



REPUBLIC OF IRAQ
MINISTRY OF HIGHER EDUCATION AND
SCIENTIFIC RESEARCH
AL-FURAT AL-AWSAT TECHNICAL UNIVERSITY
ENGINEERING TECHNICAL COLLEGE NAJAF

EXPERIMENTAL AND THEORETICAL
STUDY OF THE THERMAL PARAMETERS OF
THE HEAT SINK USING NANO PARTICLES
PACKING

HAMID MAKI BEAWAY

M.TECH
IN MECHANICAL ENGINEERING TECHNIQUES
OF POWER

2024



**EXPERIMENTAL AND THEORETICAL STUDY OF THE THERMAL
PARAMETERS OF THE HEAT SINK USING NANO PARTICLE
PACKING**

A THESIS

**SUBMITTED TO THE DEPARTMENT OF MECHANICAL
ENGINEERING TECHNIQUES OF POWER
IN PARTIAL FULFILLMENT OF THE REQUIREMENTS FOR
THE DEGREE OF MASTER OF THERMAL TECHNOLOGIES IN
MECHANICAL ENGINEERING TECHNIQUES OF POWER
(M.TECH)**

BY

HAMID MAKI BEAWAY

Supervisor By

Prof. Dr. Ali Shakir Baqir

Prof Dr. Montadhar Al moussawi

2024

بِسْمِ اللَّهِ الرَّحْمَنِ الرَّحِيمِ

يَرْفَعِ اللَّهُ الَّذِينَ آمَنُوا مِنْكُمْ وَالَّذِينَ أُوتُوا
الْعِلْمَ دَرَجَاتٍ وَاللَّهُ بِمَا تَعْمَلُونَ خَبِيرٌ

صدق الله العلي العظيم

DISCLAIMER

I confirm that the work submitted in this thesis is my own work and has not been submitted to other organization or for any other degree.

Signature:

Name: Hamid Maki Beaway

Date: / / 2024

ACKNOWLEDGMENT

All Praise to ALLAH for his uncountable blessings, assistance during the preparation of this work.

I want to submit my profound respects and sincere gratitude to my supervisors, **Prof. Dr. Ali Shakir Baqir** and **Prof Dr. Montadhar Al moussawi** , for their support during the research period and guidance to accomplish this work.

Special thanks to the head and members of the Mechanical Power Techniques Engineering department for their assistance to me. I would like to thank all lovely, helpful people who support me directly and indirectly to conduct this work.

Special thanks to my collagenous for their great assistant and great encouragement.

My deepest thanks and gratitude are due to each family member, especially my dearest parents, and brothers for their patience, support, and encouragement throughout my life. Special thanks are also due to my wife for her support and patience during my study.

Hamid Maki Beaway
2024

SUPERVISORS CERTIFICATION

We certify that the thesis entitled "**Experimental and theoretical study of the thermal parameters of the heat sink using Nano particle packing**" submitted by **Hamid Maki Beaway** has been prepared under our supervision at the Department of Mechanical Engineering Techniques of Power, College of Technical Engineering-Najaf, AL-Furat Al-Awsat Technical University, as partial fulfilment of the requirements for the degree of Master of Techniques in Thermal Engineering.

Signature:

Name: Prof. Dr. Ali Shakir Baqir

(Supervisor)

Date: / / 2024

Signature:

Name: Prof. Dr. Montadhar Al moussawi

(Supervisor)

Date: / / 2024

In view of the available recommendation, we forward this thesis for debate by the examining committee.

Signature:

Name: A. Prof. Dr. Adel A. Edan

Head of Mechanical Eng. Tech. of Power Dept.

Date: / / 2024

COMMITTEE CERTIFICATION

We certify that we have read the thesis entitled " **Experimental and theoretical study of the thermal parameters of the heat sink using Nano particle packing**" submitted by **Hamid Maki Beaway** and, as examining committee, examined the student's thesis in its contents. And that, in our opinion, it is adequate as a thesis for the degree of Master of Techniques in Thermal Engineering.

Signature:

Name: Prof. Dr. Ali Shakir Baqir

(Supervisor)

Date: / / 2024

Signature:

Name: Prof. Dr. Montadhar Al moussawi

(Supervisor)

Date: / / 2024

Signature:

Name: Asst. Prof. Dr. Rasha H. Hashim

(Member)

Date: / / 2024

Signature:

Name: Asst. Prof. Dr. Hayder H. Khaleel

(Member)

Date: / / 2024

Signature:

Name: Prof. Dr. Ahmed hashim Yousif

(Chairman)

Date: / / 2024

Approval of the Engineering Technical College- Najaf

Signature:

Name: Prof. Dr. Hassanain Ghani Hameed

Dean of Engineering Technical College- Najaf

Date: / / 2024

LINGUISTIC CERTIFICATION

This is to certify that this thesis entitled “**Experimental and theoretical study of the thermal parameters of the heat sink using Nano particle packing**” was reviewed linguistically. Its language was amended to meet the style of the English language.

Signature: Asst. Prof. Dr. Ahmed Saad Al- Hussein

Name:

Date:

ABSTRACT

Thermal management of electrical and electronic devices has become a major problem nowadays. Therefore, with the passage of time, and due to advanced technology and the increasing need for cooling in various electronic systems, there was an increasing need for research into many new materials, different designs, and innovative nanomaterials.

Most studies investigate experimental and numerical investigations into the process of heat transfer from a heat sink. In ideal design concepts that increase the heat transfer coefficient and thermal dissipation.

In this study, the heat transfer process was investigated between a traditional heatsink with rectangular fins manufactured by specialized companies and heatsinks with pin fins that we manufactured, which are (Inline, Staggered, Zigzag) and have the same surface area, which is $(21252.6 \times 10^{-3}) \text{ mm}^2$, which is equal to the area of the traditional heatsink (after removing part of it). The difference was in the arrangement of the rows of fins, and each one of these models contains a base with a thickness of (3) mm and (120) pin fins with an outer diameter of 3 mm and an inner diameter of 1.5 mm. The fins are solid in the first test (without nano), and other tests they contain a filling of a nanomaterial called Multi-Walled Carbon Nano Tubes (MWCNTs) which are characterized by superior thermal conductivity. First, all dissipators were tested to obtain the highest value of the convective heat transfer coefficient (h) and without the use of nanomaterials, in order to find out the dissipator with the optimal design in terms of the arrangement of the fins under standard working conditions (the incoming air 1.5m/s, and the temperature of the dispersant base is 95 °C at the maximum operating temperature) where the value reached h (88 W/m².C) it the highest value obtained in the dispersion (inline). From this test, the use of this dispersant was approved in other tests using nanomaterial, as this material was used in a proportion 5, 10, 15, and 20% from the total number of fins of the heat sink (Inline), Reynolds No. were obtained that ranged between (5000 - 12000) and the Nusselt No. ranged between (330 - 350) at a percentage of 5% of nanomaterial, while it ranged between (360 - 380) at a percentage of 20%, these values were at the maximum temperature, which is 95 °C, and these values are good values obtained. This indicates that the effectiveness of the nanomaterial has become effective to a very large degree, as this study shows.

CONTENTS

DISCLAIMER	I
ACKNOWLEDGMENT	II
SUPERVISORS CERTIFICATION.....	III
COMMITTEE CERTIFICATION.....	IV
LINGUISTIC CERTIFICATION	V
ABSTRACT	VI
LIST OF FIGURES.....	XIV
NOMENCLATURE.....	XIII
CHAPTER ONE	
1.1 INTRODUCTION.....	1
1.2 Definition of a Heat Sink	2
1.3 Principle of heat transfer	3
1.4 Heat Sink Systems.....	4
1.5 Thermal resistance in dispersants.....	5
1.6 Metals from which the dispersant is made.....	6
1.7 Types of heat sinks.....	6
1.8 Objective of the Thesis.....	11
1.9 Thesis Outline	12
CHAPTER TWO.....	14
LITERATURE REVIEW.....	14
2.1 INTRODUCTION.....	14
2.2 Heat sink without nano- technologies :.....	15
2.3 Heat sink with nano-technologies :.....	17
2.4 Scoop of the present work.....	35
CHAPTER THREE	
NUMERICAL ANALYSIS	
3.1 INTRODUCTION	
3.2 Numerical Side Study \ Geometry of Simulated heat sink :	
3.2.1 Governing Equations.....	38

3.3 Mesh Generation	39
3.4 Mesh Topology	39
3.5 model /In Line	39
3.6 Model Staggered :	42
CHAPTER FOUR	47
4.1 INTRODUCTION.....	47
4.2 Experimental Rig.....	47
4.2.1 Heating unit:	49
4.2.2 Voltage Regulator (Variable Transformer):.....	50
4.2.3 Watt meter (Clamp meter)	51
3.2.4 Air handling unit (Fan).....	51
4.2.5 Fan Speed Regulator	52
4.2.6 The Duct of air	52
4.2.7 Thermal silicone.....	54
4.2.8 Insulating material.....	55
4.2.9 sensitivity unit	56
4.2.9.1 Datalogger	56
4.2.9.2 Thermocouple.....	57
4.2.9.3 Digital Anemometer	58
4.3 XRD Test of Aluminum material	
4.4 Testing devices.....	60
4.4.1 Practical test form.....	60
4.4.2 - Measuring devices (Instrument)	66
4.4.3 Experimental prossedure	67
4.4.4 Charging the Nano material in the fins:	68
CHAPTER FIVE.....	70
5.1 INTRODUCTION.....	70
5.2 Choosing the heat sink :	70
5.3 Nano Material : Multi Wall Carbon Nano Tubes (MWCNTs) :.....	71
5.4 Electrical Conductivity of MWCNTs :	72
5.5 Physical Properties of MWCNTs :.....	73
5.6 Distribution of Nanomaterial on the Fins of H.S :	74

5.7 Experimental side Study :	75
5.7.1 The Variation between speed and temperature difference.....	75
5.7.2 The Effectiveness of Nano packing (ϵ_n) :	79
5.7.3 The Variation between Re and Nu :	83
5.7.4 The Variation between Re and ($Nu_n / Nu_{\text{without nano}}$) :	88
5.7.5 The Variation between Re and ($Nu_n / Nu_{\text{Classic}}$) :	91
5.7.6 The Enhansmenting Ratio of model :	96
5.8 Verification of Model :	104
CHAPTER SIX	107
CONCLUSIONS AND RECOMMENDATIONS	107
6.1 CONCLUSIONS	107
6.2 RECOMMENDATIONS	109
REFERENCES	110

LIST OF TABLES

Table 2.1: Properties material of phase change.....	19
Table 2.2 : The work of the dissipation of heat sinks.	27
Table 3.1 : The Dimensions and numbers of fins, and geometric shape in the heat sinks	54
Table 52 : XRD Test of Aluminum material.	61
Table 4.2 : The Dimensions of all heat sinks.....	69

LIST OF FIGURES

CHAPTER ONE

Figure (1.1) The cooling group in computers.[2].....	3
Figure (1.2): shows the process of heat exchange between the heat sink and the external environment.[5].....	4
Figure (1.3): Fins of HS (Epoxy-Bonded).[9].....	7
Figure (1.4): Pin fin of H.S .[12].....	8
Figure (1-5) Folded fin of HS .[13].....	8
Figure (1- 6) Manufacturing and (pros-cons) of heat sink types.[14]	10
Figure2.1: Comparison between the experiments and numerical state results for a small channel sink of heat with standard (a) and improved (b) header shapes.[22]	20
Figure (4.1) , Schematic diagram of the parts of the heat dissipation system.	48
Figure (4- 2, A) , photograph the parts of the system.	48
Figure (4- 2, B) The experimental rig	49
Figure (4-3) Electric Heater.	50
Figure (4-4) The Variable Transformer	50
Figure (4-5) Digital oveo meter.	51
Figure (4-6) Fan of cooling.	52
Figure (4-7) Fan speed regulator.....	52
Figure (4-8) , The duct with all dimensions (mm).....	53
Figure (4-9) location and dimensions of thermocouples	54
holes in the duct (mm).....	54
Figure (4- 10) , The air duct.....	54
Figure (4-11) Thermal silicone.	55
Fig (4-12) The Insulating material.	55
Figure (4-13) The Data logger.	56
Figure (4-14) K - Type Thermocouple.	57
Figure (4- 15) Digital Anemometer	58
4.3 XRD Test of Aluminum material :	58

Before that, to checked and tested the metal of model (heat sink), by XRD test in sample examination office at (Al-Kufa University), this is to ensure the metal is from Aluminum or not . The test includes the classic model too. The result of this test give us a good sign to the metal is Aluminum as shown below..... 58

Figure (4-16), XRD Diagram test of aluminumme..... 59

Figure (4-17), XRD Diagram test of aluminumme..... 60

and the figure (4- 20), expliane the dimension of the heat sink (Classic type) after cutting..... 62

Figure (4-20) , The Dimensions of Classic heat sink (after cutting) 62

Figure (4-21) shows the type of heat sinkIn Line with Dimensions (mm) 63

Figure (4-22) shows the type of heat sink staggered with Dimensions (mm). 64

Figure (4-23), Heat sink (zigzag) type. 65

Figure (4-24) Calibration curve of thermocouples. 67

Figure (4 - 25), the fins that were closed with aluminum 68

tape from the top. 68

Figure (5-1) Variation between heat transfer coefficient..... 71

and the velocity of Fan of Heat sinks at 95 °C, without nano material..... 71

Figure (5 - 2), Different between the single tube & multi tube nanomaterial 72

Figure (5- 3) (A & B) 73

show the variation in the length and dimension of the Nano material. 73

Figure (5 – 4), Distribution of the Nanomaterial in the In Line heat sink. 74

Figure (5 - 5), Variation between Velocity & ΔT at In Line heat sink 77

with 5% Nano..... 77

Figure (5 - 6), Variation between Velocity & ΔT at In Line heat sink 77

with 10% Nano..... 77

Figure (5 - 7), Variation between Velocity & ΔT at In Line heat sink 78

with 15% Nano..... 78

Figure (5 - 8), Variation between Velocity & ΔT at In Line heat sink 78

with 20% Nano..... 78

Figure (5 – 9), Variation between Re & ϵ_n at In Line heat sink..... 81

with 5% Nano..... 81

Figure (5 - 10), Variation between Re & ϵ_n at In Line heat sink 82

with 10% Nano..... 82

Figure (5 - 11), Variation between Re & ϵ_n at In Line heat sink	82
with 15% Nano.....	82
Figure (5 - 12), Variation between Re & ϵ_n at In Line heat sink	83
with 20% Nano.....	83
Figure (5 – 13) Variation between Re & Nu with Nano 5%, (Inline) H.S.	85
Figure (5 – 14) Variation between Re & Nu with Nano 10%, In Line HS.....	86
Figure (5 – 15) Variation between Re & Nu with Nano 15%, In Line HS.	86
Figure (5 – 16) Variation between Re & Nu with Nano 20%, In Line HS.....	87
Figure (5- 17) Variation between Re & Nu in Classic heat sink.	87
Figure (5 – 18), The Variation between Re & (Nu n / Nu without n) with 5% Nano.....	89
Figure (5 – 19) Variation between Re & (Nu n / Nu without n) with 10% Nano.	89
Figure (5 – 20) Variation between Re & (Nu n / Nu without n) with 15% Nano.	90
Figure (5 – 21), Variation between Re & (Nu n / Nu without n) with 20% Nano.	90
Figure (5 - 22) Variation between Re & (Nu n / Nu Classic) at 5% Nano.	94
Figure (5 - 23) Variation between Re & (Nu n / Nu Classic) at 10% Nano.	94
Figure (5 – 24) Variation between Re & (Nu n / Nu Classic) at 15% Nano.	95
Figure (5 – 25) Variation between Re & (Nu n / Nu Classic) at 20% Nano.	95
Figure (5 – 26) Variation between Re & (Nu without n / Nu Classic).....	96
Figure (5 – 27) Variation between Re & Enhancement ratio with 5% Nano.	98
Figure (5 – 28) Variation between Re & Enhancement ratio with 10% Nano.	99
Figure (5 – 29) Variation between Re & Enhancement ratio with 15% Nano.	99
Figure (5 - 30) Variation between Re & Enhancement ratio with 20% Nano.....	100
Figure (5 – 31) Variation between the Time and Temperature	101
For Classic and In Line heat sinks.	101
REFERENCE:	110

NOMENCLATURE

Symbol	Definition	Unit
A_s	Heat transfer area	m^2
B	Test section base length and width	mm
C	Clearance between the fin and duct	mm
C_p	Specific heat at constant pressure	J/kg.K
D	Diameter of pin fins	mm
D_h	Hydraulic diameter of the duct	mm
D_{hp}	Horizontal holes diameter	mm
D_{lp}	Side holes diameter	mm
D_{vp}	Vertical perforation diameter	mm
F	Friction factor	-
$g_{x,y,z}$	Gravitational acceleration component in x, y and z directions respectively	m/s^2
H	Height of the pin fins	mm
H	Heat transfer coefficient	$W/m^2 K$
K	Thermal conductivity coefficient	$W/m.K$
L	Duct cross section depth	mm
L	Duct length	mm
N	Pin fins number	-
N_p	Perforation number	-
Nu	Nusselt number	-
P	Pressure	Pa
Re	Reynolds number	-
R_{th}	Total thermal resistance	$^{\circ}C/W$

S	Pitch	mm
T	Temperature	°C
U	Components of velocity vector in x direction	m/s
V	Average inlet velocity	m/s
V	Components of velocity vector in y direction	m/s
w	Duct cross section width	mm
W	Components of velocity vector in z direction	m/s
Ψ	Effects of nanoparticle volume fraction	%

Chapter One

Introduction

CHAPTER ONE

1.1 INTRODUCTION

Electronic devices and Computers are the major pieces of equipment used in today's society, and it is common for any activity that is carried out to be directly or indirectly related to the computer such as in work, education, business daily, economic business, and air craft cockpit. For this reason, it is necessary to know its main parts, as it is classified as the first in the programs that represent a virtual memory for the development of activities in the device, and it also consists of hard it helps to cool the parts that have a high temperature due to the long operating period or the increase in storage capacity and that work together to develop an appropriate process.

The Cooling of the electronic devices, especially computers it is one of the topics that most users neglect, despite its importance .The problem is that sellers of shop owners do not care much about the temperature of the processorfor exampleIn general, a significant increase in the temperature of the processor will cause a shortening of the processor's life, slow performance, or a continuous suspension, and the problem is not related to just by cooling the processor, one of the causes of high temperature is also poor ventilation inside the computer chassis. The heat of the processor combines with the heat of the memory, hard drive, chipset, and graphics card, exacerbating the problems.

Heat can cause malfunctions in its operation but if the limit is exceeded it can become irreparable, so it is used (heat sinks) found in laptops and desktop computers, among other electronic devices. These electronic devices usually not require a high temperature to carry out their functions. What is more, they have devices that used the fans to cool the computer.

1.2 Definition of a Heat Sink

Heat sinks are the most effective parts of cooling electronic and electrical devices. Heat sinks differ from one type to another in terms of metal, the geometric shape of the fins, the number of fins, cooling fluid type, volume flow rates, and the dimensions.

The geometric shape of the heat sink that was studied in this research is of the type with small cylindrical fins. It stores heat in its walls, as it is found in the square fins, as the square fins store a part of the heat in the areas where there are angles in their walls, which causes the heat to remain in them for a longer time.

Finned piece of metal it acts as a heat exchanger that transfers the heat generated by a mechanical or electronic device to a fluid medium (and the fluid is often either air or a liquid refrigerant medium) in which the heat is transferred away from the device, as it allows the temperature of the device to be regulated at optimal levels. In computers, heat sinks are used to cool central processing units, graphics processing units, some chipsets, and random access memory (RAM) units. Heat sinks are used with high power semiconductor devices such as power transistors and optoelectronics such as lasers and light emitting diodes (LEDs), where the thermal conductivity of the element itself is insufficient to modulate its temperature[1].

The heat sink is designed so that the surface area in contact with the cooling medium around it - air for example - is as large as possible. Air velocity, material selection, ridge design, and surface treatment were affect on heat sink performance. The methods of installing the heat sink and the materials used in the thermal exchange interface (thermal paste) also affect the temperature of the integrated circuit template. Thermal adhesive or thermal grease improves the performance of the heat sink by filling the air pockets between the heat sink and the heat diffuser on the device.



Figure (1.1) The cooling group in computers.[2]

1.3 Principle of heat transfer

The heat sink transfers heat energy from the temperature device high to a fluid medium to lower temperature. Mostly the fluid medium is air, but it can also be water , or coolant , or oil. If the fluid medium is water ,is called heat sink(cold plate). heat sinkas it's known in the thermodynamic a heat reservoir that can absorb an unlimited amount of heat without a significant change in temperature . Heat sinks in electronic devices must have temperatures higher than ambient to enable convective, radiant and conductive heat transfer. Power feeders in electronic devices are not 100% efficient, so they generate excess heat that can be harmful to device operation . Therefore, the design includes a heat sink to dissipate the heat .the figure (1.2) explains the process of heat exchange between the heat sink and the external environment.[3,4]

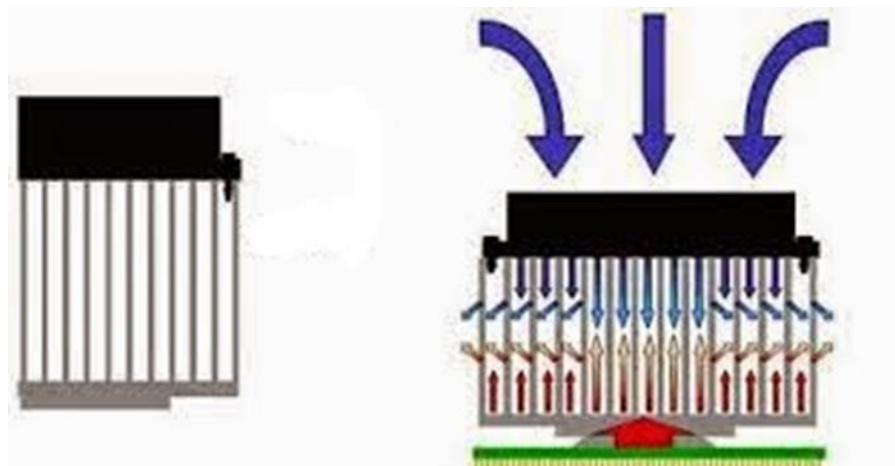


Figure (1.2): shows the process of heat exchange between the heat sink and the external environment.[5]

1.4 Heat Sink Systems

The pin-fin array system's heat transfer characteristics have been the subject of extensive investigation because of its importance. Commonly used heat sink is pin-fin type. A pin-fin is an element attached perpendicular to a wall against the fluid flow. There are various parameters characterizing the pin-fins are, by shape, height, diameter and height to diameter ratio. In addition to the physical geometry, pin-fins are positioned in arrays either inline or staggered with respect to the flow direction. The pin-fin finds a variety of engineering applications like compact heat exchangers and the cooling of advanced gas turbine blades and electronic devices. For a given base plate temperature, Heat transfer rate could be enhanced based on the Newton's law of cooling by altering the values of heat transfer coefficient or surface area and while limiting the temperature difference. An increase in heat transfer coefficient can be achieved via forced convection or changing fluid (not practicable always). The alternate is by changing the geometry of the heat sink to enhance the heat transfer.[4]

Heat sink for electronics depends on conduction from the electronic package to the heat sink base, followed by conduction into the extended surfaces and

convection to the cooling fluid[6] . The rate of heat dissipation depends on the following :

- (i) temperature distribution in pin-fins and its assembly
- (ii) pin-fin geometry
- (iii) pin-fin arrangement
- (iv) fluid flow rate
- (v) tip clearance
- (vi) fluid flow direction.

1.5 Thermal resistance in dispersants

In devices in which it is semiconductors used in a number of industrial or consumer electronic devices The idea of thermal resistance simplifies the selection of heat sinks. The heat flow between the semiconductor die and the surrounding air is modeled as a series of resistances to the heat flow; There is resistance from the die to the device case, from the case to the heat sink, and from the heat sink to the surrounding air[7]. The sum of these resistances is the total thermal resistance from the mold to the surrounding air. Thermal resistance is defined as the temperature rise corresponding to a unit of power, which is similar to electrical resistance, and is expressed in degrees Celsius per watt ($^{\circ}\text{C}/\text{W}$). If the amount of heat discharge of the device in watts is known, and the total thermal resistance is calculated, the temperature rise of the die over the ambient air can be calculated.

The idea of thermal resistance of a semiconductor heat sink is used as an approximation . It does not take into account the uneven heat distribution on the device or the heat sink. They only model a system in thermal equilibrium, ignoring the change in temperature with time. And do not reflect linearity of both radiation and convection with respect to temperature rise. However, manufacturers include

typical values for the thermal resistances of heat sinks and semiconductor devices , which facilitates the selection of commercial heat sinks.

1.6 Metals from which the dispersant is made

The heat sink mostly made from aluminum or copper, this is because these two elements are widely available in nature and have high advantages in thermal conductivity and performance.

1.7 Types of heat sinks

The use of heat sinks to improve the heat transfer rate from a module has been implemented with great care. The increased surface area usually requires an increase in the air pressure drop in that region, and if there are other paths for the air to flow through at a lower pressure drop, the resulting air starvation in an enhanced region may actually result in a lower heat transfer rate [8]. Careful analysis

or testing is therefore necessary under the actual system condition to ensure effectiveness of the design. Flow through heat sinks refers to heat sinks wherein the flow enters the heat sinks from one end and travels more or less in a straight line to exit from the other end. One of the simplest and most cost-effective heat sink designs used is the linearly extruded aluminum heat sink, Figure (1-3).

Aluminum alloys (6063 or 6061) are most common, followed by copper (which is 4-6x more expensive, 3x as heavy, by having 2x the conductivity).



Figure (1.3): Fins of HS (Epoxy-Bonded).[9]

These heat sinks consist of an extruded or machined base, which is flat on the module-facing side and grooved on the fin side. The fins are then epoxied into the grooves. The epoxy interface does, however, add a thermal resistance to the system. This difficulty can be overcome by brazing or soldering the fins to the base, resulting in reduced overall resistance at a higher cost [10,11]. Both aluminum and copper can be used to construct this type of heat sink, depending on the system requirements and allowable overall weight. Pin-fin heat sinks are also commonly used and have the added advantage of not requiring specific positioning relative to flow direction. Pin-fin heat sinks can be manufactured either by starting with a linearly extruded parallel plate heat sink and then cutting the plates to form the pins, or by building them using more costly specialized techniques such as epoxy bonding, brazing and soldering.

Round pins or other cross-section shapes can also be manufactured using casting as shown in Fig. (1-4).

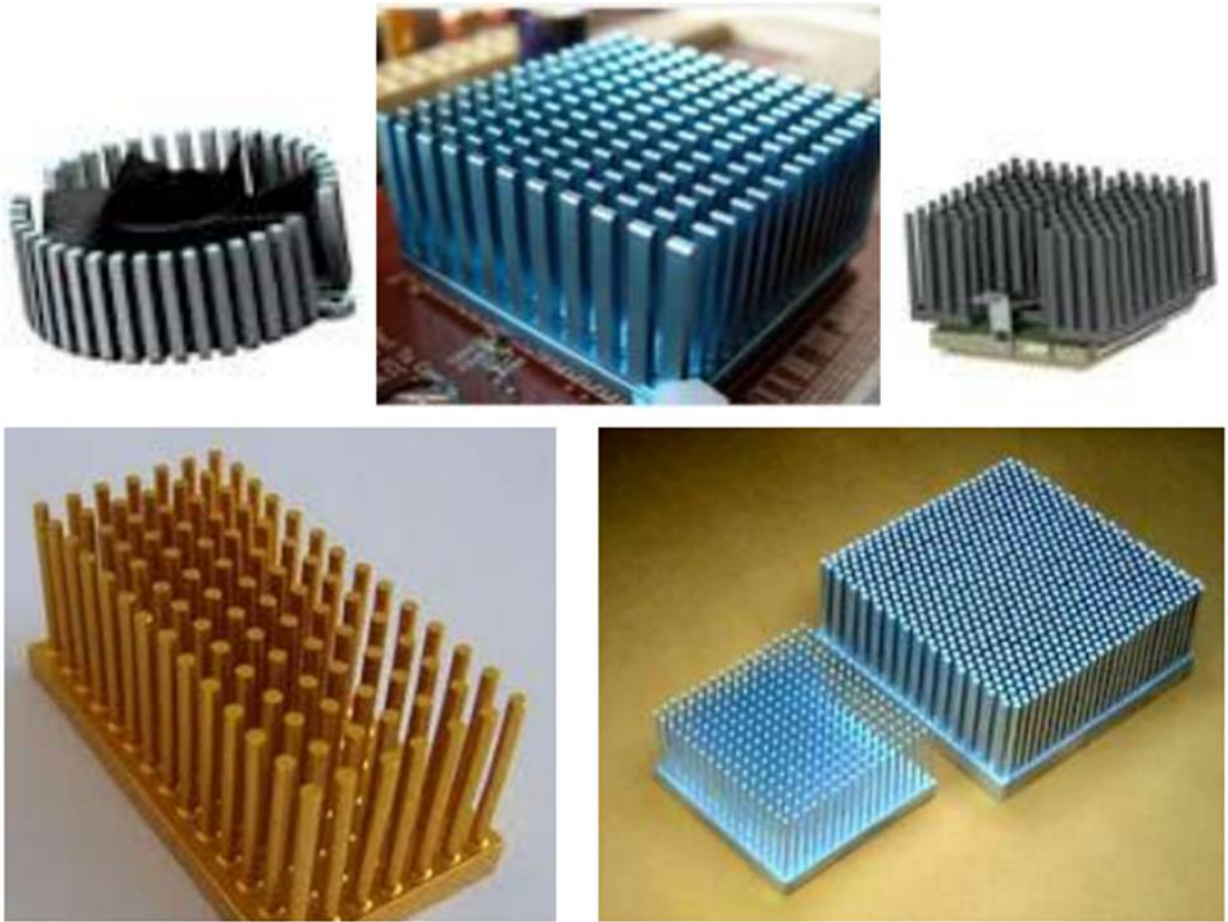


Figure (1.4): Pin fin of H.S .[12]

Other commonly used heat sinks include folded-fin heat sinks where sheet metal (0.005) to (0.08) cm is corrugated to form fins as in Fig. (1-5).



Figure (1-5) Folded fin of HS .[13]

Manufacturing of heat sinks widely spreads to provide thermal solutions for fast development in electronics production (growing energy and declining volume). Heat sink types, manufacturing and its pros and cons are illustrated in Fig. (1-6).

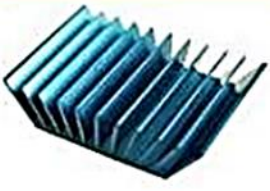





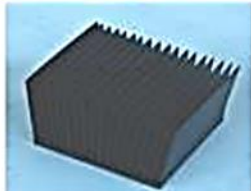
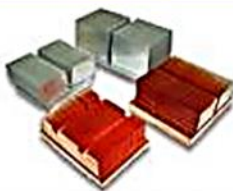
Heat Sink Types & How They Are Made				
Extruded	Stamped	Bonded	Folded Fin	
				
Heated metal is forced through a profiled die	Metal stamped to form a particular shape	Individual fins are bonded with epoxy to a pre-grooved base	Fins are pre-folded and then brazed or soldered to a plate base	
Single Fin Assembly	Swaged	Forged	Skived	
				
Individual pieces of fin and spacer material are stacked and then brazed to create the desired shape	Individual fins are placed in a pre-grooved base and then a roller or punch will swage the sides to the fins	Heated metal is compressed into a form mold to the desired shape	Fins are "skived" from a solid piece of material, usually copper	
Heat Sink Types: Pros and Cons				
Type	Best For	Performance	Pros	Cons
Extruded*	Most applications	Low-High	Cost-effective	Limited dimension
Stamped*	Low power	Low	Inexpensive	Low performance
Bonded Fin*	Large applications	Moderate	Large sizes	Expensive
Folded Fin	Ducted air	Very High	High heat-flux density	Expensive, needs ducting
Active Heat Sink	When necessary	High	Band-aid Solution	Reliability, cost, warm air recirculation
Forged	Many applications	Medium	Inexpensive	Limited in design and flow management
Swaged	High power applications	Medium	Good for power devices	Heavy and bulky, limited ability for flow management
Single Fin Assembly	All applications	Low-High	Light weight and low profile with high degree of flow management options	Expensive
Skived	Many applications	Medium-High	High fin density	Thick base, higher weight, directional sensitive

Figure (1- 6) Manufacturing and (pros-cons) of heat sink types.[14]

1.8 Objective of the Thesis

- 1- Investigate the effect of fins arrangement on the important parameters (Q , h , ΔT) at steady state conditions, also at constant surface area.
- 2- Compare the best arrangement heat sink with a classical heat sink to study the heat sink performance.
- 3- Proposed a new strategy (MWCNTs packing) for CPU heat sink cooling with (5, 10, 15, and 20) % inlet of fins .
- 4- Comparison between the Inline heat sink and the classical heat sink to find out which one has more performance and effectiveness in heat transfer process.

1.9 Thesis Outline

This master's thesis is divided into five chapters, as follows:

1. The first chapter (Chapter One) includes an introduction to heat sinks and their types, as well as their uses and importance in the process of cooling electrical and electronic devices, and the metals from which they are made.
2. The second chapter (Chapter Two) included previous literature that dealt with the use of heat sinks in the cooling process, as well as the types of nanomaterials added to them.
3. The third chapter (chapter Three) includes the Numerical Analysis by used Ansys (R18.1) program with insert the B.C (velocity of air inlet and temperature).
4. The forth chapter (Chapter Four) includes the work method, materials, and devices used in this experiment, in addition to measuring devices.
5. The fifth chapter (Chapter Five) presents a discussion of the experiments obtained from the process of cooling the heat sink (without the nanomaterial, and after adding it to the heat sink).

6. The sixth chapter (Chapter Six) dealt with the conclusions reached from the experimental study and some recommendations for future work.

Chapter Two

Literature Review

CHAPTER TWO

LITERATURE REVIEW

2.1 INTRODUCTION

Pin-fin heat sinks are a good type of CPU cooling in electronic and electrical devices. The use of nanomaterials in this field played a major role in the process of cooling the dissipator quickly, saving time and effort.

This chapter provides a review of the studies conducted on the cooling process for various heat sinks, including micro channels or rectangular fins or other types, with use of various nanomaterials and knowing how effective they are in lowering temperatures in a way that helps these devices continue to work for longer periods of time.

2.2 Heat sink without nano- technologies :

Anmar Adnan, et al. [2014][15], Reduced pressure drop and enhancing heat transfer on pin fins with holes nested in a rectangle duct with orthogonal airflow was studied experimentally and numerically using ANSYS-CFX-12. The dimension used are channel width of a cross-section (w) 62 mm. depth of cross section (l) 167 mm. channel long (L) 1200 mm. Experimentally results showed that. Reynolds No. is ranged 28000-113000 for pin fins with a solid form and horizontal/vertical (HV) holes & Pin fins have horizontal/lateral/vertical (HLV) holes respectively. Findings from Experiments showed that the (Nu) of horizontally/vertically (HV) pins is almost 11% which is greater than the value of solid pins, whereas; HLV (horizontal/lateral/vertical holes) is approximately 21% more than solid pins. Pressure decrease with horizontally/vertically (HV) punches is lowered by 23% when compared to solid screws, the pressure drop is decreased

by roughly 19% when using (HLV) punches to solid screws. Additionally, the experimental outcomes showed that the holes of (HLV) nails have a good improvement in heat transfer as well as a significant weight reduction of about 21.65% compared to solid nails. Correlation equations for heat transfer have been created to study heat transmission and pressure decrease. The numerical analysis explained that the intensity of the velocity vectors was found to be high in the results of the HLV pin fin, which is greater than that of the HV pin fin because the lateral perforations provide less pressure inside the horizontal holes and enable flow to pass through them. And, the HLV perforated screw fins provided a greater drop in temperature on the surface compared to solid and HV perforated screw fins. Finally, the current numerical findings are shown to be in great agreement with the experimental data.

Hossein Lotfizadeh, et al. [2015][16], Studied experimentally the thermal performance of four types of heat sinks including; a heat sink with extruded longitudinal fins, an aluminum nanoparticle extruded longitudinal fin heat sink, a commercially available rectangular block of metallic revolutionary aluminum foam, and a water-as-liquid heat sink working with a velocity of 1.17 m/s. The four heat sinks have the same dimensions ($9 \times 16 \times 3.5$) cm. Spherical and monodisperse 10 nm aluminum nanoparticles, nano-coated aluminum metal foams, and uncoated metal foams were used. The restricted stream from the ambient air was used to cool each heat sink. The experiments were conducted in an air tunnel 120 cm long, and 19.05 cm in diameter, with an air exit hole diameter of 20.06 cm. The air velocity varied between 1 and 3 meters per second. The temperature of the application-specific IC chip (ASIC) is represented by the temperatures at the base of the heat sinks. The influence of airflow velocity on the thermal resistance of the heat sinks was also investigated. The results indicated that the unique heat sink with aluminum nano-coating outperformed the other heat sinks utilized in the study. Although the metal foam heat sink has better performance than the uncoated and coated, it cannot be an

economical alternative for industrial applications due to its price and technical issues.

Patil, et al. [2022][17], Measured the number of Nusselt, factor of friction, and performance of thermal-hydraulic (THP) of several heat sink geometries. The effectiveness of a plate-fin sink of heat and a screw-fin sink of heat in a forced-flow condition was evaluated in this investigation. A heat sink consisting of dimpled plate fins and a new pin-fin design with winglets are tested experimentally at Reynolds numbers between 6800 and 15100. The pin-fin sink of heat is expected to operate at full thermo-hydraulic capacity ($S / D_f = 4.52$) at a pitch ratio ($S / D_f = 2$) and wing length ratio ($L_w / D_f = 2$). The optimal thermal-hydraulic efficiency of dimpled plate fin sink of heat is seen for D/d values of 0.5 and P/d values of 0.5. It is shown how different fin designs with an aspect ratio (s/d) of 2.5 affect the relationship between factor of friction & Nu . It is essential to optimize the spacing between the fins on pin-finned heat sinks for effective heat dissipation since the space between the fins allows for about twice the heat transfer of plate heat sinks.

2.3 Heat sink with nano-technologies :

Tu - Chieh Hung, et al. [2012][18], Employed nanofluids to investigate heat transport in a 3D rectangular microchannel heat sink (MCHS) experimentally and numerically. The type of nanoparticles, base fluid, particle size fraction, particle size, and pumping force was found to have a significant impact on the coolant's thermos physical properties. The lowest thermal resistance was achieved by appropriately adjusting the volume fraction and pumping force under specific engineering conditions. However, according to the calculations done for this study, a system with Al_2O_3 -water-cooled nanoparticles MCHS can achieve the greatest heat transfer improvement. The outcomes also demonstrate if the volume portion of nanofluid particles is elevated, the thermal resistance initially was low and

subsequently high. When using nanofluids with smaller nanoparticles, MCHS performs better over a modest range of particle sizes. Additionally, if the pumping power is about 0.5 W, that will lead to lower total heat resistance in MCHS. Nanofluids containing Al_2O_3 and water had performance 21.6% better in terms of heat transmission than pure water. The MCHS is a prospective cooling device for uses like electromechanical system cooling systems and high large-scale integrated circuits. It was found that the primary determinants of the cooling performance of MCHS employing nanofluids are The heat capacity, thermal conductivity, and dynamic viscosity of the work materials.

Ismaila Zarma, et al. [2019][19], Measured a Concentrator Photovoltaic (CPV) Nanoparticle-PCM hybrid system's performance in a solar concentration 20% proportion. The effects of Al_2O_3 , CuO, and SiO_2 nanoparticles on a concentrator solar system's overall efficiency at loading ratios of 1% and 5% are evaluated. A two-dimensional hybrid model was created and computationally simulated, featuring photovoltaic layers and a heat sink composed of nanoparticles and PCM. The results of numerical and experimental analyses are confirmed. Al_2O_3 greatly improves the thermal conductivity of PCM in comparison to CuO and SiO_2 nanoparticles, resulting in a cooler solar cell and a faster rate of heat transfer and melting. The usage of nanoparticle-PCM has also been linked to improvements in electrical efficiency and thermal uniformity. Whereas electrical efficiency in pure PCM it was 6.36 percent and stability of temperature was 20 °C, 5% Al_2O_3 -PCM achieved an efficiency of 8 %. Because of the CPV-Nanoparticle-PCM system's cutting-edge energy-saving and safety-enhancing capabilities, it may be recommended for usage in both residential and commercial properties.

Nadezhda S. Bondareva, et al.[2020][20] mentioned that the electronic of cooling parts is the most essential topic in electronic technology design

development. One of the methods in advanced and promising cooling is heat sinks depends on materials of phase change (PCMs) reinforced with particles of the Nano-sized solid . They used a closed radiator with fins to test the effect of PCM physical characteristics and nanoparticle concentration on heat and mass transmission while maintaining a constant heat output volume. The melting phase-change materials of nano-enhanced (NePCMs) is investigated, taking natural convection into consideration in the (NePCMs) under the effect on outside convection cooling. A closed metal rectangular made of copper with dimensions [Length = 3.0 cm, High = 1.5 cm], and the nanoparticles of Al_2O_3 were employed. Other PCM's in this paper (n-octadecane with melting point 28.05 °C, melting point of capric acid with 32 °C, melting point of lauric acid 46 °C, RT-50 with point of melting 49 °C, and RT-80 with point of melting 81 °C). They found that the best PCM's n- octadecane because it has low melting point temperature. That mean, when using the material of phase change (PCM) with low temperature of melting it help to cooling the heat sink, while if using the PCM with high melting temperature that not useful in this process. Table No.2-1 showed the alter phase material characteristics .

Table (2-1) Properties material of phase change

Material of phase change	T_m (°C)	L_f (kJ/kg)	K_s/k_l W/(m.k)	ρ_s/ρ_l (kg/m ³)	cs/cl , J/(kg·K)	μ , Pa·s	β (K ⁻¹)
n-octadecane	28.05	241	0.39/0.157	814/770	1900/2200	3.8×10^{-3}	8.5×10^{-4}
Capric acid	32	152.7	0.372/0.153	1018/888	1900/2400	2.7×10^{-3}	10^{-3}
Lauric acid	46	187.2	0.16/0.14	940/885	2180/2390	8×10^{-3}	8×10^{-4}
RT-50	49	168	0.2	780	2000	4.8×10^{-3}	6×10^{-4}
RT-80	81	175	0.2	920/770	2400/1800	7.2×10^{-3}	10^{-3}

Zhang, et al. [2020][21], Improved a topology optimization technique, a two-dimensional (2-D) nanofluid-cooled microchannel heat sink (NMHS) geometric structure. They explained the heating & flow transmission in the NMHS using a Convective flow using a single-phase of nanofluid heating model. Also because thermos physical characteristics of the nanofluid are substantially affected by temperature, fluid characteristics that vary with temperature are taken into account in the design. To maximize NMHS designs, a topology optimization strategy based on density is used to study a maximizing of heat transfer issue when the pressure differential is constant. The density of the substance is used as element of design in the optimization to limit a variant of flow field. This section investigates the implications of temperature-dependent fluid characteristics on optimum designs. The pressure differential and the coefficient of heat production were set to constant values of $\Delta p = 10 \text{ Pa}$ & heat generation coefficient $\beta = 108 \text{ W}/(\text{m}^3 \cdot \text{K})$, respectively. As a coolant, a Nano fluid with $d_p = 13 \text{ nm}$ & $p = 9\%$ is employed. The implications of fluid that varies in temperature characteristics on ideal NMHS model are first investigated numerically. Furthermore, the influence of nanofluid properties such as base fluid and nanoparticles on optimum designs, volume percentage, and diameter are evaluated. The quantitative outcomes demonstrate that fluid is temperature dependant characteristics exist. have a significant influence on As the differential of pressure or heat production coefficient rises, more branching flow channels are formed in the best topologies; and an enhanced optimum arrangement was gained through decreasing the proportion of nanoparticle volume. From the perspective of engineering, this research presents a useful optimization tool for the development of a high-performing NMHS.

Awais,et al.[2020][22], Examined the impacts of head geometry, nanoparticle concentration, and coolant flow rate on the overall heat transfer coefficient, where the hydraulic performance of micro-channel heat sinks with two distinct head geometries using nanofluids. Some ineffective designs in the tiny channel heat sink

result in poor flow distribution, which has a significant risk of worsening the sink's thermal and hydraulic performance. Several tests were performed on the tiny channel heat sink with traditional and enhanced head geometries utilizing nanofluids and pure water. In this study, Al_2O_3 was utilized as a nanofluid, and the velocity of water flowing through the small canals was constant (0.5 L/min) at the inlet and (1.5 L/min) at the outflow, as shown in Fig. (2-1). The findings from both experiments and calculations agreed well; the microchannel sink of heat with better head shape had a greater heat transfer coefficient of 17% than traditional heat sinks. The temperature in the optimized header at the entry was 316°K and 331°K , while the temperature in the standard dispersant at the entrance was 318°K and 334°K .

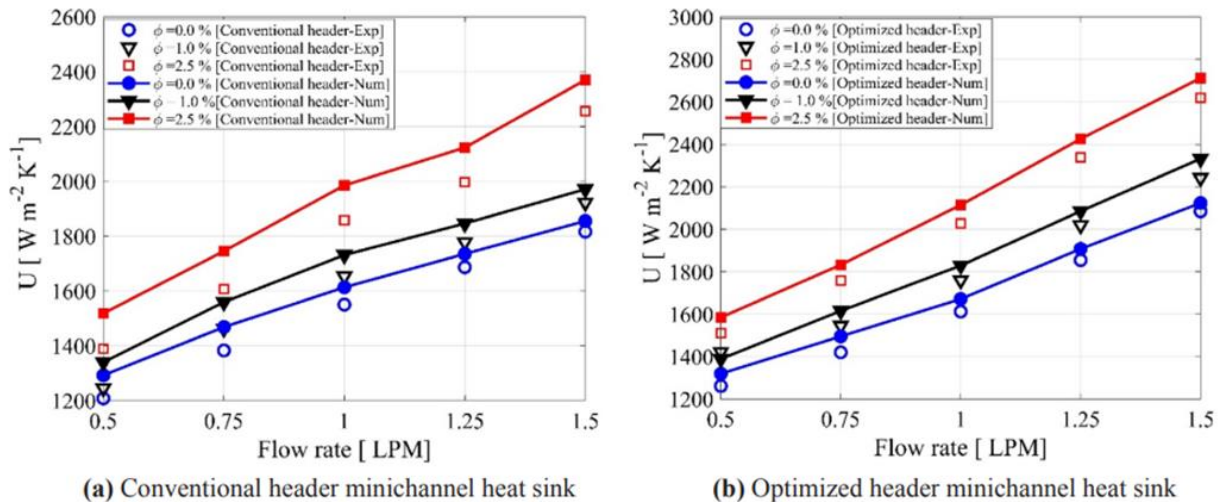


Figure 2.1: Comparison between the experiments and numerical state results for a small channel sink of heat with standard (a) and improved (b) header shapes.[22]

Yulin Ma, et al.[2020][23], Researched in the effects of nanoparticle volume fraction (ψ) and Reynolds number (Re) on the convective coefficient, CPU temperature at the surface, pumping power, heat transfer, and irreversibility of fluid friction. Using a microchannel heat sink and a biodegradable water-Ag nanofluid, they examine the effect of fin configuration on irreversibility and hydrothermal

heat. All three variations of bifur heat sinks with micro channels (straight channel, inline fin, and staggered fin) were analyzed in detail. To realistically model the behavior of nanofluids, the two-phase blending technique is employed. The results showed a lower average CPU temperature, a lower peak CPU temperature, and a lower thermal resistance. The inline-finned heat sink has the lowest pumping power and the greatest Performance Evaluation Criterion (PEC), whereas the staggered-finned sink of heat has maximum temperature resistance under constant conditions temperature. Further, it was shown meaning the rates of heating transmission and fluid friction irreversibility are lowest includes both in-line and staggered fins . First-law and second-law thermodynamic performance is optimal for heat sinks with inline and staggered fins, with the exception of $\psi = 0.1\%$, $\psi = 0.5\%$, and $Re = 500$. In addition, water-Ag nanofluid proved more preferable for use in the tested heatsinks at high Re and ψ . It was also found that the performance of the nanofluids under the second law in the considered heatsinks improves with increasing Re and ψ .

Balaji, et al. [2020] [24], Measured the convective heat transfer coefficient, temperature drop, Nusselt Number, and pressure drop while functionalized graphene nano-platelets (f-GnP) were floating in distilled water. They employed a copper microchannel heat sink ($L_{ch} = 30$ mm, $W_{ch} = 0.5$ mm, $H_{ch} = 5$ mm, $W_{fin} = 0.5$ mm, $N_{ch} = 30$) in their studies. The heat transfer characteristics were discovered to be modified by the mass flow rate (5 g/s to 30 g/s) and the GnP content (0 vol % to 0.2 vol%). In heat sink studies, GnP-based nanofluids reduce the temperature of the heat sink by 10 °C while increasing the Nusselt number and convective heat transfer coefficient by 71% and 60%, respectively, with only a modest increase in drop of pressure, which is only about 12% higher than with water; however, viscosity was found to increase by 13.3%. The results reveal that by enhancing coefficient of thermal convection and heat conduction, with modifications GnP-

based nanofluids can successfully replace conventional nanofluids and improve the performance of electronic circuits.

Kumar, et al. [2021] [25], Studied the thermal energy storage system's thermal performance based on nano-phase-changing cooling material (NePCM) of electronic components, where the researcher demonstrated that sink of heat (HS) cooling based on NePCM is a passive cooling technology that can eliminate the traditional fan-based cooling technology. In order to break a fixed size of the fin material, several models of heat sinks were used, including a heat sink without fins (HSNF), a sink of heat with rectangular shape fins (HSRPF), a sink of heat with square shape pin fins (HSSPF), and a sink of heat with fins, and round shape pin (HSCPF). Aluminum, paraffin wax, and copper oxide nanoparticles (CuO) were used. The results showed that there was an increase in the conductivity of thermal and viscosity of NePCM it 150% and 100%, respectively, and the performance of sink of heat configurations were looked into the various nanoparticle concentrations ranged ($\phi = 0.5 - 3.0$), with heat flux values ($q'' = 1.5 - 3.0 \text{ kW/m}^2$). The HSSPF square pin fin heat sink incorporating PCM / NePCM was shown to have improved thermal performance in comparison to previous sink of heat designs, where the max. drop in the temperature was discovered to be between 13°C & 15°C . HSSPF type according to the research result is better than other types.

Jung, et al. [2021] [26], Employed the parameters of heat transmission employing flow behaviors and temperature and distribution in micro-channels (MCHS). A micro-channel heat sink with nanofluid in this experiment to increase heat transfer performance in small-sized mechanical systems, where Al_2O_3 was used as a nanofluid with deionized water (DI). A number of research have proven the heating transfer processes of nanofluid (Al_2O_3) in micro channel sink of heat, however the flow and heat transfer properties do not have well explored because of lack of sufficient experiments data. Temperature and velocity field measurements

in the MCHS are critical for evaluating these heat transfer processes because flow factors determine how well heat travels. The temperature and velocity domain measurements of the MCHS were carefully investigated using methods include laser-induced fluorescence (LIF) and particle image velocimetry (PIV). Because of the large absorption of energy, the use of nanofluids in heat transfer has an improved and good performance when compared to ordinary or basic fluids, so the modification of viscosity or thermal conductivity led to the enhancement of the physical properties of nanofluids, as adjusting the concentration of nanofluid or changing it helped on it. After 20 seconds, temperature and velocity data were collected, ensuring that the recorded temperature and spatial gradient did not alter over time.

Kothari, et al.[2021] [27], Evoluted and propagated of the melt front within the heat sink HS through photographic observation, where to learn more about the, experimental research into the joint effect in the thermal management system through the concentration of nanoparticles and the number of fins in heat sinks based on a phase change material (PCM). Because of their high heat capacity, non-toxicity, high melting point, and chemical stability, PCMs derived from paraffin are frequently employed for the control of heat applications related to electronics. The experiment used three heat sink models (one without fins, one with one fin, and one with three fins) with the same length, breadth, and height ($110 \times 110 \times 27$) mm. As heat sinks, paraffin and aluminum wax were utilized, and Al_2O_3 as a nanofluid with varying percentages of nanoparticles (0, 2, 4, 6 wt%). The highest operating time value was (6470 s) for the traditional heat sink with three fins made of PCM material, and the maximum reduction in melting time was 9%, 13%, and 26% for the heat sink made of NePCM, indicating that NePCM, when mixed with a low value of nanoparticle concentration, is useful for heat sinks with an SPT (Set Point Temperature it maximum operating of electronic devices up to which the electronic devices can work without failure) value. (1.48) is the largest possible improvement

ratio. achieved for SPT of 60 °C and unfinned HS loaded when the quantity of nanoparticles is 2%. The greatest value of the enhancement ratio for the usual pure PCM-based system is determined to be 1.35 and 1.32 for SPT of 65 °C and 70 °C, respectively.

Oguzhan Ozbalci, et al. [2022] [28] Studied the transmission of heat from plate fin and pin fin-type sinks of heat put in an electrical system's water block. The studies were carried out with volumetric flow rates ranging from 100 to 800 ml/min and heat flux levels ranging from 454.54 W/m² to 1818.18 W/m², basic liquid (pure water) and a mass concentration of 0.1% Al₂O₃-H₂O nanofluid were used as a cooling fluid for an heat sink from aluminum with dim. (2.5 × 2.5 × 1) cm, and the maximum thermal improvement was determined by 56.4% for the basic liquid and 70.27% when using of nanofluids by making a similar comparison to the heat sink with pin-fins. The max. heat transfer improvement in comparison to the blank the surface achieved at the base fluid contains roughly 64.25% and the nanofluid contains around 82.8%. The findings revealed that the efficiency was raised by 1.6% when using 100 (ml/min) volumetric flow with nanofluid in the plate, and 1.55% when using 100 (ml/min) volumetric flow in the pin fin, while the efficiency was 1.1% when using 800 (ml/min) volumetric flow for both cases (in plate and pin fin). It was observed the pressure decrease was more than that because of the basic fluid the flow frictions in nanofluid applications. It has been observed that the quantity of pressure drop rises with the influence of both viscosity and the increase in area of the surface when making use of nanofluid. With the increase of the pressure loss was greater than the volumetric flow rate that of because of the basic fluid the friction of the nanofluids.

Tiwary, et al. [2022][29], Studied the apparent flow behavior of nano fluids numerically through a micro-channel when placed in a sink of heat with oblique fins in a Reynold number (Re) range (100 - 300). The researcher presented an experimental and numerical investigation on the performance of thermal fluids by

0.5 - 2.0% of the volumetric concentration of aqueous nanofluids by performing the experiment on two types of heat sinks, an oblique fin heat sink (OFHSMC) under the light of inclination of the fin of ($\theta = 27^\circ$), & a straight fin sink of heat (SCHSMC) with the same hydraulic channel diameter. About the flowing fluid, the RNG-k model was used for simulation in both cyclic and full-field numerical analyses. In comparison to the straight channel sink of heat, the angled fin microchannel encouraged secondary flow, and one of the essential phenomena for increasing heat transfer is the disruption of the a layer that forms a border and the producing whirlpools in the secondary channels. The thermal conductivity of the oblique fin nanofluid sink of heat group is found to be significantly improved. When the concentration of nanoparticles increases, so does the heat transfer coefficient. When $Re = 300$ in the heat sink was found with the inclined fin, this increased the heat transfer coefficient by 2%. When compared to the straight channel heat sink, it works to improve the temperature rate.

The table below (Table 2-2) explains the significance differences between the investigations in this paper.

Table No. (2-2) The comparison between all the studies in the review.

No of Resaarch	Materials	Dimensions	Temp.(in , out)	Efficiency	Velocity	Objective	Limitation
[15]	Aluminum(without nano particles)	Width = 60 cm High = 40 cm Length = 100 cm Type of Fin (HV) & (HLV) Pin fin shape.	Input air (18 – 25) °C	HV\ Low η_{th} HLV\ High η_{th} HV\Nu =11% more than solid fin . HLV\ Nu =21% more than solid fin HV\pressure low than 23% from solid fin. HLV\ low than 19% from solid fin. HV\Low Velo. Vectors intensity HLV\High	Velocity 3 -20 m/s	This study aims to achieve the highest thermal and dynamic performance of the dissipator by implementing the staggered arrangement of the fin arrays.	The researchers limited themselves to finding solutions to the problems of high temperatures, but the effect of time should be considered and the term unstable state should be included in the governing equations, while studying the same problem experimentally and numerically in the case of flow collision.

[16]	<p>1\Extruded uncoated longitudinal fin heat sink</p> <p>2\Extruded coated longitudinal fin heat sink by aluminum nanoparticle</p> <p>3\Rectangular block of commercially available aluminum metallic foam.</p> <p>4\innovative heat sink using water as a working fluid with the velocity.</p>	<p>1\Rectangular block of aluminum metal foam\</p> <p>Aluminum: Surface per volume = 15 (1/cm) PPI = 0.33</p> <p>Weight = 21 g</p> <p>2\ Innovative heat sink \</p> <p>Aluminum metallic foam</p> <p>Dim(9X16X3.5)cm</p> <p>Weight =780 g</p> <p>Dia tube in =19.05 cm</p> <p>Dia tube out=20.06 cm</p> <p>Length = 1.2m</p>	<p>Thermal resistance = 0.29 °C/W</p> <p>power in axial tube = 38 W.</p>	<p>Velo. Of air \</p> <p>Input =1 m/s</p> <p>Output = 3 m/s</p> <p>Velo. Of water =1.17 m/s</p>	<p>The current study evaluates the use of metallic foam liquids in the cooling process of electronic devices, which is one of the modern methods of cooling, and the use of an aluminum-coated heat sink has a higher performance than the uncoated heat sink.</p>		<p>This study suffers from the problem of the high financial cost of using these materials in the process of cooling heat sinks (it cannot be an economical alternative due to its high price).</p>
[17]	<p>1.Aluminum pin – fin heat sink.</p> <p>2.Aluminum plate fin heat sink.</p>	<p>1.Rectangular channel (180 mm width, 80 mm height)</p> <p>2.Dia. of pin-fin= 10 mm.</p> <p>3.plate fin heat sink (spacing of 16 mm).</p> <p>4.Re range(6800- 15100).</p> <p>5.Nu= 9.19</p>		<p>Max. thermal-hydraulic performance = 4.67 at dimple dia. Ratio (D/d)of 0.5.</p>		<p>The presented study explored the performance of pin fin and similar base plate extended turbine under similar operating conditions.</p>	<p>The researchers limited themselves to conducting comparisons and experiments between heat sinks with pin fins and heat sinks with plate sheets, and they did not conduct experiments on more than these two types of heat</p>

		at(pin-fin) 6.Nu=5.1 at (plate fin).					sinks, such as heat sink with micro channels and heat sink with fins and others.
[18]	1\ Nano fluids(AL ₂ O ₃) 2\heat transfer enhancement 3\micro channel heat sink (MCHS)	3-Dim micro channel rectangular shape .Particle size of nano fluid (d = 38 nm) .	T _{in} = 25 °C	The heat transfer performance of Al ₂ O ₃ -water and diamond-water Nano fluids was 21.6% better than that of pure water		This study assesses the 3D numerical simulation of the heat transfer performance of a very small channel heat sink (MCHS) optimally.	-----
[19]	1.Concentrator photovoltaic . 2.Nanoparticles(AL ₂ O ₃ , CuO, SiO ₂). 3.Nanoparticles (PCM). 4.Heat sink. 5.Rectangular container of Aluminum.	1.Two-Dimensional hybrid model consisting of photovoltaic layers. 2.Rectangular CPV-Nanoparticle (L= 100 mm, H= 125 mm) 3.Rectangular container of Aluminum = 3 mm wall thick. .	Al ₂ O ₃ – PCM → 5wt % : T = 12 °C Pure PCM (0 wt T = 20 °C	η _{ele} = 8 % η _{ele} =6.36%		The main objective is to improve the thermal conductivity of the phase change material while reducing the rise in the photovoltaic temperature of the concentrator, in order to obtain the ideal and effective performance.	This innovative CPV Nano particle -PCM system may be thought of as an effective renewable energy source with secure operating conditions for domestic and commercial use.

[20]	<p>1. Closed metal rectangular from copper</p> <p>2. PCMs (AL₂O₃)</p> <p>3. Thermal insulation</p>	<p>L X H (L=3.0) & (H=1.5)cm</p> <p>Plate surface .</p>	<p>T_{in} = 34 °C</p> <p>T_{out} = 4.5 °C</p> <p>(with nanoparticles AL₂O₃)</p> <p>T_o = 23 °C</p>	-----	-----	<p>The study assesses the increase the throughput of the heat sink, it is preferable to use PCM with the highest melting point.</p>	<p>The problem of this study is that it is within the temperatures that are less than (70 °C) and that there are no solutions when the temperature reaches this degree or a degree higher than it.</p>
[21]	<p>1\ Microchannel heat sink Aluminum)</p> <p>2\ Nano fluid (Al₂O₃)</p>	<p>1\ geometric design 3-D nanofluid microchannel heat sink.</p> <p>2\ inlet width (L= 10⁻³ m)</p> <p>3 \ ρ particles = 3970 kg/m³</p> <p>4\ Cp particles = 765 J/kg.k</p> <p>5\ dia of nanofluid particles (d= 13 nm)</p> <p>6\ ΔP = 10 Pa , β= 10⁸ W/m³.k</p>	<p>T_{in}= 300 °K</p> <p>T_{out} = 340 °K</p>		<p>V in = 0 m/s</p> <p>V out = 0.7 m/s</p>	<p>The study addressed the physical problem in (NMHS) Nano fluid Microchannel heat sink.</p>	
[22]	<p>1\ heat sink minichannels with convectional and optimized headers from copper.</p>	<p>1\ Rectangular minichannel heat sink (L= 65 mm, W= 55 mm).</p>	<p>For optimize d header\</p> <p>T_{in}= 316 °K</p> <p>T_{out}= 331 °K</p>	<p>η th= 17%</p> <p>η hy = 41%</p>	<p>Water flow</p> <p>V in= 0.5 L/min</p> <p>V out= 1.5 L/min</p>	<p>The study was keen to discuss the effects of the improved geometry of the head on the performance of the hydraulic heat sink with</p>	<p>Due to limitations in the preparation, the researchers limited themselves to calculating the pressure drop numerically</p>

	<p>2\nanofluids (AL₂O₃—H₂O).</p> <p>3\plexi-glass cover.</p> <p>4\ 2- nozzles (inlet,outlet)</p> <p>.5\heater.</p> <p>6\copper cylinder.</p> <p>7\rubber sheet</p>		<p>For convec-tional header\</p> <p>T_{in}= 318 °K</p> <p>T_{out}= 334 °K</p>			<p>small channels.</p> <p>only.</p>
[23]	<p>1\copper heat sink (In line, Staggered).</p> <p>2\Insulated cover .</p> <p>3\Nanofluid s (water-Ag).</p> <p>4\ micro channel H.S (straight channels).</p>	<p>H.S (bifucation)1</p> <p>Distance between the H.S=0.2 mm.</p> <p>2\Re=1500 .</p> <p>3\HF=40000 W/m2 .</p>	<p>T in = 300 °K</p> <p>T out = 356.3°K</p> <p>Reductio n:</p> <p>sample A (0.01-14.77) °C</p> <p>sample B (0.01-12.72).</p> <p>sample C (0.03 – 14.96).</p>			<p>In this study, the evaluation and comparison of the cooling performance of biological water (nanofluid with silver particles) in three models of heat sinks (with straight channels, staggered fins, and inline fins) from the point of view of the first and second laws of heat transfer.</p>

[24]	<p>1.Graphene nanofluid Particles (GnP).</p> <p>2.Distilled water .</p> <p>3.Nitric acid .</p> <p>4.Copper microchannel heat sink .</p>	<p>1.GnP dia. =25 μm .</p> <p>2.copper heat sink: [L ch= 30 mm, W ch= 0.5 mm, H ch= 5 mm, W fin= 0.5 mm, No. ch= 30] .</p> <p>3.mass flow rate of nanofluid is varied (5 g/s) To (30 g/s) by mass flow meter.</p> <p>4.The viscosity increment with addition of (GnP) is found to be (13. 3 %) higher than water.</p>	The different of temp. between nanofluid inlet and outlet = 10 °C	1. K max (11 %) higher as compared with water.		This study assesses the effect of using nanofluids based on (Gn-f) on the thermal transfer process of electrical and electronic devices.	The study was limited to the heat dissipation of electronic chips, which reached 40 watts only, and the variable flow rate was up to 10 mm / sec.
[25]	<p>1\Plate heater(4 mm thick)</p> <p>2\Copper Oxide (CuO)</p> <p>3\Paraffin wax</p> <p>4\Aluminum nanoparticle</p> <p>5\Phase change material (PCM)</p> <p>6\Heat sink material</p>	<p>1\Heat sink with no fin (HSNF)= (160 X 160)mm</p> <p>2\Heat flux = 1.5→3.0 Kw/m²</p> <p>3\various mass fraction of CuO ($\Phi=0.0\rightarrow3.0$)</p>	$T_{in} = 65$ °C	$\eta = \text{high}$		The aim of the study is to analyze the physical properties of (NePCM) such as latent heat, specific heat, density, thermal conductivity, and viscosity. It also aims to explore the effect of different values of heat flux, nanoparticle concentration and (SPT) on the base temperature with the operating time.	CuO nanoparticle addition that is more than 0.5 significantly reduces HS performance because it causes a significant rise in base temperature and viscosity.

[26]	<p>1\Microchannel heat sink.</p> <p>2\Nanofluid AL_2O_3.</p> <p>3\Laser induced fluorescence (LIF).</p> <p>4\Deionized water(DI).</p> <p>5\Two plano-convex lenses by length (0.25 & 0.5)m.</p> <p>6\Electronic heater.</p>	<p>1\Nanofluids particles size (500 nm).</p> <p>2\ hight (e) & width(W) of the ribs = 0.5 mm.</p> <p>3\Hight(H) of the microchannel = 1 mm.</p> <p>4\Distance between adjacent ribs = 0.5 mm.</p> <p>5\ Thickness(t), depth-wise(z) direction of the microchannel = 1 mm.</p>	<p>$T_{in} = 298$ °K</p> <p>$T_{out} = 327$ °K</p>		<p>Wind speed (in wind tunnel) :</p> <p>$V_w = 5$ m/s</p>	<p>The study was keen to conduct a large-scale investigation of the phenomenon of heat transfer in small channels to obtain high efficiency through a cooling process that is sufficient for continuous use. R Operating precision devices.</p>	<p>The researchers limited themselves to numerical results only, due to the absence of T experimental results.</p>
[27]	<p>1\Aluminum .</p> <p>2\Paraffin wax (H.S from paraffin wax).</p> <p>3\Nano particles (Aluminum Oxid).</p> <p>4\PCM .</p>	<p>Square heat sinks :</p> <p>1\ H.S unfinned (110X110X27) mm³.</p> <p>2\ H.S 1 finned (110X110X27) mm³.</p> <p>& 1 finned from inside dim. (100 L X 5 thick X 20 H)mm³.</p> <p>3\H.S 3 finned (110X110X27) mm³ & dim. H.S from inside (100 X 100 X 22)mm³</p> <p>4\ Dim. Of each</p>	<p>$T_{in} = 60$ °C</p> <p>$T_{out} = 70$ °C</p> <p>H.F (q) = 2.0 Kw/m²</p>			<p>This study assesses the concentration determination of nanoparticles, the HS composition and temperatures on various parameters such as the HS core temperature, the enhancement ratio and the operating time.</p>	<p>The problem of this study is that it applies to electrical devices whose temperature is less than 60 °C during the operating period.</p>

		<p>fin</p> <p>a\ 1_ finned (100X9X20)mm³.</p> <p>b\ 3_ finned (100X3 thick.X20) mm³.</p>					
[28]	<p>1.nanofluid (AL₂O₃)</p> <p>2.water block (pure)</p> <p>3.H.S (Aluminum)</p>	<p>(2.5 X 2.5 X 1)cm</p> <p>1\ plate fin .</p> <p>2\ pin fin .</p>	<p>Heat flux =454.54 W/m²</p> <p>and 1818.18 W/m² .</p>	<p>$\eta=1.6$ at 100 ml /min volumetric flow for plate fin.</p> <p>$\eta=1.55$ at 100 ml /min volumetric flow for pin fin.</p> <p>$\eta=1.1$ at 800 ml /min volumetric flow for both</p>	<p>Volumetric flow rate $\approx 100 \rightarrow 800$ ml/min.</p>	<p>The study aims to develop cooling systems for electronic devices through the use of nanomaterials in cooling different surfaces.</p>	<p>Most of the study that the researchers showed was a numerical study and a little of the experimental study.</p>
[29]	<p>1\Oblique fin H.S micro channel (OFHSMC).</p> <p>2\Water Nano fluids(Al₂O₃) .</p> <p>3\straight channel H.S micro channel (SCHSMC).</p>	<p>◆ Re No range(100-300).</p> <p>◆ The oblique fin :</p> <p>P fin = 2 mm</p> <p>$\theta = 27^\circ$</p> <p>H fin = 1.5 mm</p> <p>W fin = 0.23 mm</p> <p>W ch = 0.5 mm</p> <p>◆ Holes of thermo couple :</p> <p>Dia. = 2 mm</p> <p>◆ Holes of screw:</p>	<p>T water nano fluid inlet = 298 .15 ° K</p> <p>T_{out} = 324. 75 ° K</p> <p>H.F = 64 W/cm²</p> <p>(given at the H.S bottom).</p>			<p>The current study explored the thermal properties of fluids in a tilted fin heat sink with nanofluids at different concentrations starting from 0.5% to 2%.</p>	<p>-----</p>

		<p>Dia. = 4 mm</p> <p>◆ The straight H.S: H = 1.5 mm</p> <p>Space between channels= 0.5 mm</p> <p>L(H.S)=W(H.S)= 25 mm .</p> <p>◆ Holes of screw:</p> <p>Dim. = 4 mm .</p>					
--	--	---	--	--	--	--	--

2.4 Scoop of the present work :

From a summary of the literature, it can be summarized as follows:

- 1- According to the literature review, previous researchers have reviewed, designed and tested many forms of heat sink.
- 2- Adding nanomaterials increasing heat transfer parameters.
- 3- There are shortage of experimental data and able of design correlations concerning the packing of nanomaterials(as governing equations).

The design of the fins has certain limits that cannot be exceeded, such as dimensions (dimensions of the heatsink and fins), and these dimensions are affected by the dimensions of the device.

As for the nanomaterial (liquid), it is considered a toxic substance and may be affected or interact with the metal of the heat sink or form deposits that will be harmful in the future.

Therefore, a previously unexplored method was proposed in the field of manufacturing and arranging fins, which is a new, pioneering and unique method in the field of designing heat sinks. A method of filling the fins with solid, non-liquid nanomaterials that have a very high thermal conductivity of more than $3500(\text{W}/\text{m}\cdot^{\circ}\text{C})$ was also proposed. .degrees, and these are considered nanochannels to withdraw heat from the hot base towards the surface area for heat exchange.

Chapter Three

Numerical Analysis

Chapter Three

Numerical Analysis

3.1 Intruduction

Numerical simulations allow complex phenomena to be analyzed without resorting to expensive prototypes and difficult experimental measurements. Over the past few years, computational fluid dynamics has become one of the most powerful and useful tools for forecasting by the behavior of turbulent air vortices that form between the pin fins of the heat sink. Any modification required in the design can be made using software Ansys (R18.1) available. Hence, the repetition of these the operation allows achieving optimal design at lower operating cost. Therefore, full numerical analysis was used in this work to simulate the flow in Pin-fin heat sink model and predicting the improvement of heat transfer inThis state is between the external environment.

3.2 Numerical Side Study \ Geometry of Simulated heat sink :

In order to obtain better results for the transfer of heat from the heat sink to the external environment, we must study the subject in all respects, and here we will work to find the best results through the simulation program (Ansys R18.1), which in turn will be a good and effective test to give results by entering similar values of the dimensions of the heat sink to the program (length, width, base thickness of the heat sink , number of fins, fin diameter, height of the heat sink). Enter the velocity of the air entering to the H.S and the temperature relative to the base of the H.S that is in direct contact with the electric heater.

Here it should be noted that all models in the program have been designed in accordance with the real dimensions, in order to ensure obtaining results that are closer to reality.

The models entered into the simulation program are (In line , Staggered , Zigzag) which are the same models on which practical experiments were conducted in reality, and we

will come to mention all the cases that the simulation program showed us in terms of temperature distribution, air velocity, Nu number, and heat transfer coefficient (h).

In the beginning, the dimensions of all models on which the simulation program tests were conducted must be mentioned, and the table below shows that:

Table (3 - 1), The Dimensions of the heat sinks

Sample	Length(mm)	Width (mm)	Thickness of base (mm)	No. of Fins	Highest of HS(mm)
In Line	81	67	3	120	14
staggered	81	67	3	120	14
zigzag	81	67	3	120	14

3.2.1 Governing Equations

The Navier-stokes equation and the following conservation equations were used to simulate the nanofluid thermal performance. [36]

Continuity equation:

$$\rho \left(\frac{\partial u}{\partial x} + \frac{\partial u}{\partial y} + \frac{\partial u}{\partial z} \right) = 0 \quad (3.1)$$

Momentum equation in 3D:

$$\begin{aligned} \rho \left(\frac{\partial u}{\partial x} + \frac{\partial u}{\partial y} + \frac{\partial u}{\partial z} \right) &= -\frac{\partial p}{\partial x} + \mu \left(\frac{\partial^2 u}{\partial x^2} + \frac{\partial^2 u}{\partial y^2} + \frac{\partial^2 u}{\partial z^2} \right) \\ \rho \left(\frac{\partial v}{\partial x} + \frac{\partial v}{\partial y} + \frac{\partial v}{\partial z} \right) &= -\frac{\partial p}{\partial y} + \mu \left(\frac{\partial^2 v}{\partial x^2} + \frac{\partial^2 v}{\partial y^2} + \frac{\partial^2 v}{\partial z^2} \right) \\ \rho \left(\frac{\partial w}{\partial x} + \frac{\partial w}{\partial y} + \frac{\partial w}{\partial z} \right) &= -\frac{\partial p}{\partial z} + \mu \left(\frac{\partial^2 w}{\partial x^2} + \frac{\partial^2 w}{\partial y^2} + \frac{\partial^2 w}{\partial z^2} \right) - g \end{aligned} \quad (3.2)$$

Energy equation:

$$\rho \cdot C_p \cdot \left(u \frac{\partial T}{\partial x} + v \frac{\partial T}{\partial y} + w \frac{\partial T}{\partial z} \right) = k \cdot \left(\frac{\partial^2 T}{\partial x^2} + \frac{\partial^2 T}{\partial y^2} + \frac{\partial^2 T}{\partial z^2} \right) \quad (3.3)$$

Where (u) is velocity vector (m/s), (ρ) the nanofluid density (kg/m³), (P) is the static pressure (Pa), (C_p) the nanofluid specific heat at constant pressure (J/kg. K), (T) temperature of flow (K), and (k) is the nanofluid thermal conductivity (W/m. K).

3.3 Mesh Generation

From the previous sections, in order to perform numerical calculations the representative domain of the problem under consideration must be divided into several small subdomains called mesh or grids. The studied problem was analyzed for an air flow system on the surface of a pin-finned heat sink when the base temperature and the inlet air it constant.

In this thesis To facilitate data management, the appropriate grid for the state of air turbulence was applied to the pin fins of the heat sink, where a simulation program (3D) was used to find out the areas where the air turbulence is so great that it needs to distribute nanomaterial inside the fins for the purpose of accelerating the exchange process. Thermal temperature between the heat sink and the external environment.

3.4 Mesh Topology

Through the process of topological construction, it is possible to know the areas where there are gaps and problems in the geometric shape of the heat sink in terms of the distribution of fins from the models presented in this study.

In this process, the areas that are somewhat weak in the heat exchange process (through the presence of a certain gap or an incorrect geometric arrangement of the fins) will be identified, and some problems from this aspect can be corrected.

3.5 model /In Line

When conducting the test on this model by Ansys (R18.1)[40], as mentioned earlier, the basic special data must be entered in terms of temperature and air velocity entering the dispersant, as the temperatures start from 60 °C and reaches a maximum of 95 °C in

reality. The Figure shows how the temperatures are distributed in the In line heat sink, where we notice a significant rise in temperatures at the base of the heatsink, especially at the edges of the base, because the base is in direct contact with the heatsink (separated by thermal silicone only), also notice the transfer of heat from the base to the fins (but by the effect of the air pushed from the fan that is above the diffuser) we find that the temperatures in the fins are lower than the temperatures in the base, up to the upper ends of the fins we find that they are the lowest region in temperature, and as shown in Figure (3 – 1).

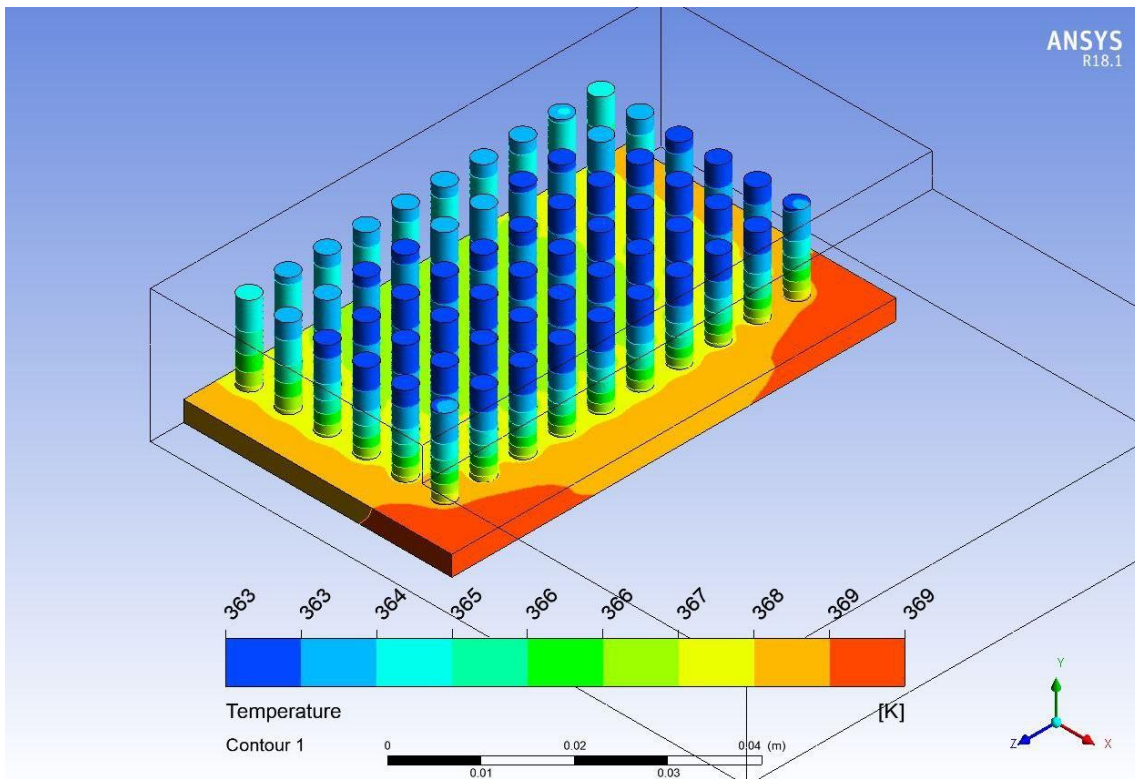


Figure (3 - 1) represents the temperature distribution of the heat sink (Inline) in the simulation program.

Where the temperatures in the base range between (367- 369) ° K i.e. equal to (93 - 95) °C and it is, as we mentioned, the region with the highest temperature, while we notice that the fins have the lowest temperature and range between (363 - 366) ° K which is equal to (90-93) °C.

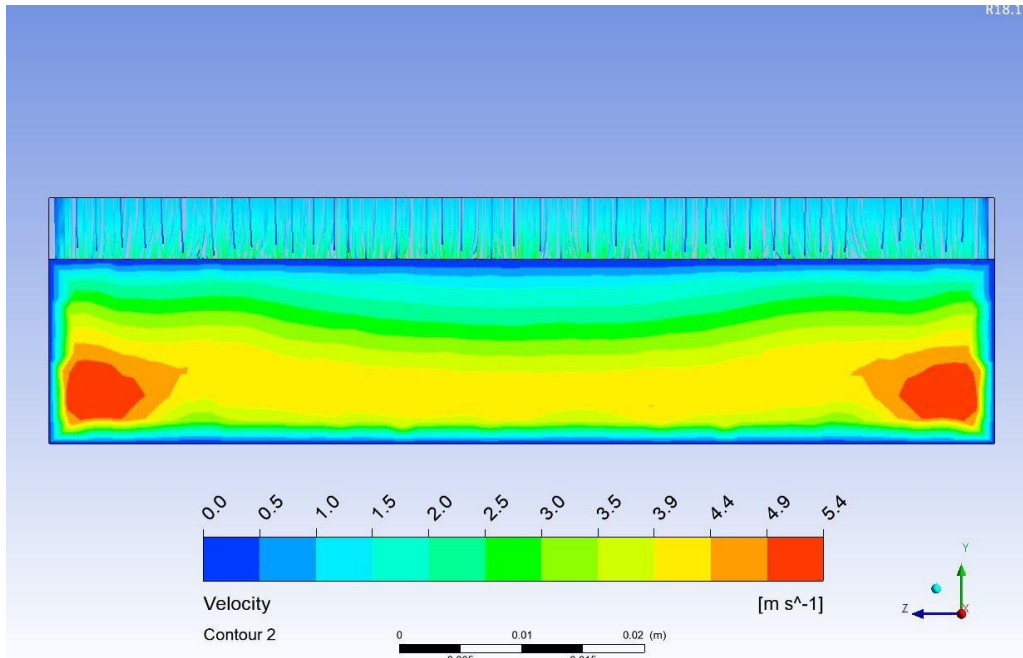


Figure (3 – 2) represents the speed of the air entering the heat sink and its effect on temperature.

In Figure (3 – 2), we notice that the effect of the speed of the air entering the fan, which is confined by the duct (where the air exits only from the two side openings through the heat sink) is at several different speeds, as it starts at a speed of 0.8 m / s and increases until it reaches 1.5 m / s, as a maximum in reality. Because of the speed of the incoming air, we find that the areas of temperature distribution in the parts of the heat sink differ greatly between the base of the heat sink and the fins, as the speed ranges between (0.0-5.4) m/s.

In Figure (3 – 3) below, we also notice the incoming air flow lines at the required speed when entering from the top and exiting from one of the side openings, where we notice here how hot the air (which is in red) is at the edges of the lower base of the heat sink, and the air flow

lines when entering It is the lowest temperature of the outside air due to the collision of cold air particles with the hot fins, and here is a heat transfer process from the hot body

(the heat sink) to the outside environment, and the speed here ranges between (0.0-6.0) m/s.

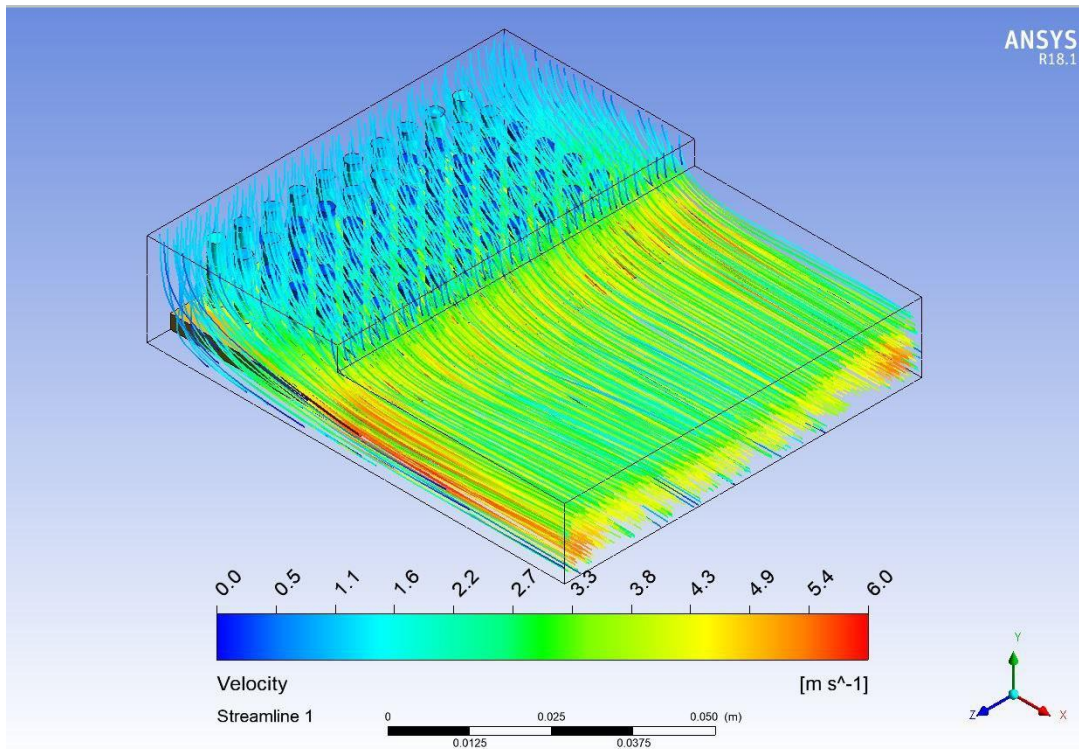


Figure (3 – 3) represents air flow lines at different velocity.

3.6 Model Staggered :

This model is different from the model In Line in terms of the arrangement of the fins as shown in the figure (3 – 4, 5) below, and when the simulation program is running for this model with the entry of all data and special values (B.C) of temperature, speed and temperature of the incoming air, we find that the temperature distribution differs from the first model in the base and fins area, where The temperature in the base is the highest in the disperser and reaches in the base and fins area, as the temperature in the base is the highest in the disperser and reaches 368° K i.e. 95° C and there is no difference in temperature in the middle or the edges of the base . In the Stagg diffuser fins.

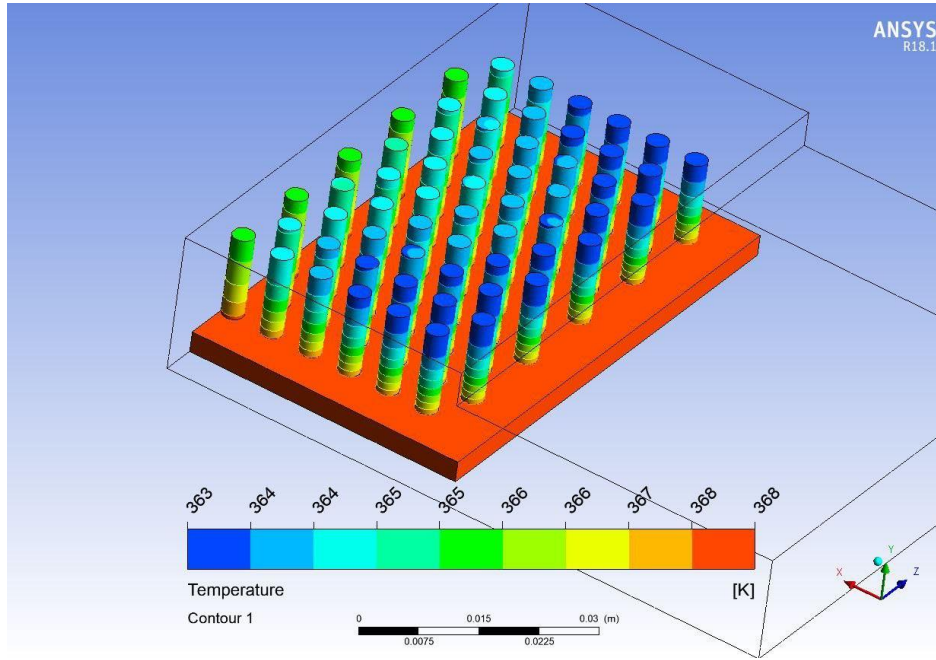


Figure (3 – 4) represents the temperature distribution in the heat sink.

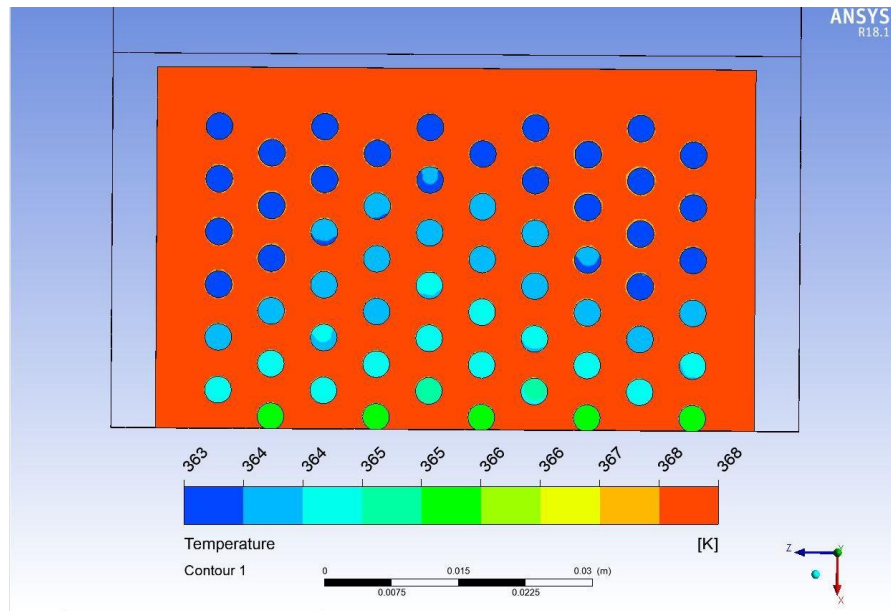


Figure (3 – 5), represents a vertical show the distribution of temperature for Stagg. heat sink.

In Figure (3 – 6), we notice that the speed of the air entering the disperser through the fan greatly affects the distribution of temperatures in the surfaces of the disperser, and we

note here that the maximum speed affecting the temperature in the base reaches 4.6 m / s , which are at the base edges, then gradually decrease until they are in the fins, which are less than what they are in the base.

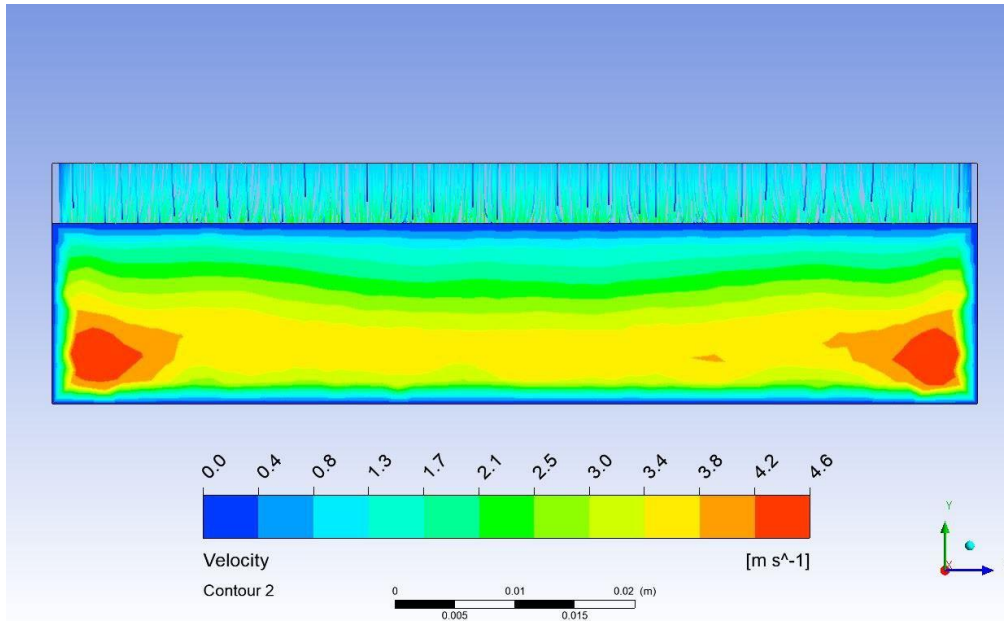


Figure (3 – 6) Represents the effect of air velocity on the heat sink Staggerd.

As for the image below, Figures (3 – 7), it shows the distribution of a Nu number on the areas of the disperser and differ from one region to another, where we note that the Nu in the lower base of the disperser is less than in the fins. The fins also have a Nu number that differs from one fin to another, so we notice that the fins that are at the edges of the diffuser (on the side where the air exits from the duct) are less than the Nu number on the fins in the middle of the diffuser, because the fins that are in the middle have a coefficient The heat transfer is higher than in the edges, through the intense air vortices in the middle of the disperser.

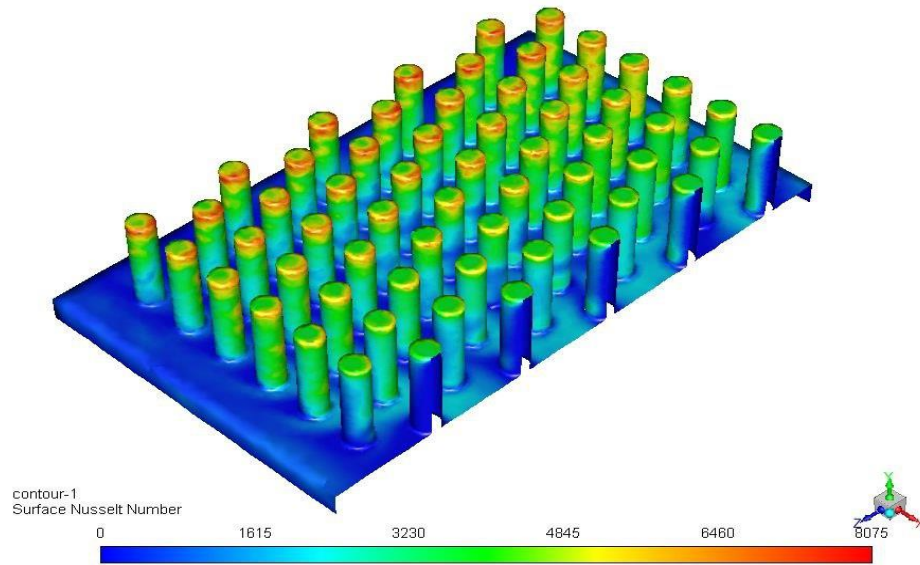


Figure (3 - 7) represents the distribution of a Nu number on the scattering surface Stagg.

Chapter Four

EXPERIMENTAL WORK



CHAPTER FOUR

EXPERIMENTAL WORK

4.1 INTRODUCTION

According to the review work, it has been seen that no studies have been published on nano practical packing on cooling the CPU technique. The previous studies, as mentioned in the literature review, gave a clear indication of the possibility of improving the performance of the heat sink withpin fin using nanomaterials of various types, and the presented study refers to the use of a nanomaterial (Multi Wall carbon Nano Tube) or in short called (MWCNT) used as a filling inside the fins, and the following is a breakdown of the work sections for this study.

4.2 Experimental Rig

The heat dissipation system that was manufactured consists of a heat sink, an air duct, sensors to measure air temperatures at entry and exit, a small air fan (to push the air), thermal silicone material, a layer of thermal insulation , a voltage regulator, an electric heater, and a device. Fan speed control, data logger, computer. Figure (4-1) and (4.2 A,B) show the schematic and photograph view of the parts of system respectively.

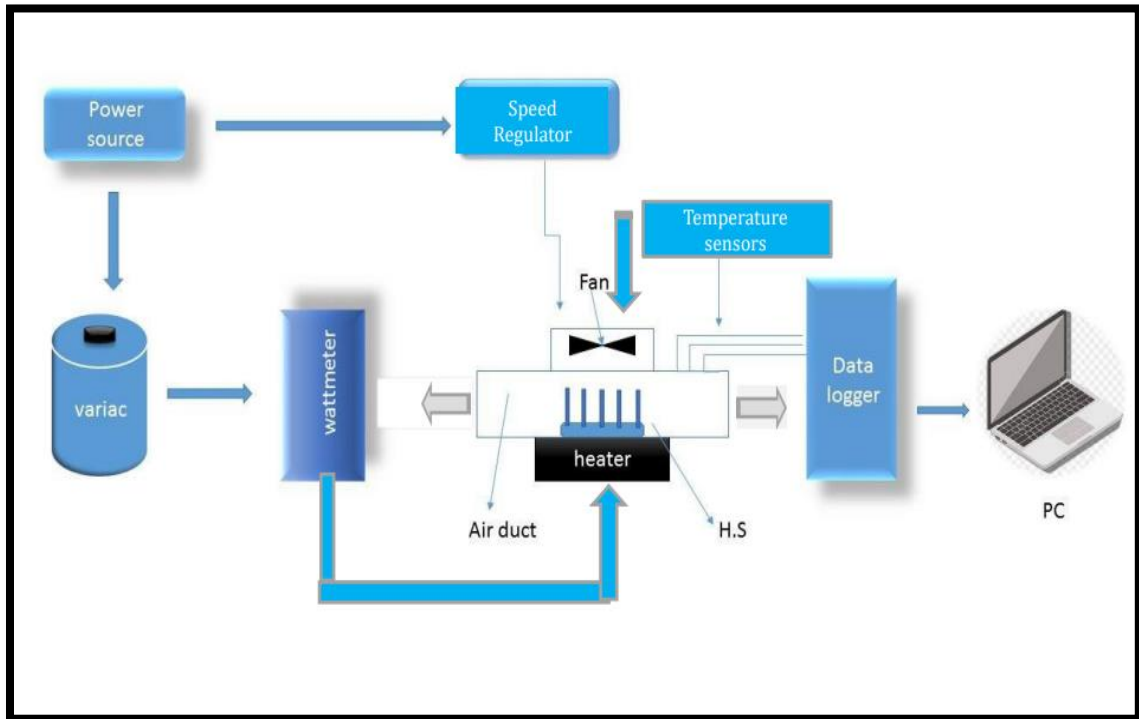


Figure (4.1), Schematic diagram of the parts of the heat dissipation system.



Figure (4- 2, A), photograph the parts of the system.

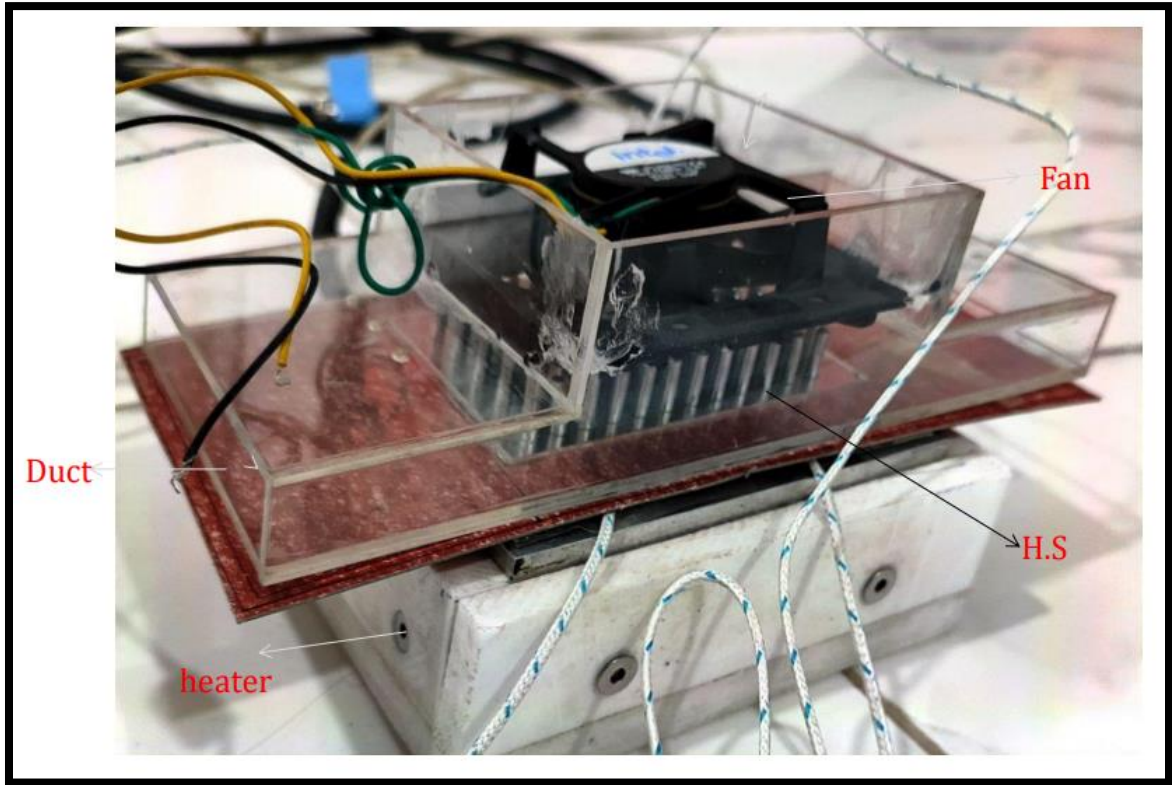


Figure (4- 2, B) The experimental rig.

In general, the main parts of the experimental rig (test devices) can be classified into:

4.2.1 Heating unit:

This unit is responsible for heating the test sample to the required temperature in a constant manner. It consists of:

electric heater: a heater (Flat Plate) has dimensions of (98×98) mm and works with AC (220 volts) as shown in Figure (4-3).



Figure (4-3) Electric Heater.

4.2.2 Voltage Regulator (Variable Transformer):

It is a device used to control the voltage (voltage regulation) given to the heater, through which the temperature to be heated can be controlled. It is of a type (HSN 0103 220 – 250 V, 50- 60 Hz) and as shown in Figure (4-4).



Figure (4-4) The Variable Transformer

4.2.3 Watt meter (Clamp meter)

It is a instrument for measuring the amount of watts entering the heater, through which the amount of watts supplied to the heater is known, and it connects the voltage regulating device and the heater. And the shape. Figure (4-5) show the types of wattmeters used in the experiment.



Figure (4-5) Digital oveo meter.

3.2.4 Air handling unit (Fan)

Supplying the system with the necessary air for the purpose of cooling the heat sink that is on the heater. This unit consists of fan it's used to cool the heat sink in regular computers (Desk top), It is of the type (Intel \ E18764-001), its speed ranges between (0.5 - 1.5 m/s) and it has dimensions of (97×73) mm, as shown in the figure (4-6).



Figure (4-6) Fan of cooling.

4.2.5 Fan Speed Regulator

It is used for the purpose of knowing the speed of the fan being used (related to it) by controlling the power that is given to the fan, as it works with alternating current 220 volts and is equipped with an electrical transformer (12) volts, as shown in figure (4-7).



Figure (4-7) Fan speed regulator

4.2.6 The Duct of air

It is an air duct made of transparent plastic called (acrylic) and its purpose is to make the air enter from one hole (air intake hole) by means of the fan, and exit from sides

with placing thermal sensors in each direction for the purpose of knowing the temperature of the outside air Its dimensions (mm), are as shown in the Figure (4-8) below, and figure (4-9) show the locations of the thermocouples on the air duct, and Figure (4-10) it's a photograph to the air duct.

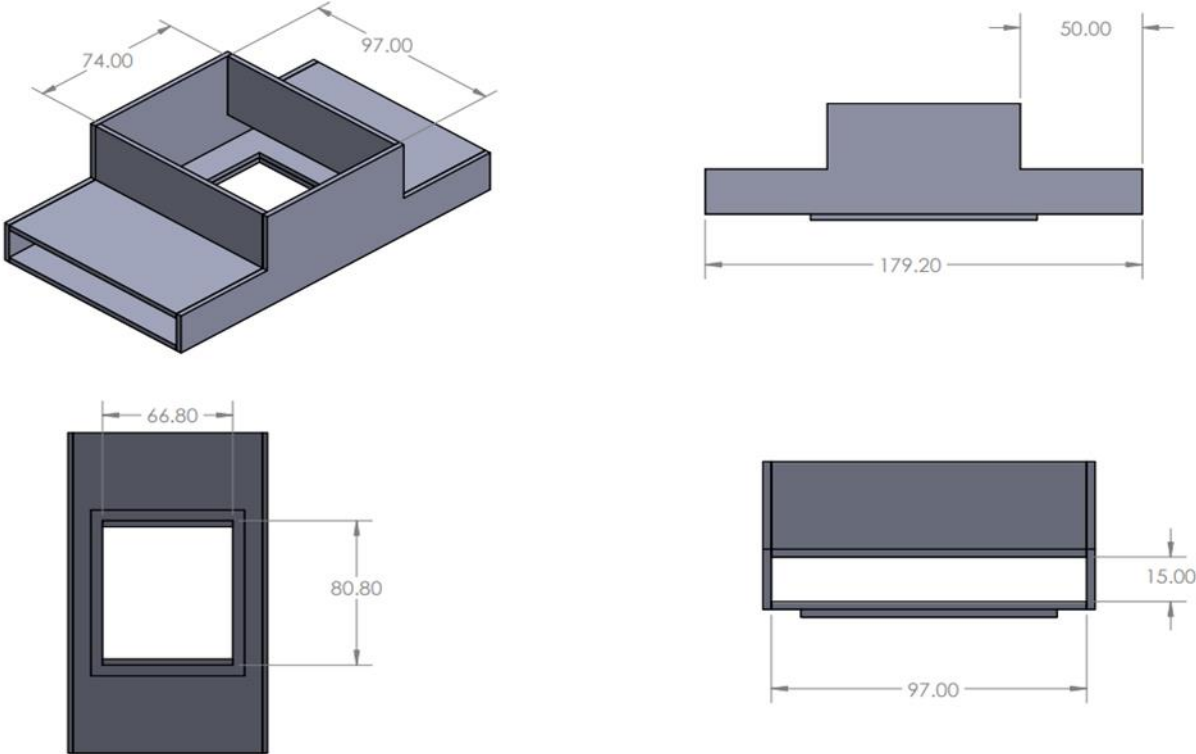


Figure (4-8), The duct with all dimensions (mm).

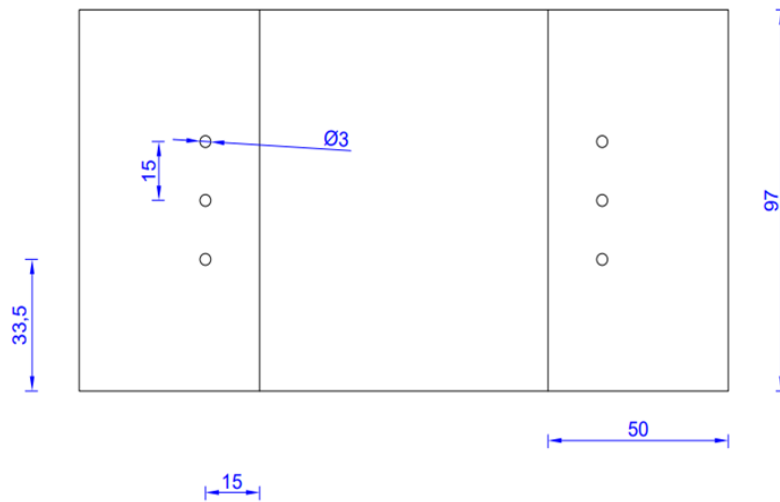


Figure (4-9) location and dimensions of thermocouples holes in the duct (mm)

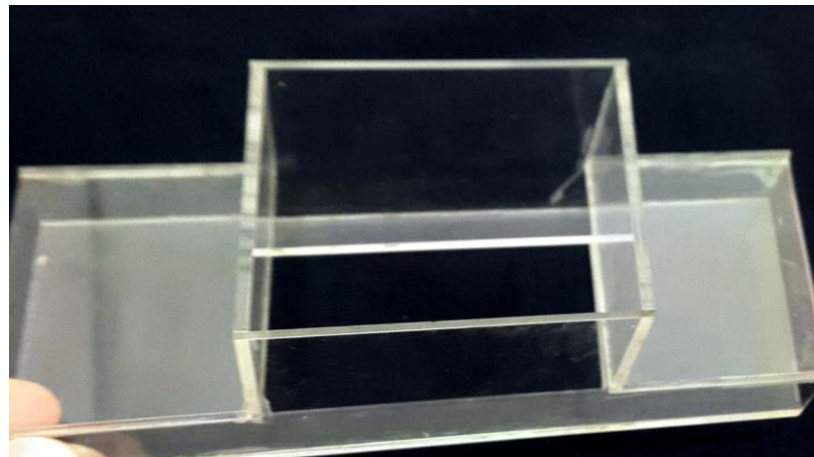


Figure (4- 10), The air duct

4.2.7 Thermal silicone

It is a material with low thermal resistance and high conductivity for superior heat transfer. It is a kind of paste placed between the surface of the heater and the heat sink. Its purpose is to assist in cooling by dissipating heat and not storing it on the surfaces of the heatsink. It is of a type (thermal grease HY 400) Figure (4-11).

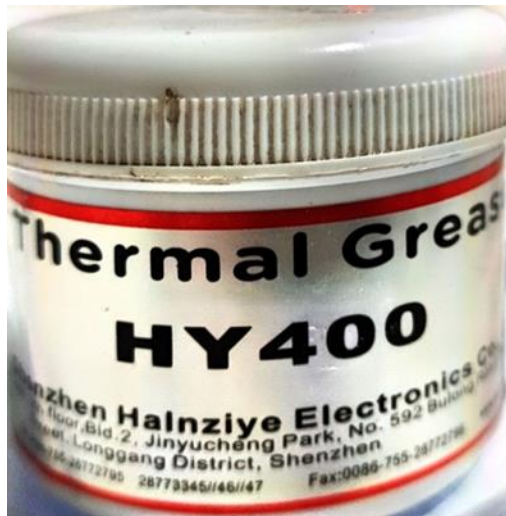


Figure (4-11) Thermal silicone.

4.2.8 Insulating material

It is a heat-resistant asbestos material that is placed between the plastic duct and the electric heater for the purpose of preserving the duct from exposure to melting due to the high temperature. Its dimensions are (185 × 119) mm,

as shown in the figures (4-12) .

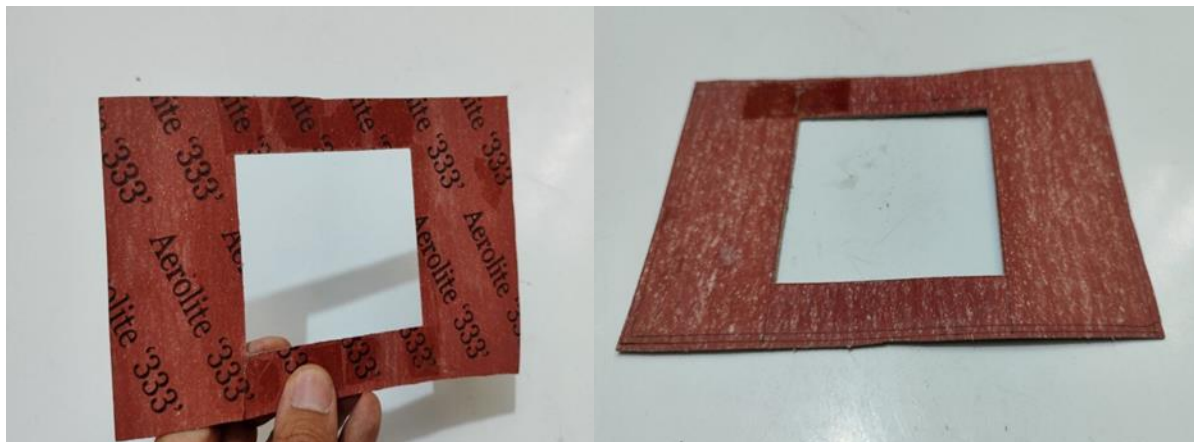


Fig (4-12) The Insulating material.

4.2.9 sensitivity unit

This unit is responsible for knowing the temperature of the heat sink and the base of the heater and knowing the air temperatures at entry and exit, in order to know the difference in temperatures.

This unit consists of:

4.2.9.1 Datalogger

The 8-channel data logger (fig 4.13), with the following parameters, was used:

1. Eight-channel data loggers for thermocouples.
2. Supports all common forms of thermocouples.
3. Measures from -270 to +1820 °C.
4. High resolution and accuracy (For common K type thermocouples, the TC-08 can sustain a resolution of 0.025°C, over a range of -250 to +1370°C).
5. Fast sampling rate up to 10 measurements per second.
6. The USB interfaces.
7. Pico Log is used for Windows data logging applications.

The data logger is directly attached to the PC with a USB link, where the thermocouple reads directly on the PC.



Figure (4-13) The Data logger.

4.2.9.2 Thermocouple

It is of type (K-Type) , (Nickel Chromium) Calibrated thermocouples with extension wires (RS component Ltd Nothants, UK).

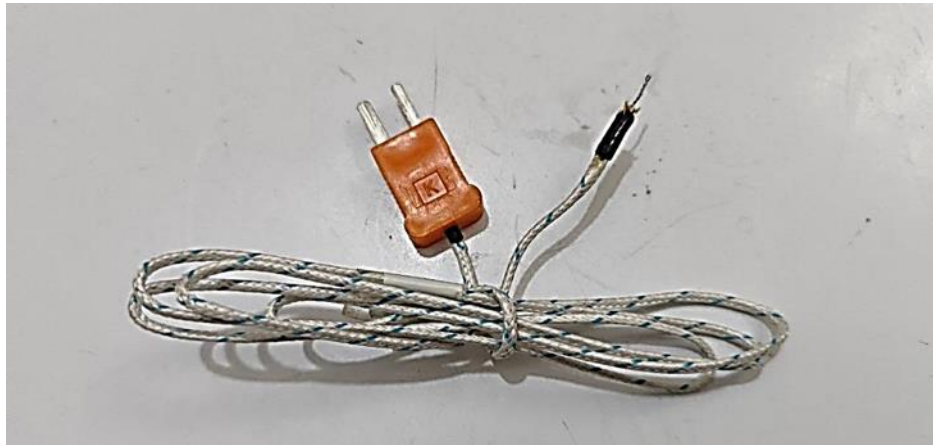


Figure (4-14) K - Type Thermocouple.

Where the thermocouple is connected directly with the data logger device as shown in the Figure (4-14), the data logger device is also connected directly to the computer (PC).

Thermocouples are used in most applications, due to their high corrosion resistance. In addition, it has a wide operating temperature range.

The qualitative specifications of this type are as follows:

Temperature Range

- 1\ Thermocouple grade wire - 270 To 1260 °C .
- 2\ Extension wire grade 0 To 200 °C.
- 3\ Melting point 1400 °C.
- 4\ Special limit of error (± 1.1 °C OR 0.4 %

4.2.9.3 Digital Anemometer

This device used to measure the average air velocity at inlet and outlet of the air duct and its content from fan with digital readability as shown in Figure (4- 15). When the air comes inside the duct , it is necessary to know the speed of the air to need of cooling the heat sink. The air at exit has temperature more than at inlet, because the air takes the heat from the heat sink to the out.



Figure (4- 15) Digital Anemometer

4.3 XRD Test of Aluminum material :

Before that, to check and test the metal of model (heat sink), by XRD test in sample examination office at (Al-Kufa University), this is to ensure the metal is from Aluminum or not . The test includes the classic model too. The result of this test gives us a good sign that the metal is Aluminum as shown below.

Peak Search Report (10 Peaks, Max P/N = 47.0)								
[diwani#1#20230128-033909_200.mdi] XRD SSC 30KV/20mA Slit:1deg&1deg&.2mm Monochromator: ON Ts-Td 200								
PEAK: 15-pts/Quartic Filter, Threshold=0.0, Cutoff=0.1%, BG=1/2.8, Peak-Top=Summit								
2-Theta	d(nm)	BG	Height	I%	Area	I%	FWHM	crystal sizeXS(nm)
37.222	0.24136	0	12	0.1	259	1.4	3.669	2
38.403	0.2342	0	398	4.5	884	4.9	0.378	24
39.592	0.22744	0	11	0.1	234	1.3	3.616	2
43.934	0.20592	0	15	0.2	254	1.4	2.879	3
44.63	0.20287	0	1143	12.9	2053	11.4	0.305	31
45.195	0.20046	0	15	0.2	328	1.8	3.717	2
64.412	0.14453	0	61	0.7	1047	5.8	2.918	3
65.069	0.14323	0	8837	100	18005	100	0.346	30
65.806	0.1418	0	59	0.7	1209	6.7	3.484	3
77.553	0.12299	0	52	0.6	1096	6.1	3.583	3

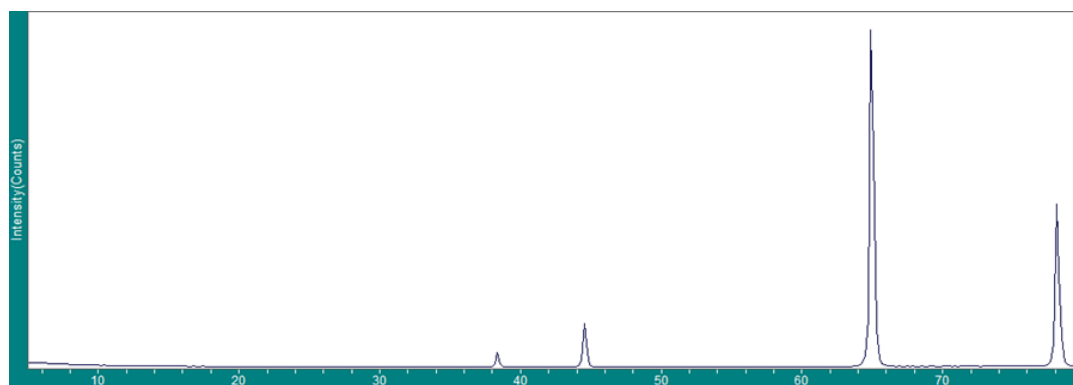


Figure (4-16), XRD Diagram test of aluminumme.

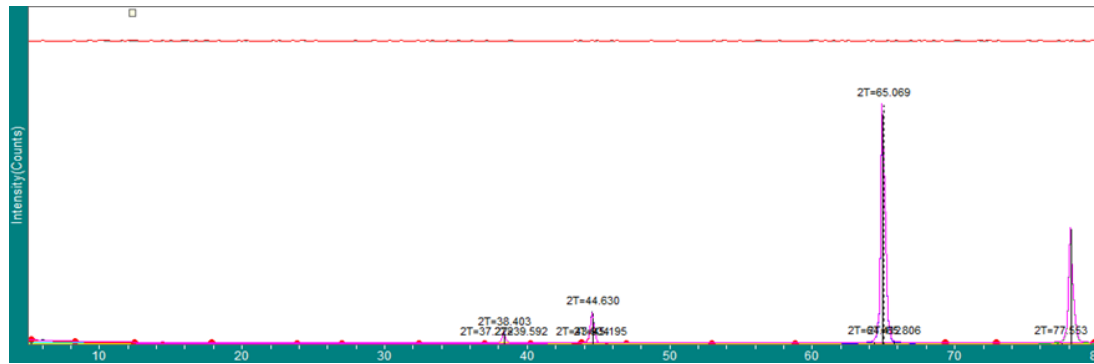


Figure (4-17), XRD Diagram test of aluminum.

4.4 Testing devices

4.4.1 Practical test form

The important details of the practical test form consist of

A- The heat sink / consists of four models

1. Heat sink (classic) type.
2. Heat sink (In Line) type.
3. Heat sink (staggered) type.
4. Heat sink (zigzag) type.

Here, it should be noted how the dispersants are manufactured in the presented study (except for the classic dispersant), which was manufactured as follows:

1. Supplying an aluminum sheet that conforms to the specifications of the dispersant manufactured by the company, with a thickness of (3) mm.
2. Set the dimensions (height and width) of the scatterer with the same dimensions as the classic scatterer.
3. The holes were made in the aluminum plate in the blacksmithing and welding workshop of the Holy Shrine in Najaf.
4. The work of 3 models of dispersants (In line , Staggered , Zigzag) with the same dimensions of length and width.
5. All forms contain (120) pin fin, and the difference is in the arrangement of the fins arrays only.

The following is a detailed diagram with a picture of each type of heat sink, according to the above sequence:

Heat sink type (classic)

It is the dispersant used in computers of the type (Desk Top), made of aluminum, but this model is somewhat large compared to other models, so a large section of the fins

in it was cut in order to make the surface area equal to other models, and the Figures below (4-18) and (3- 19) show the shape of the diffuser in its case

Regular before cutting and after cutting

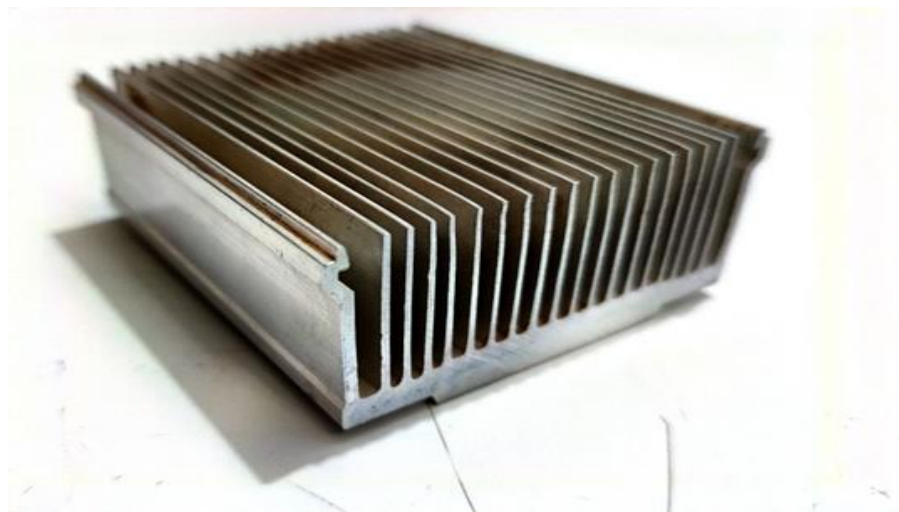


Figure (4-18) shows the heat Sink Classic before cutting.

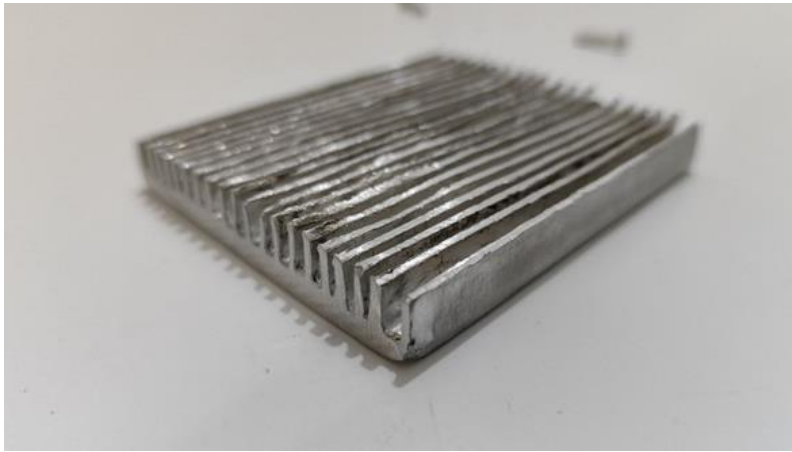


Figure (4-19) shows the shape of the classic scattering after cutting

and the figure (4-20), explain the dimension of the heat sink (Classic type) after cutting.

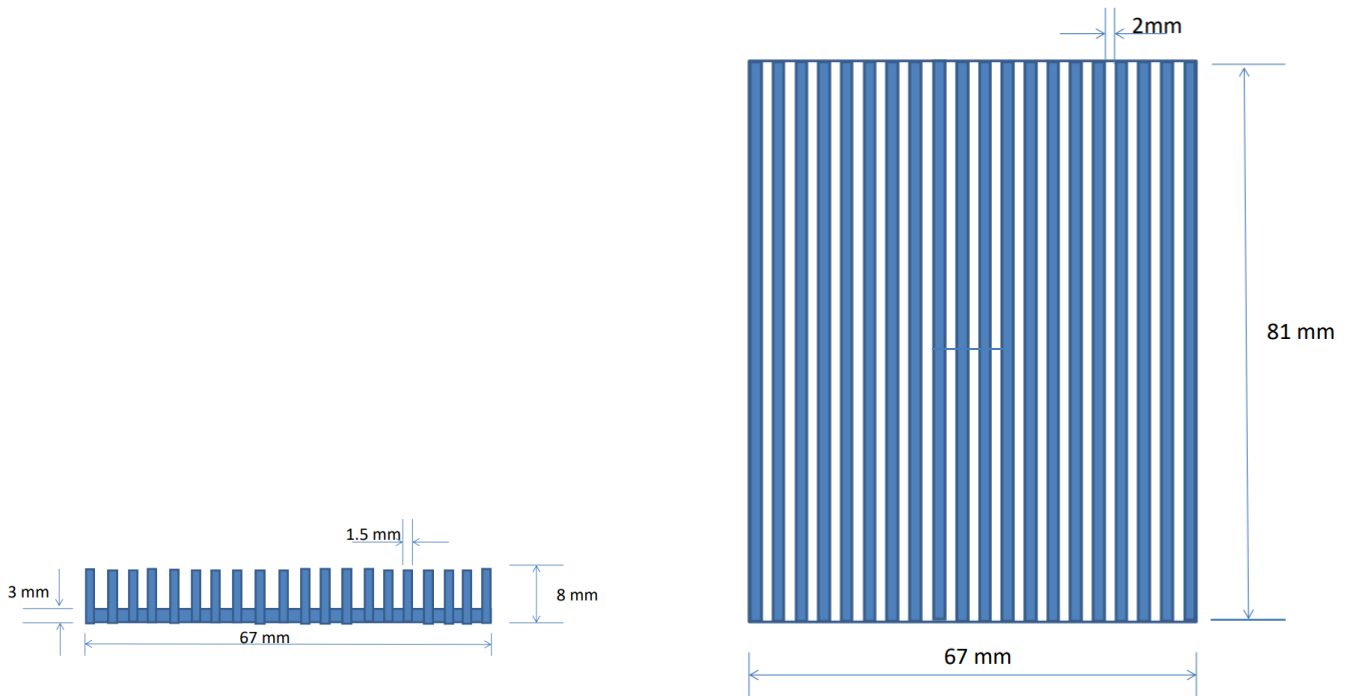


Figure (4-20), The Dimensions of Classic heat sink (after cutting).

1. Heat sink type (In Line) as in the figure (4-21).

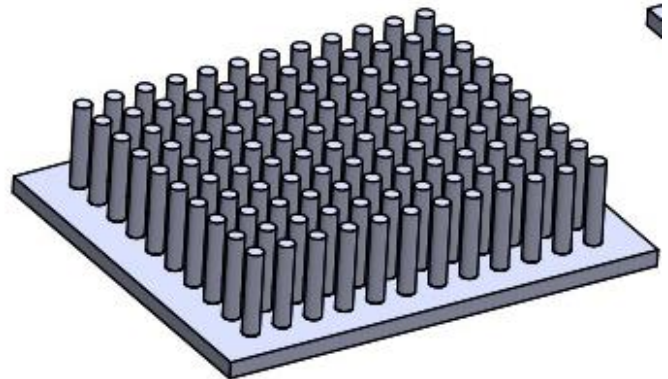
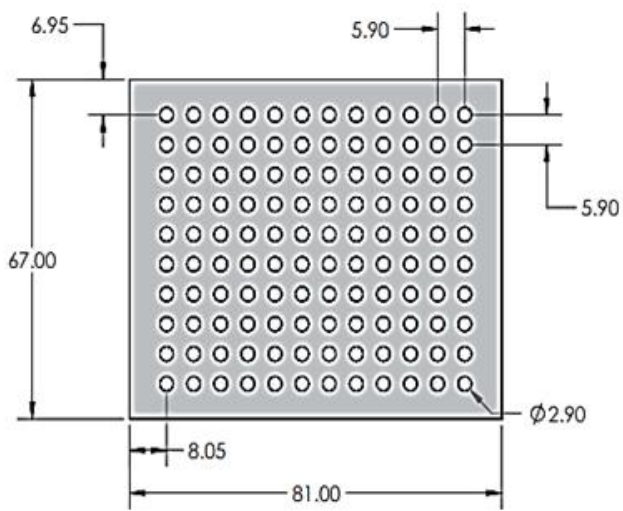
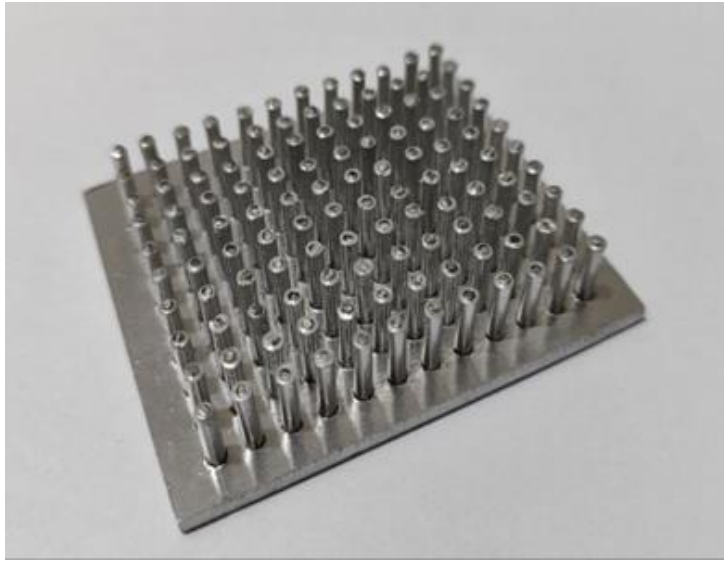


Figure (4-21) shows the type of heat sink In Line with Dimensions (mm)

2.heat sink type (staggered) with dimensions as in the figure (4-22).

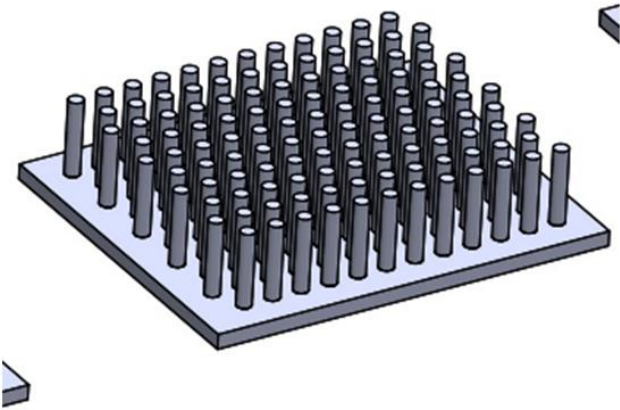
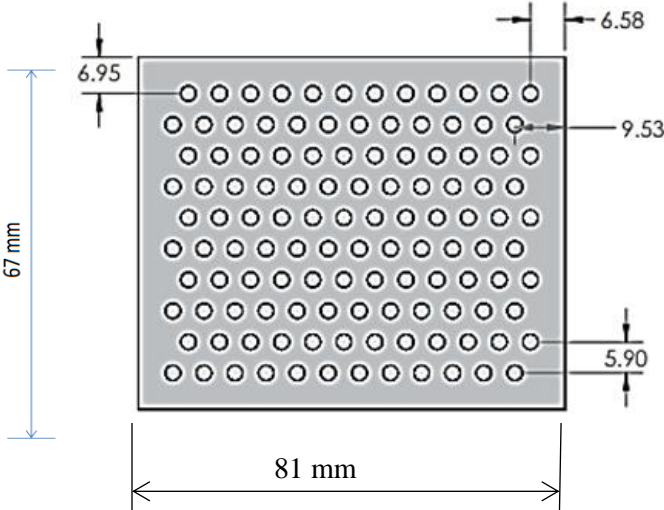
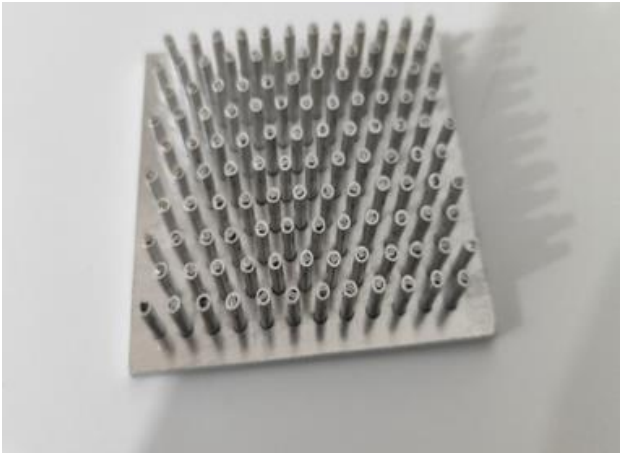


Figure (4-22) shows the type of heat sink staggered with Dimensions (mm).

3.Heat sink (zigzag) type as shown in figure (4- 23) below.

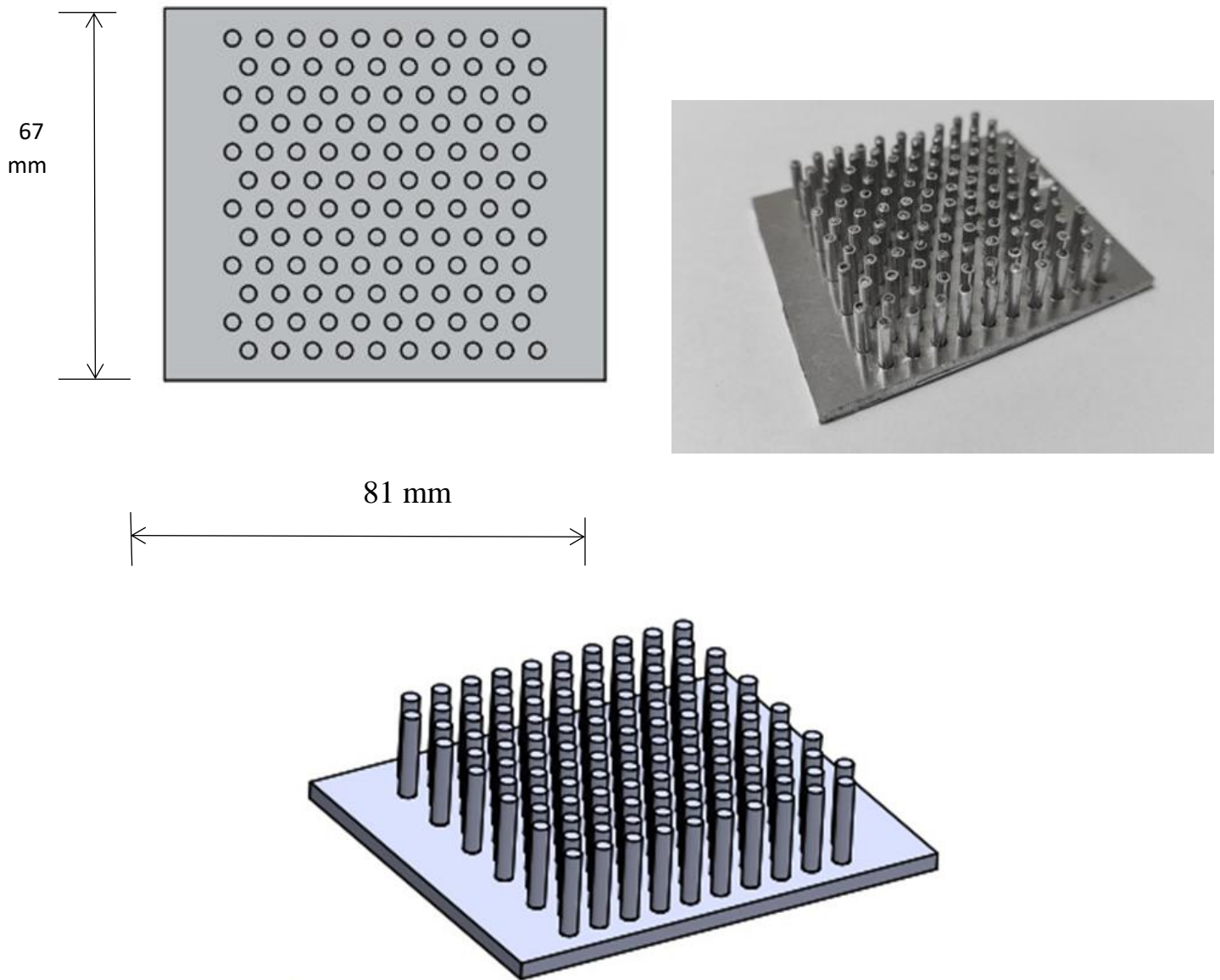
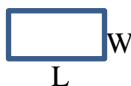





Figure (4-23), Heat sink (zigzag) type.

Table No. (4-1) shows the dimensions, number of fins, and geometric shape of the said dispersers.

HS	Classic	In Line	staggered	zigzag
Area (mm ²)	21252.6X10 ⁻³	21252.6X10 ⁻³	21252.6X10 ⁻³	21252.6X10 ⁻³
FinType	Straight	Pin Fin	Pin Fin	Pin Fin
Dim. Of Fin(mm)	L=81 W=5 	L=14 D = 3 	L=14 D = 3 	L=14 D = 3 
Nu. Of Fins	20	120	120	120
Thick of Base (mm)	3	3	3	3

4.4.2 - Measuring devices (Instrument)

To know the air temperature at the entrance and exit from the sides airway (Made of translucent plastic) which passes through the fins of the heat sink, there must be devices commensurate with this work, including thermocouples, which are very important in measuring and knowing temperatures. The thermocouple used in this study is of the type (K-Type) which is used in most applications because of its high corrosion resistance in addition to its wide operating temperature range.

Where a thermocouple has been placed with six doubles Type of (K-Type) In the air outlet area and installed on both sides of the air duct Where the airway wall was perforated with six holes to fix it, the diameter of the hole is (3) mm. These sensors are directly connected to the previously described data reader device, which is also directly connected to a device (PC) in order to record all readings and confirm them, while keeping a copy of the charts for practical experiments. The thermocouple was placed between the surface of the electric heater and the base of the heat sink, in order to measure and know the temperature of the surface of the heater and the heat sink together, and it is also connected directly to the data reader device.

In order to know the ambient temperature (room), a mercury thermometer of the very sensitive type was used. Its purpose is to know the temperature of the air entering the airway and to take the temperature difference at entry and exit.

The thermocouple was calibrated as follows:

Calibration method: Thermometer and thermocouples were put in ice cup as a first point for calibration. The calibration carried out under five variat temperature value. Temperature values of thermocouples were recorded from data logger and temperature of thermometer recorded directly. The temperature value of ice water warm up gradually by using a water heater. Approximately the temperature different between of thermometer and thermocouples was 0.5 °C at the most point as seen in the curves in Figure (4- 24) .

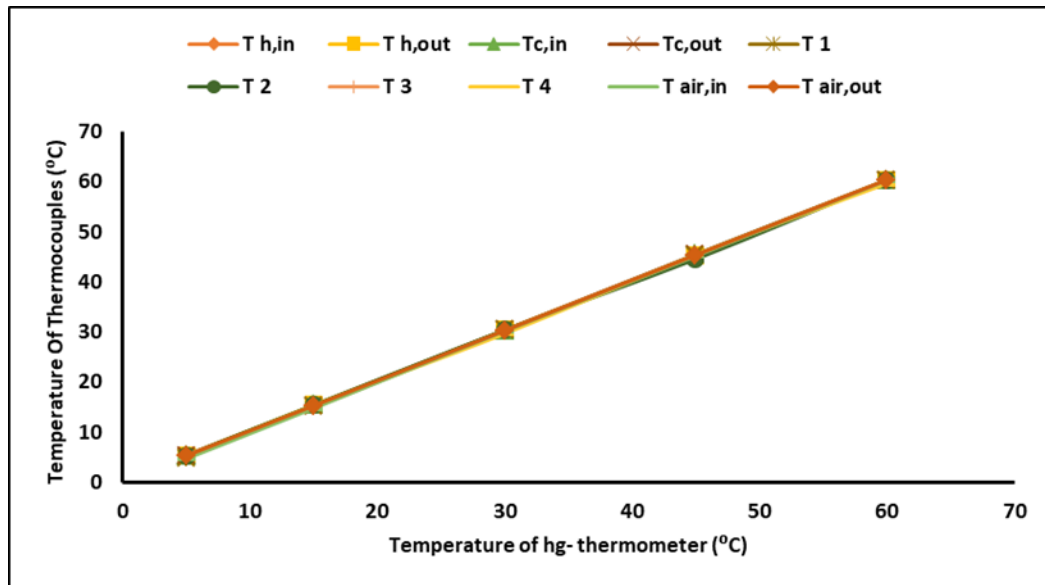


Figure (4-24) Calibration curve of thermocouples.

4.4.3 Experimental proessedure

The practical experiments were carried out under normal conditions inside the room, where the temperature in the room ranged between (23 - 24) °C, with no intense air current close to work, so was the work with constant alternating current (220V, 50 Hz, 0.35 Amp).

Equivalence was donec, the original (classic) heatsink with the test models in terms of the total surface area, taking into account the use of thermal silicon, which in turn acts as an aid in the cooling process as it is found in regular computers.

After conducting tests on the Classic heat sink and obtaining the required results, we place the heatsink (In line) Instead of the previous scatterer, in order to obtain the readings and results, and to ensure this, the study was carried out under the same working conditions for both mod els so that there would be no difference due to the difference in these conditions.

4.4.4 Charging the Nano material in the fins:

In this part we discussed the process of placing the nanomaterial in the fins of the heat sink. As we previously talked about, the inner diameter of one fin is 1.5 mm. This means that this measurement is very small, and because the fin is open from both sides (top and bottom), we have closed the bottom side of the base with aluminum tape. It is very thin, its thickness does not exceed 0.1 mm so as not to affect the addition of additional thickness to the base. Accordingly, the nano material was placed in the fin from the upper side and ensured that it was completely filled with a slight shaking process to ensure that the material descended to the bottom (to the base of the fin).

After completing the placement of the nanomaterial in the fin, we closed the fin from the top with the same aluminum tape with small pieces only for the purpose of ensuring that the material remains inside the fin and does not come out while taking readings. And the Figure (4 - 25) shows the closure of the fins at the top.



Figure (4 - 25), the fins that were closed with aluminum tape from the top.

Chapter Five

Results and Discussion

CHAPTER FIVE

Results and Discussion

5.1 INTRODUCTION

In this chapter specifically, we will discuss the practical results that were conducted on the previously mentioned of heat sinks without the types of use of any auxiliary materials (or Nano materials) on the transfer of heat to the external environment and knowing which type of these dissipators had the most effective performance than others in the process of improving heat transfer. The effect of the nanomaterial used in these experiments will also be discussed for the purpose of knowing the effectiveness of this material in terms of accelerating and shortening the time in the process of thermal transfer.

5.2 Choosing the heat sink :

The types of heat sinks used in these experiments are (Classic, Inline, staggered, and zigzag). The experimental work in the beginning was to expose the heat sink to different temperatures without use of Nano material. The work showed that the heatsinks manufactured in this study had a greater impact on the heat dissipation process than the classic heatsinks manufactured by the private manufacturing company. Therefore, the necessary tests were conducted to determine which of these three types (inline, staggered, and zigzag) is better than others in this work, by conducting a chart showing the relationship between the speed of the air forced on the heatsink and the heat transfer coefficient by convection, and it became clear to us from the tests the best of these types is the (Inline) model, because the heat transfer coefficient by convection in this model was higher than in other models, as in Figure (5-1).

Therefore, it was decided to use this model alone to complete the study.

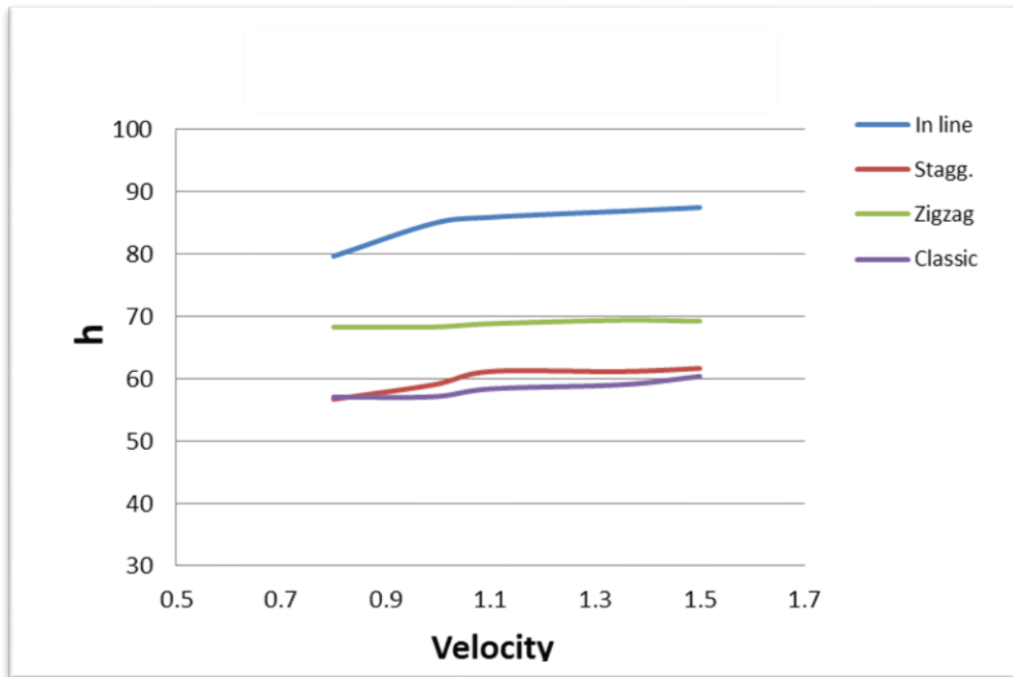


Figure (5-1) Variation between heat transfer coefficient and the velocity of Fan of Heat sinks at 95 °C, without nano material.

5.3 Nano Material : Multi Wall Carbon Nano Tubes (MWCNTs) :

- 1- Most commercial applications dealt with multi wall carbon nanotubes (MWCNTs) , which can be thought of as a number of tubes nested inside each other.
- 2- A bit like the rings of a tree or folded telescopic antenna, Figure (5 – 2).

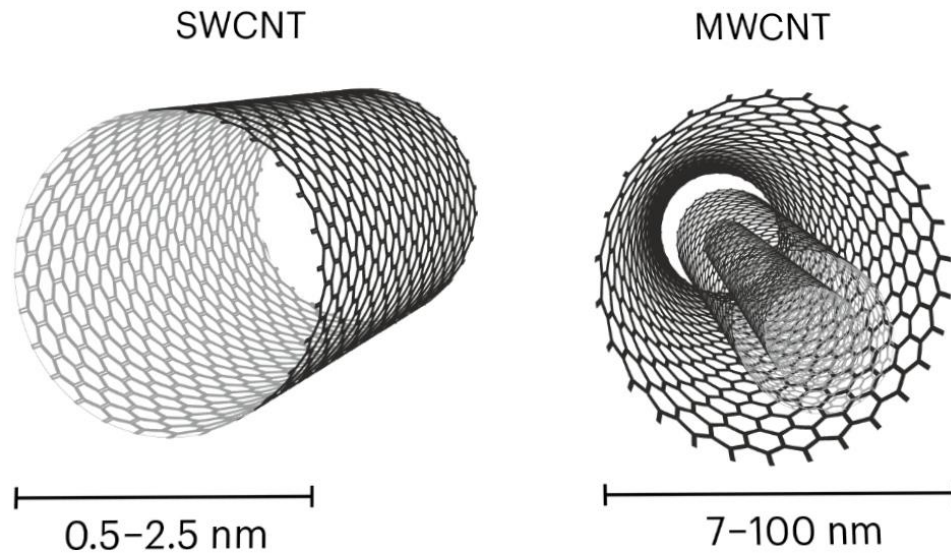


Figure (5 - 2), Different between the single tube & multi tube nanomaterial.[30]

5.4 Electrical Conductivity of MWCNTs :

1- One of the most advantageous properties, is their high electrical conductivity. The good thing about it that when even relatively small amounts of MWCNTs are mixed into normally insulating materials, the materials can gain significant conductivity.

2- The length-to-diameter ratio of multi wall carbon nanotubes makes it possible to achieve that at much smaller amounts, because the long tubes can contact each other over longer distances and form a conductive network through the material.

Thermal conductivity of multi-walled carbon nanotubes:

A- MWCNTs also have high thermal conductivity and can be used in normally insulative materials to increase their ability to transmit heat.

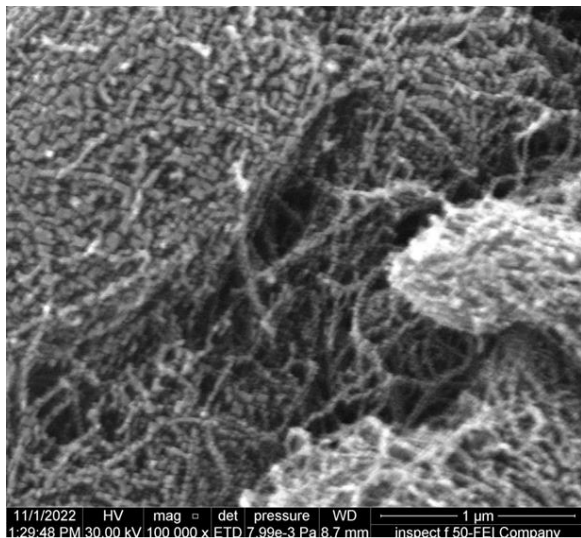
B- The thermal conductivity of MWCNTs ($K = 3500 \text{ W/ m. C}$).[31]

5.5 Physical Properties of MWCNTs :

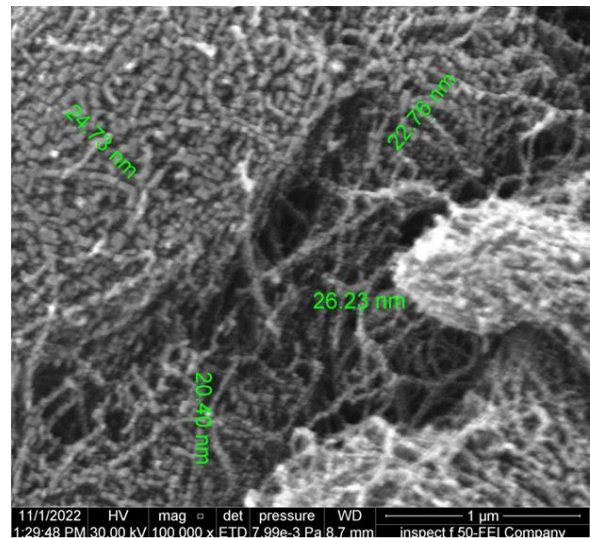
It is one of the things that we must mention, the Nanomaterial it used in this study, also we checked and tested in lap (Areej Al-furat) in Baghdad, to inspect the materials, we get the pictures under scoop to explain the particles and bonds of interconnection between them, and these some of the properties of the Nano.

1- The MWCNTs are a long tubes, but the length itself is not the crucial characteristic in many applications. The ratio of the length to the diameter, is often more important.

2- For MWCNTs with typical dia. between 7 & 100 nm, the aspect ratio is typically between 50 & 4000. These ratios have a significant impact on the performance of MWCNTs and other materials such as various plastic, Figure (5-3 , A and B).



(A)



(B)

Figure (5- 3) (A & B)
show the variation in the length and dimension of the Nano material.

5.6 Distribution of Nanomaterial on the Fins of H.S :

The nanomaterial was charged and extruded into the fins in a very precise manner. The amount of nanomaterial in one fin was by an amount (0.0247) gram , and the percentage taken for each experiment was as follows:

The use of nanomaterial is 5% in the dispersion, and this means that we use (5%) of the total fins in the dispersion, and since the number of fins is (120) fins in one dispersion, this means that we use nanomaterial in (6) fins only. As for the percentage of (10%), the number of fins used will be (12), the percentage of (15%), the number of fins will be (18), and the percentage of (20%), the number of fins used will be (24).

In figure (5 – 4) , explain to the distribution of the nanomaterial in the In Line heat sink.

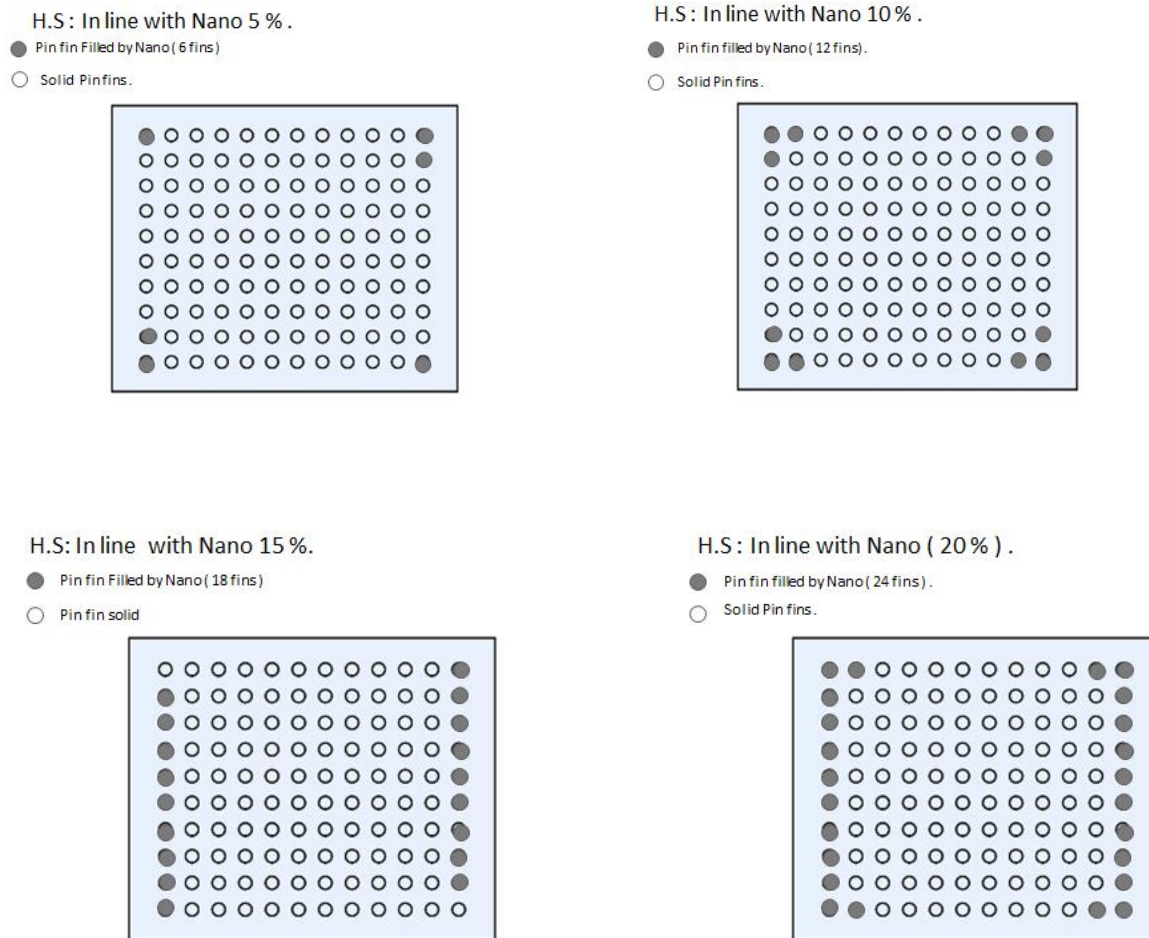


Figure (5 – 4) , Distribution of the Nanomaterial in the In Line heat sink.

5.7 Experimental side Study :

5.7.1 The Variation between speed and temperature difference

When making a chart to explain the relationship between the velocity of the air entering the heat sink through the fan and the difference in the temperatures of the air entering and leaving through the air duct (ΔT), The relationship is direct, because the greater the speed of the air through the fan, the greater the difference in air temperature at the exit. Also, we notice the effect of the nanomaterial in the process of heat transfer between the heatsink and the external environment. Therefore, the nanomaterial affects the temperature rise the air coming out of the air duct transfers the heat sink to the outside.

When using nanomaterial at a rate of 5%, we see in the figure (5 – 5), The first curve is at a temperature of 60 °C, which is between the minimum and maximum air speed (0.8 - 1.5) m/s. The curve ranges between a value (3.05 - 3.3), while we find that the last curve, which was at a temperature of 95 °C (which is at the lowest and maximum air speed), ranges in value between (5 - 5.4), and this indicates that the difference in temperatures was very clear and high, which indicates the heat transfer process between the In Line heat sink and the external surroundings was very good due to the geometric shape of the aforementioned dispersion and the proportional distribution of the fins.

we find that the increase in temperature is greater when using the nanomaterial to a greater extent, even by a little and a little, in the Figure (5 – 6) it shows the use of nanomaterial at a rate of 10%, and here we notice that the values of the curves in this figure are more than they were in the previous figure, and this means that the difference in temperatures here is greater. Whereas the first curve, which is at a temperature of 60 °C has a value between (4.2 - 4.5), while we find that the last curve, which is at the maximum temperature in the presented study, which is 95 °C, ranges in value between (5.31 - 5.57), which indicates that the heat transfer process was more severe here.

We also notice that the difference in temperature is greater with an increase in the nanomaterial by 15%. The values of the curves, as we find that the values of the curves in the figure (5 - 7) it is higher than it was previously due to the speed of thermal dissipation or heat transfer between the dissipator and the external environment as a result of the use of a nanomaterial with a very large thermal conductivity coefficient. We notice that the first curve, which is at 60 °C, ranges in value between (5 - 5.38), while we find that the last curve, which is at the maximum temperature of 95 °C, ranges in value between (6.95 - 7.22) and these values are more than the previous values.

The last chart in this aspect indicates the use of nanomaterial at a rate of 20%, which is the highest percentage of use in the study presented, as the values refer to the curves in the figure (5 – 8), The difference in temperature with speed is the highest among the charts mentioned previously, as the first curve, which is at 60 °C, indicates a value ranging between (6.35 - 6.54), while the last curve, which is at the maximum temperature, which is 95 °C ranged between (7.2 - 7.4), and these values are higher than before in all previous charts, and this indicates here that the difference in temperatures is the largest practical results we have achieved in this presented study.

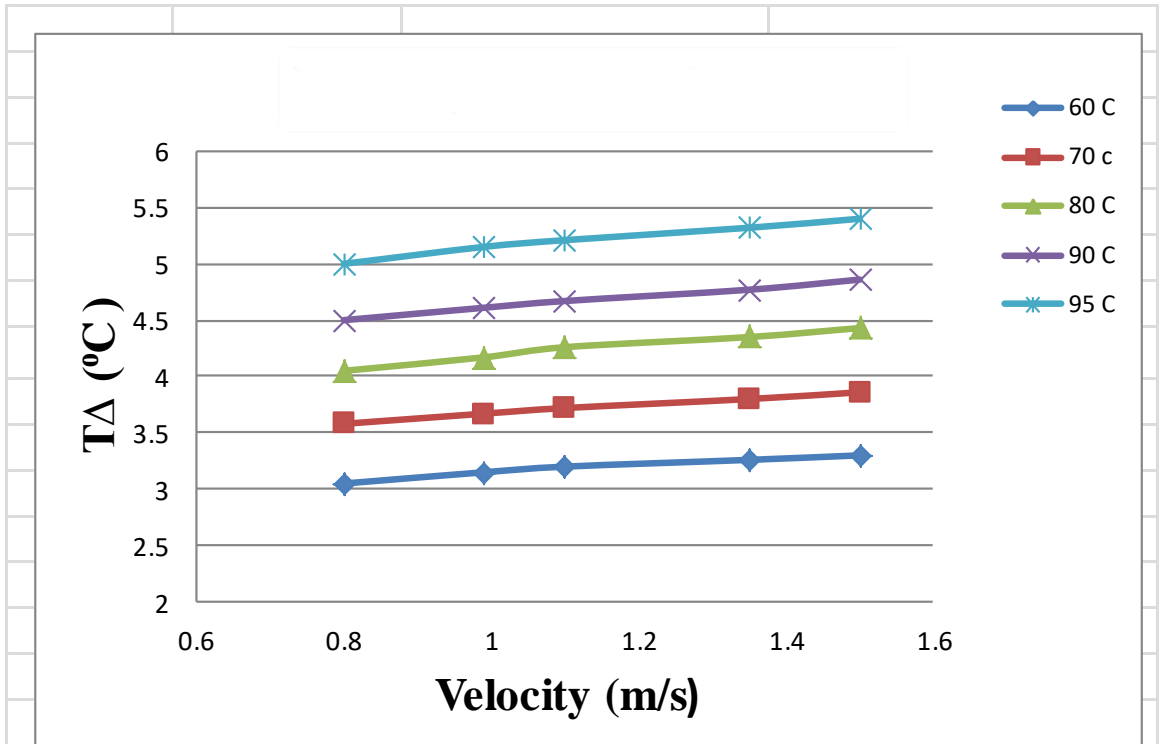


Figure (5 - 5), Variation between Velocity & ΔT at In Line heat sink with 5% Nano.

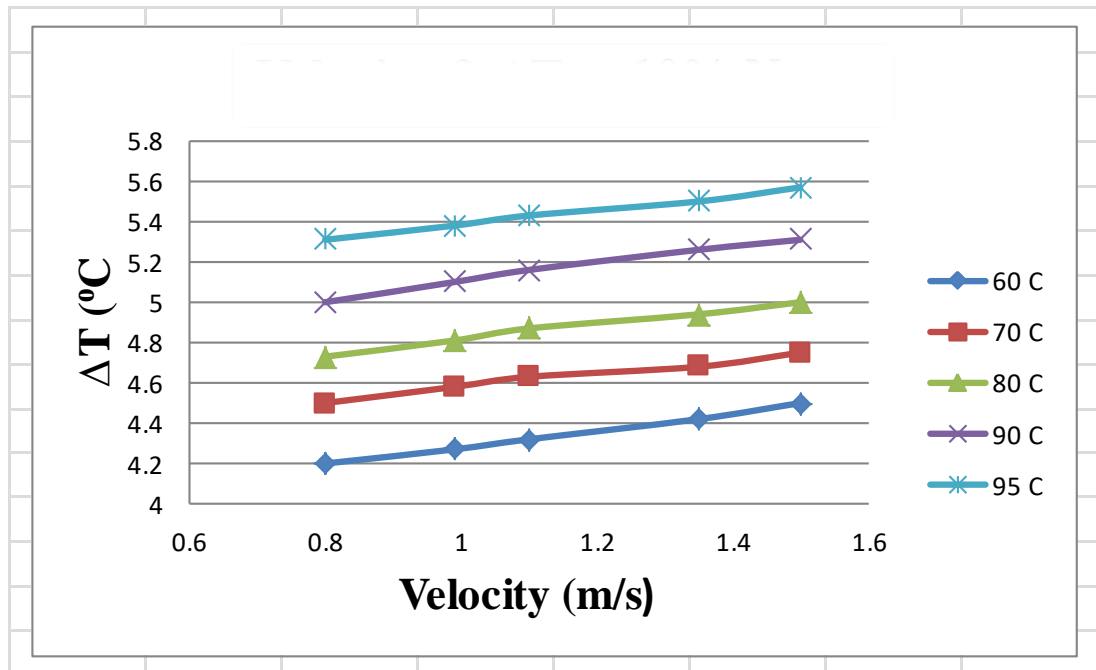


Figure (5 - 6), Variation between Velocity & ΔT at In Line heat sink with 10% Nano.

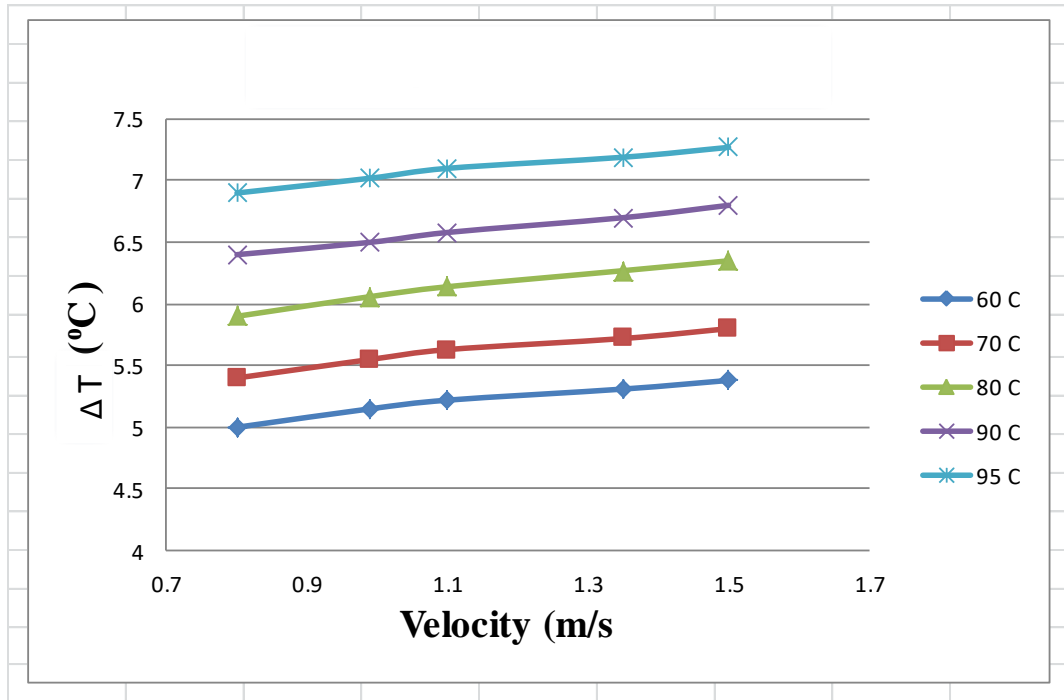


Figure (5 - 7), Variation between Velocity & ΔT at In Line heat sink with 15% Nano.

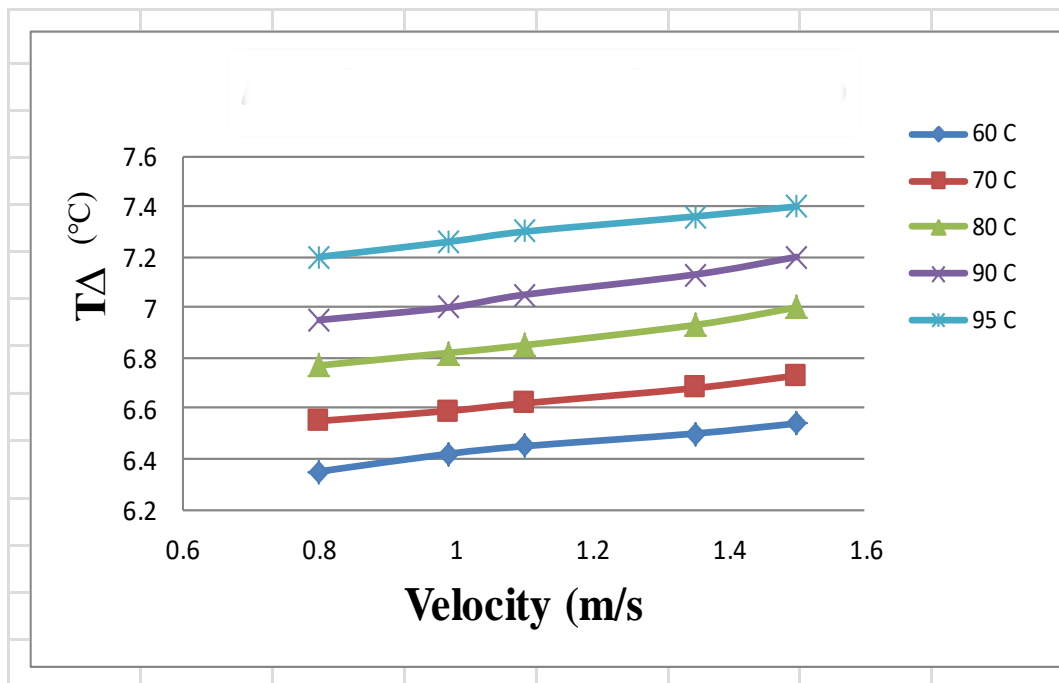


Figure (5 - 8), Variation between Velocity & ΔT at In Line heat sink with 20% Nano.

5.7.2 The Effectiveness of Nano packing (ϵ_n) :

The use of nanomaterial, as we mentioned previously, led to significant progress in the process of heat transfer between the heat sink and the external environment, thus shortening the time factor, which has long been considered one of the important factors for which researchers wanted to find appropriate solutions. Also, the geometric shape has a major impact on this process (heat transfer process) in terms of the arrangement and shape of the fins in the heat sink.

Here, it is worth noting that the more the size and area of the heat sink are proportional, the more the cost is also proportional. While the fins contain the nanomaterial (and the nanomaterial is somewhat expensive), however, reducing the area of the fin size leads to the nanomaterial filling being less (and this is considered Good from an economic and material perspective), and vice versa, the larger the area and size of the fin, this means that the nanomaterial filling is also large, which means that the nanomaterial dissipator is very expensive, which does not help people with expertise to use it in the process of cooling electrical and electronic devices.

In this aspect of presented work , we address the effectiveness of nanopacking and its effect on the area and size of the fins in the heat sink by finding a coefficient (ϵ_n) which is considered to be the effectiveness factor of the nanomaterial and to know the extent of its effect) in the diagrams that show this, and to know the value of (ϵ_n) We divide the value of the total amount of heat Re with ($Q_{\text{Total nano}}$).

Used in dissipators (with the nanomaterial) divided by the total amount of heat without the nanomaterial ($Q_{\text{Total without nano}}$), Define the new parameter for all ratios used, as in the following equation :

$$\epsilon_n = \frac{Q_{\text{Total nano}}}{Q_{\text{Total without nano}}} \dots\dots\dots(5.1)$$

We find that the value of (ϵ_n) If it is greater than (1), this means that the heat transfer in the heat sink with the nanomaterial is much better than the effectiveness of the heat sink without the nanomaterial, and this, as we said before, is good and useful in terms of the size and area of the heat sink. But if the value (ϵ_n) Less than (1), this is an indication that the heat transfer process with the nanomaterial is ineffective at work.

In Figure (5 - 9), relationship between (ϵ_n) And the Reynolds coefficient when using 5% nanomaterial, we notice that the values in the chart are values greater than (1), and this means that the curves are on the rise, which gives good results in the presented work.

As the first curve, which is at a temperature of 60 °C, the value ranges from (1.05 - 1.13), and this value is at the lowest and maximum fan speed fan speed, which is (0.8 - 1.5) m/s. While we find that the last curve, which is at a temperature of 95 °C, has a value ranging from (1.17 - 1.23) in same range speed of the fan.

Either in the figure (5 – 10), we notice that the values began to rise from what they were in the previous figure, which means that the effectiveness of the nanomaterial increases little by little, as the percentage of nanomaterial in this figure is 10%, and the first curve, which is at 60 °C, ranges between (1.08 - 1.14). While the last curve in the chart, which is at 95 °C, ranges between (1.20 - 1.26).

In the figure (5 - 11), the nanomaterial used is 15%. This means that by increasing the nanomaterial, the effectiveness of the dispersion in the heat transfer process increases. We notice that the first curve, which is at 60 °C, ranges between (1.11 - 1.17) These values are greater than they were previously. At 95 °C, which is the maximum temperature, the last curve ranges between (1.23 - 1.28), we also find that the values are higher than the previous ratios and figures.

And in the figure (5 - 12), The nanomaterial used is 20%, which is the highest percentage of nanomaterials used in this study, as we find that the first curve at a temperature of 60 °C ranges between (1.16 - 1.21).

We find that the last curve, which is at 95 °C, ranges between (1.27 - 1.30), and this indicates that the effectiveness of the nanomaterial is large if compared with the effectiveness of the heat sink without the nanomaterial.

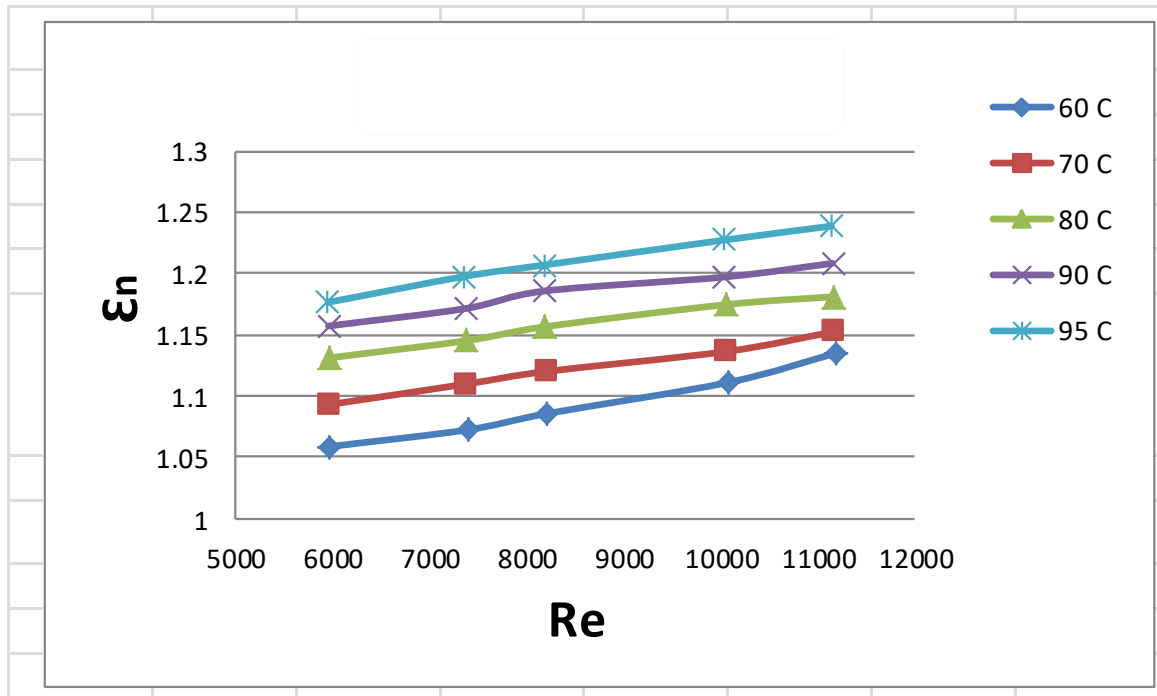


Figure (5 – 9), Variation between Re & ϵ_n at In Line heat sink with 5% Nano.

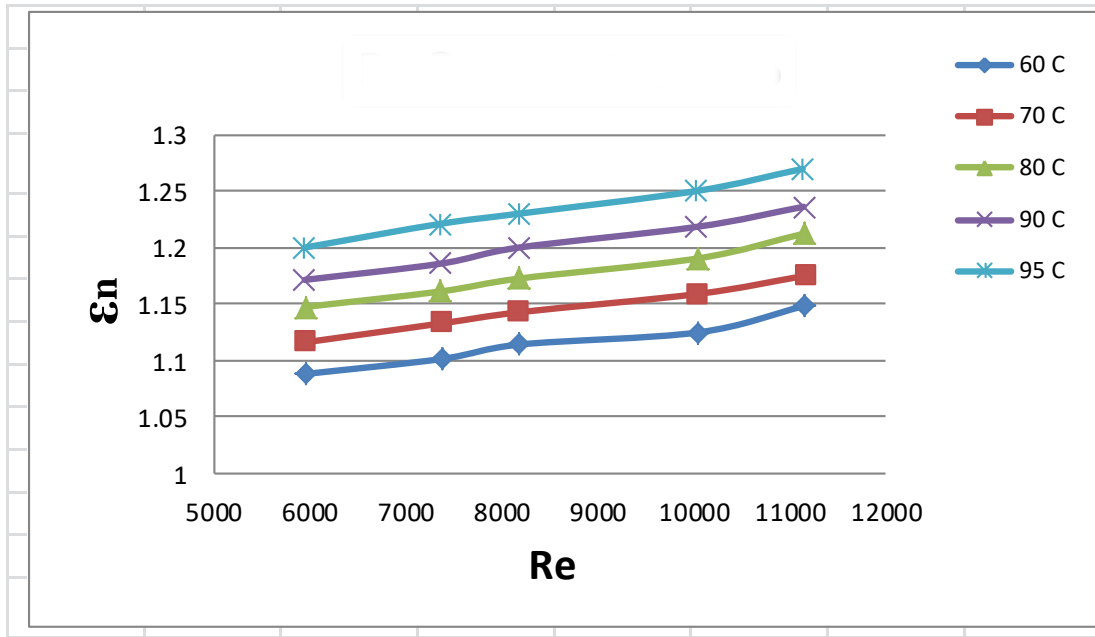


Figure (5 - 10), Variation between Re & ϵ_n at In Line heat sink with 10% Nano.

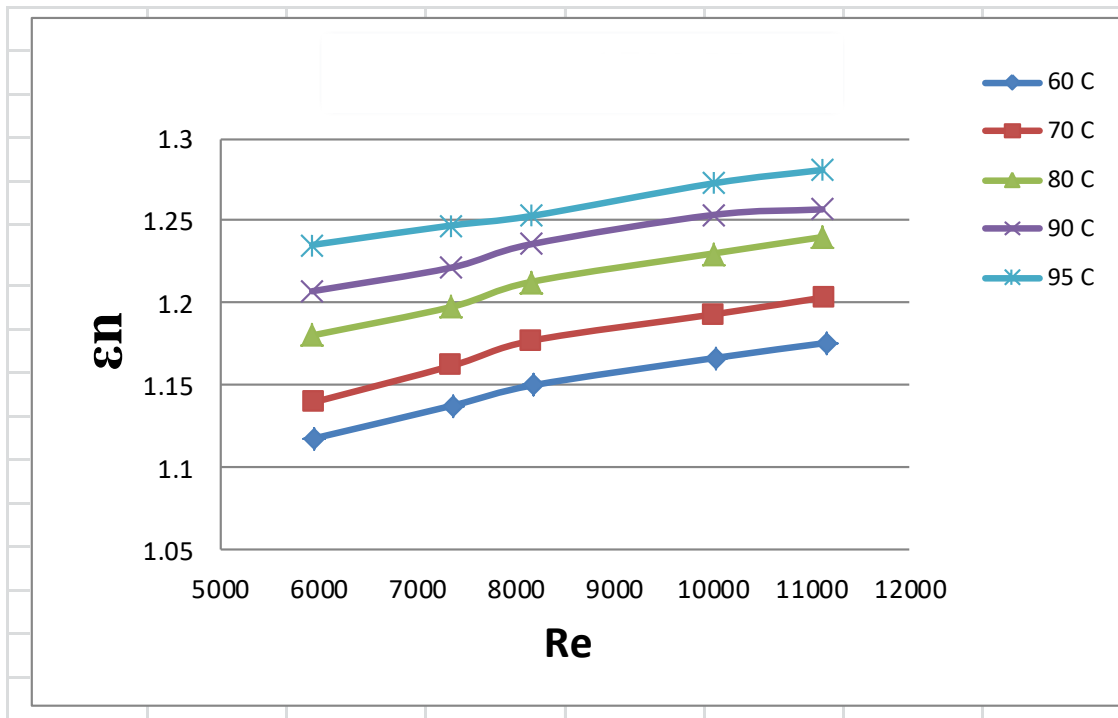


Figure (5 - 11), Variation between Re & ϵ_n at In Line heat sink with 15% Nano.

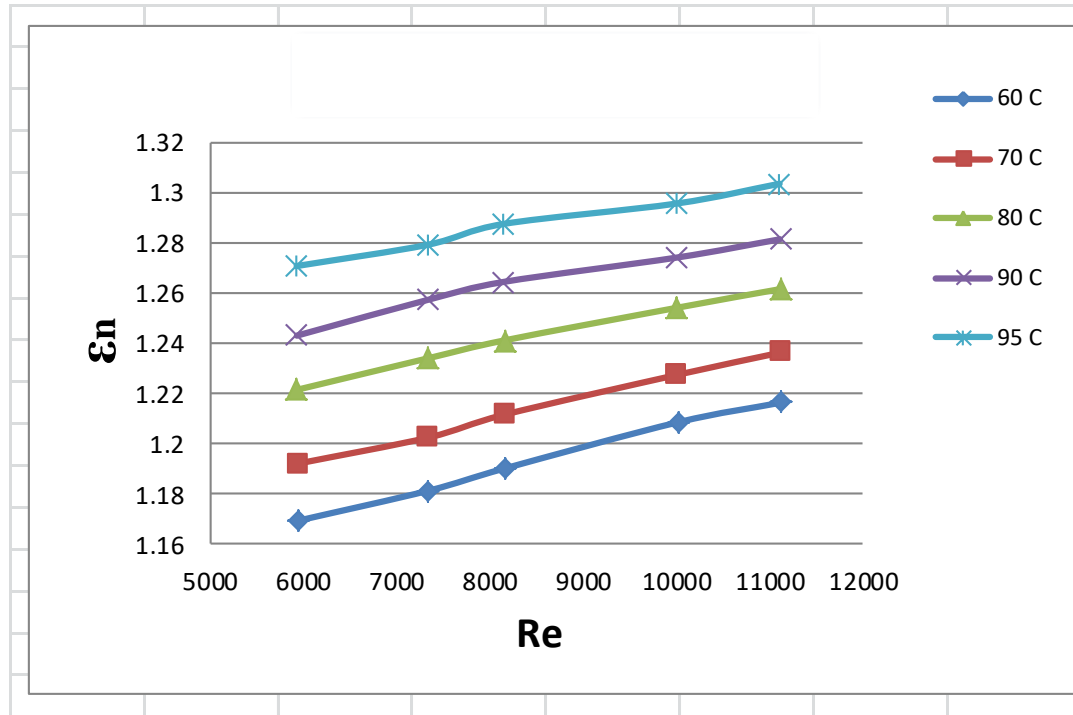


Figure (5 - 12), Variation between Re & ϵn at In Line heat sink with 20% Nano.

5.7.3 The Variation between Re and Nu :

It is very important to know the effectiveness of nanomaterial in the process of thermal dispersion, through several things, and one of these things is knowing the type of relationship between Reynolds number And Nusselt number, Knowing this was through conducting the necessary plans between them. Figure (5–13) shows that Nusselt laboratories It increases gradually with an increase Reynolds number ,but this increase was small because the nanomaterial used was 5%, so we find that Reynold it ranged between (5000 - 12000) and Nusselt it ranges between (230 - 243) at 60 °C, which is the lowest temperature tested, while we find that Nusselt number it increases at a temperature of 95 °C (maximum temperature) until it reaches between (335 - 350), as shown in figure (5-13) .

While we find in Figure (5 – 14) that the increase in the Nusselt number is greater due to the increase in the percentage of nanomaterial to (10%), which is more than in the previous figure, which means that as the percentage of nanomaterial increases , the rate increases. Nusselt number more. This means that the number of fins containing the nanomaterial has doubled from the first percentage, which leads to an acceleration of heat transfer between the heat sink and the external environment. We find that the Nusselt number ranges between (250 - 277) at a temperature of 60 degrees Celsius. While we find it ranges between (338 - 358) at a temperature of 95 degrees Celsius.

We note here in Figure (5 - 15) that the rates Nusselt number It is increasing because the heat transfer coefficient by convection is high because it is included in the calculation process Nusselt number Also, because the nanomaterial has increased from the previous percentages, it has become here by (15%), which means that the process of heat transfer is faster between the heat sink and the external surroundings.

We find that the first curve, which is at 60 degrees Celsius, ranges between (263-297), while we find that the last curve, which is at 95 degrees Celsius, ranges between (360-370). For Nusselt number, while We find that Reynolds number It remained within the previous range between (5000-12000) because Reynold It is affected by the difference in temperature, which is small compared to the high heat transfer coefficient by convection.

In Figure (5 – 16), we find that the curves have increased in value more than all previous diagrams, because the percentage of nanomaterial reached (20%), which is the largest percentage in this study. It is very natural that there is a difference in the rates Nusselt number In this chart where the rate ranges Nusselt number at the lowest temperature, which is 60 °C (275-300), and at the maximum temperature, which is 95 °C, between (361-376), which is much higher than all the curves in the other charts.

Another important thing is knowing the relationship between Reynolds number and Nusselt number as for the regular dispersion (classic), this is to know the amount of these rates and compare them with the rates Reynolds and Nusselt for the dispersant used in this

study, which is Inline heat sink through the presented study, we found that these rates for the dispersion (Inline it much more than distracted Classic) as shown in Figure (5 – 17), which shows the change between Reynold number and Nusselt number, where we note that Nusselt rate it ranges between (183-208) at temperature of 60 °C, while it ranges between (252-268) at maximum temperature of 95 °C.

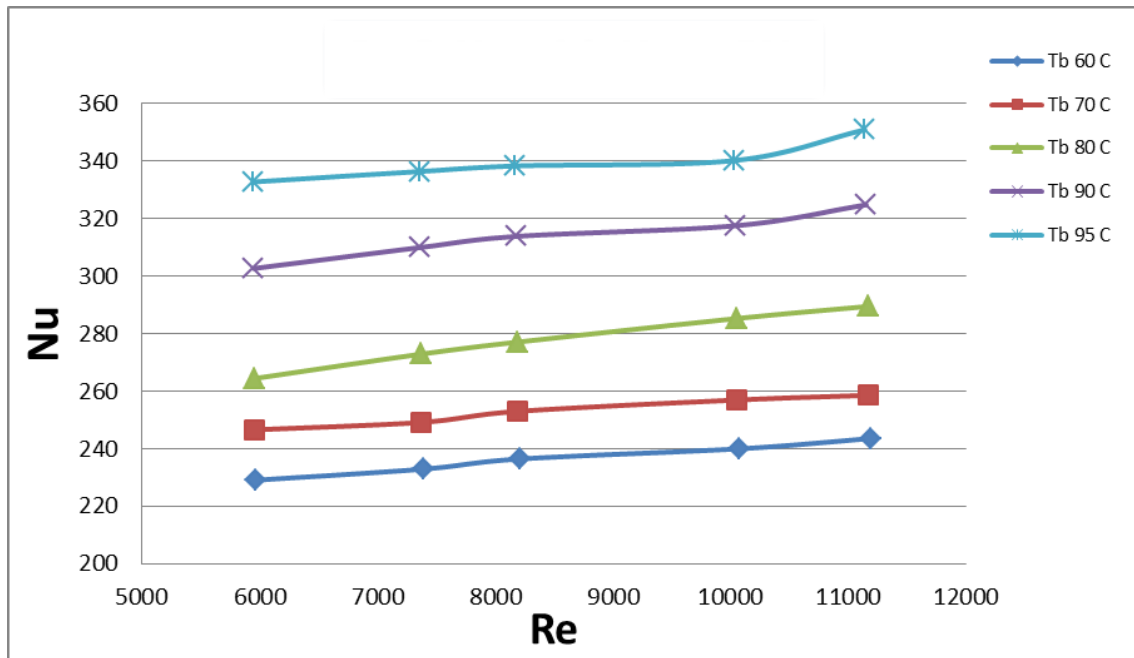


Figure (5 – 13) Variation between Re & Nu with Nano 5%, (Inline) H.S.

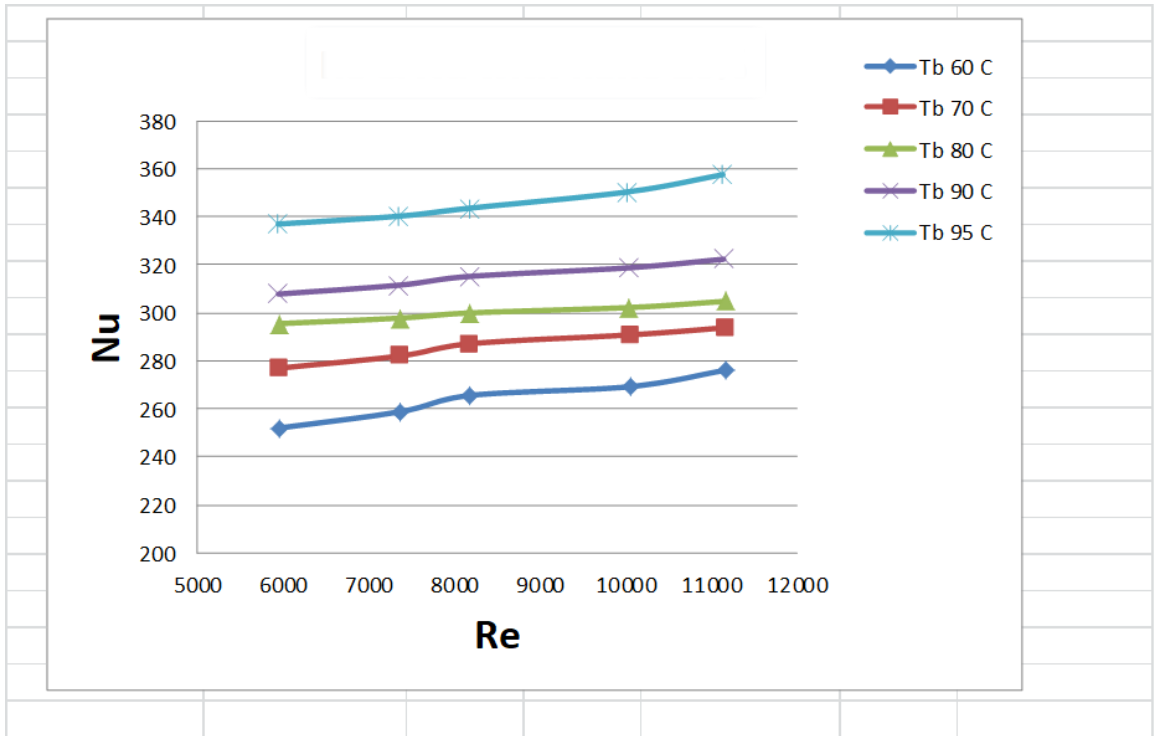


Figure (5 – 14) Variation between Re & Nu with Nano 10%, In Line HS.

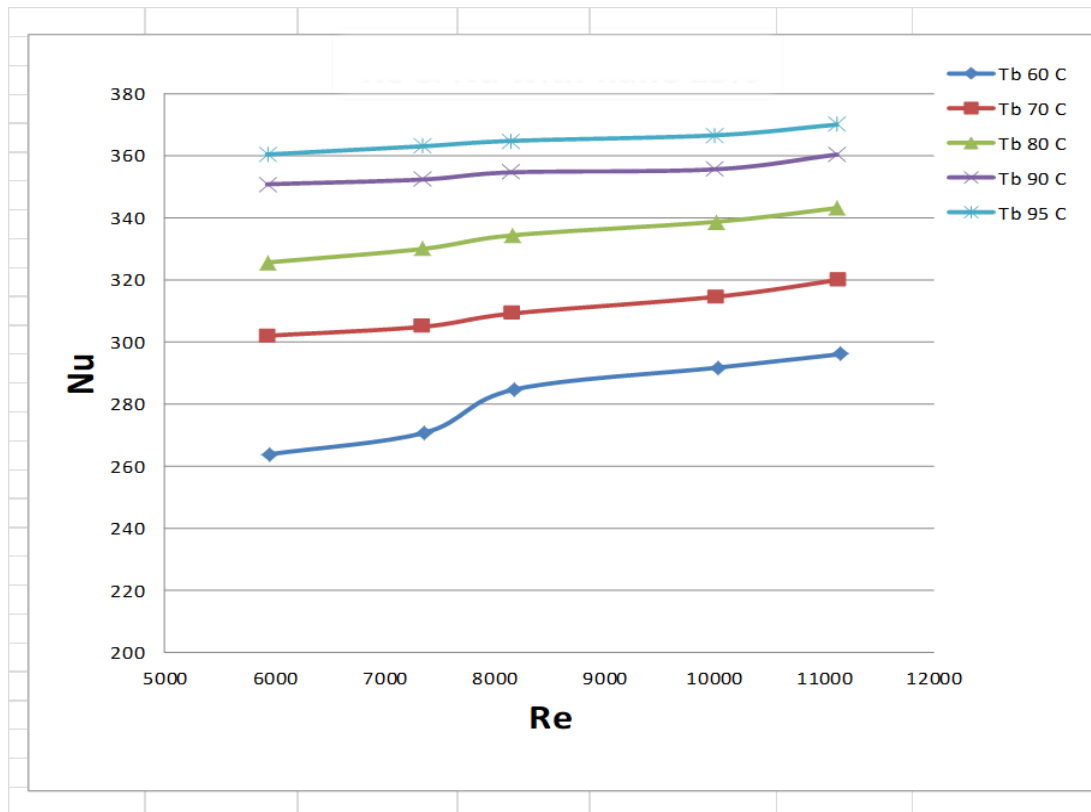


Figure (5 – 15) Variation between Re & Nu with Nano 15%, In Line HS.

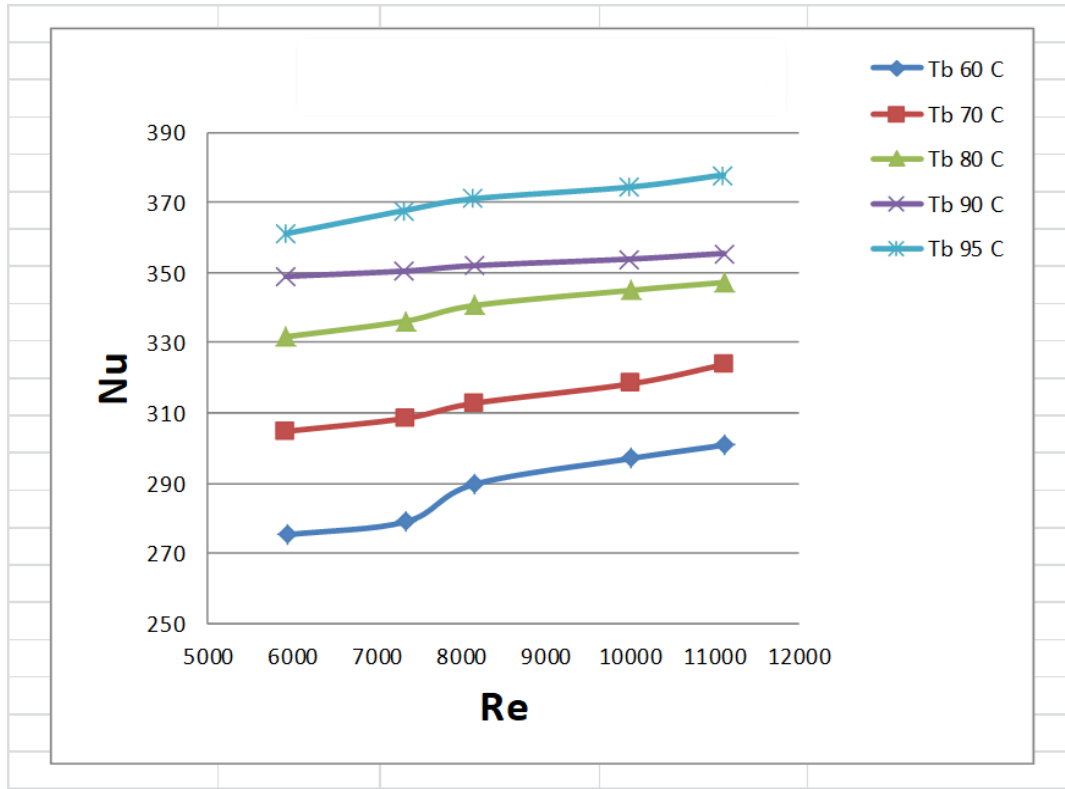


Figure (5 – 16) Variation between Re & Nu with Nano 20%, In Line HS.

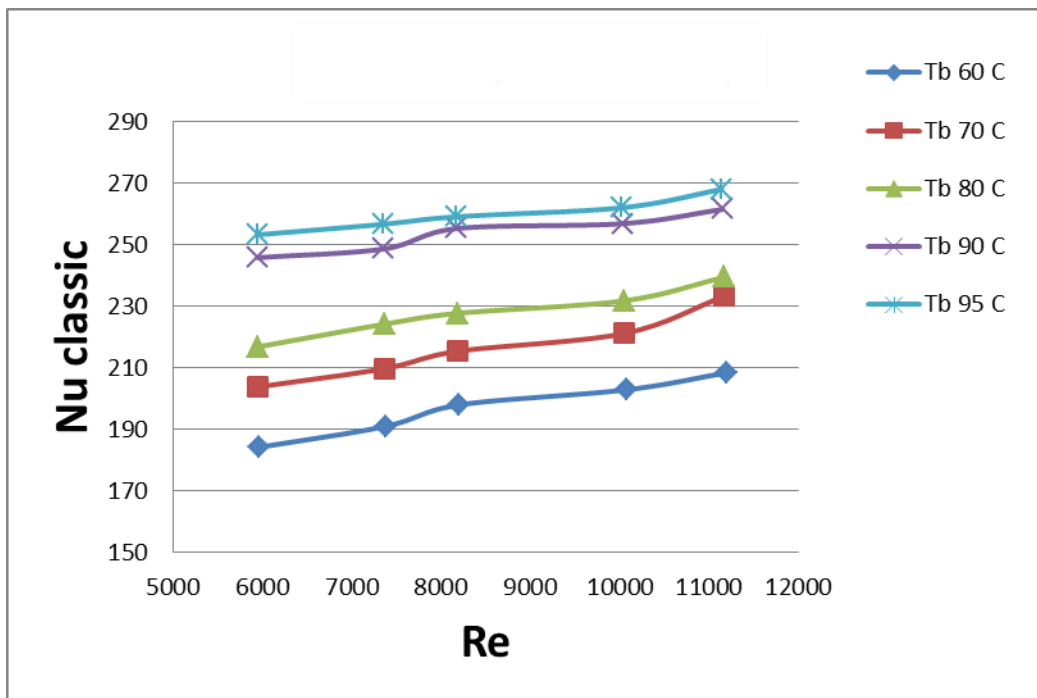


Figure (5- 17) Variation between Re & Nu in Classic heat sink.

5.7.4 The Variation between Re and $(Nu_n / Nu_{\text{without nano}})$:

As for knowing the effect of the nanomaterial and its effectiveness in the process of improving heat transfer, the change between rates must be known Nusselt when using this material in the heat sink (Inline) and without using it for the same heat sink, therefore we extracted the value Nusselt rate With the nanomaterial of the dispersion divided by Nusselt rate For the same dispersion, but without the nanomaterial, and find out the change between these two values relative to Reynolds number when using this material in all the proportions mentioned previously. Through this equation it becomes clear to us If the result is greater than (1), this means that the effectiveness of the nanomaterial in the dispersion is effective At work If the result is less than (1), this means that the heat dissipator is doing the process of dispersing heat well without using the nanomaterial (this contradicts reality because the work of the nanomaterial is to accelerate the heat transfer between the surfaces of objects and the external environment), so the result was greater than (1).) in all the proportions that were used, and this is evidence that the nanomaterial is effective in thermal work. Figure (5 –18) shows the amount of change occurring between the Reynolds number and the Nusselt rates (with and without the nanomaterial) at using 5%.

Where we notice that Nusselt rates on axis (Y) is more than (1), so we find that Nusselt it ranges between (1.08-1.10) at 60 °C, while we find that Nusselt high at 95 °C and ranges between (1.15 - 1.17), at the same rate Reynold Which remained within the previous rates and ranges between (5000 - 12000).

The increase also increases if the percentage in the use of nanomaterial increases, as we notice in figure (5 – 20) and Figure (5 – 21) that the curves are higher than in the previous two figures. In figure (5 – 20), the nanomaterial was used at a rate of 15%, meaning that (18) fins was charged. we find the change or increase in the Nusselt value with the nano, divided by the Nusselt value without the nano, so the first curve ranges between (1.22-1.3) at a temperature of 60 °C, while the last curve ranges between (1.45-1.54) at a temperature of 95 °C. As for figure (5 – 21), the nanomaterial was used at a rate of 20%, meaning that

(24) fins were charged out of (120) fins out of the total number of fins. We find that the curves rise more than all previous percentages.

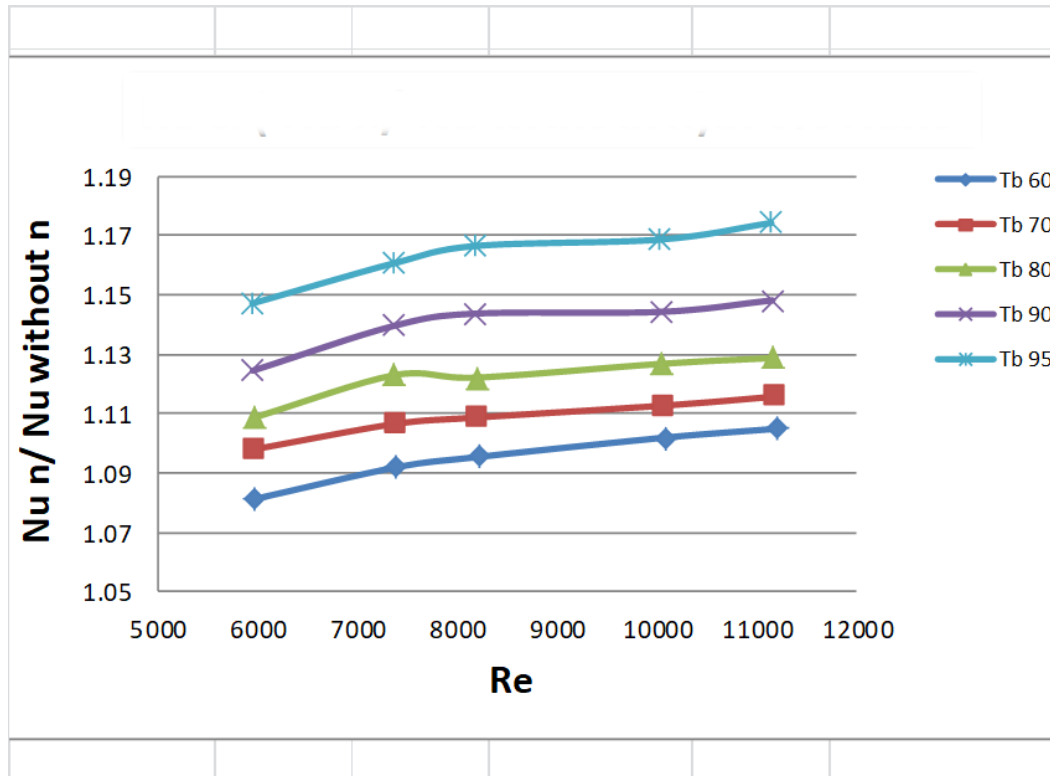


Figure (5 – 18), The Variation between Re & $(Nu_n / Nu_{without\ n})$ with 5% Nano.

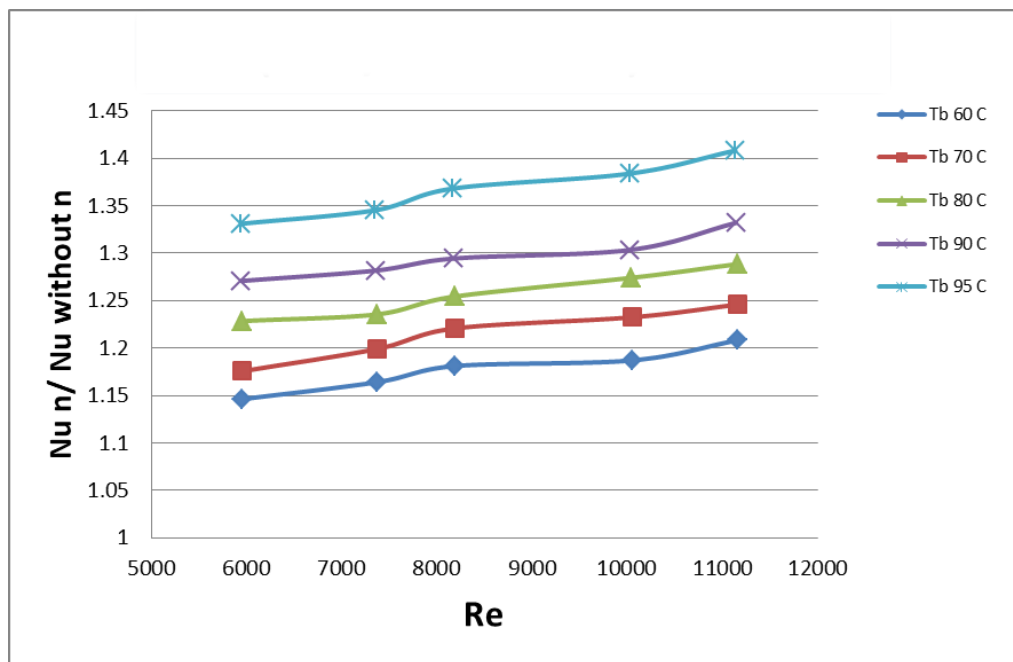


Figure (5 – 19) Variation between Re & $(Nu_n / Nu_{without\ n})$ with 10% Nano.

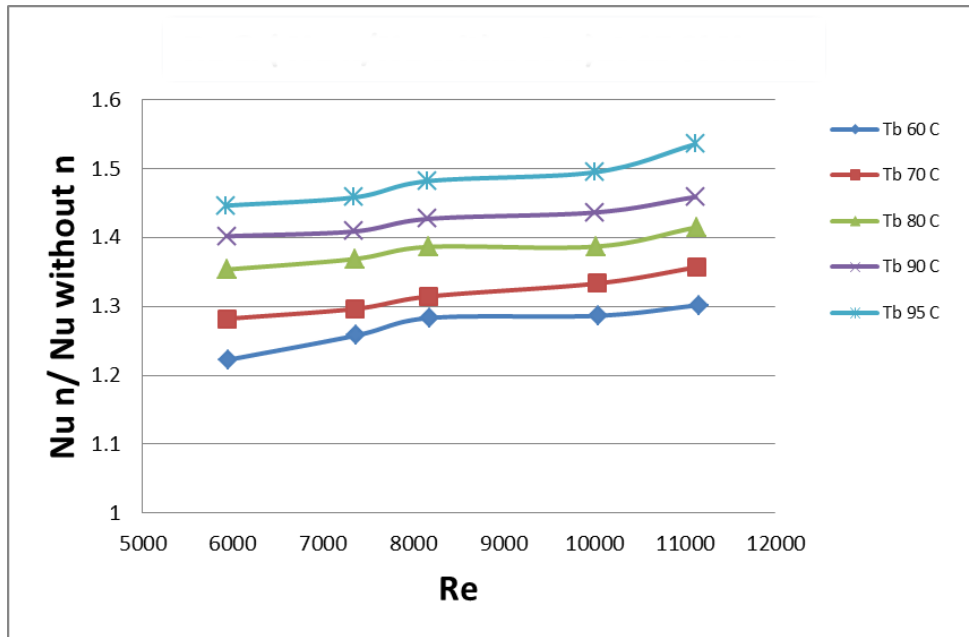


Figure (5 – 20) Variation between Re & (Nu n / Nu without n) with 15% Nano.

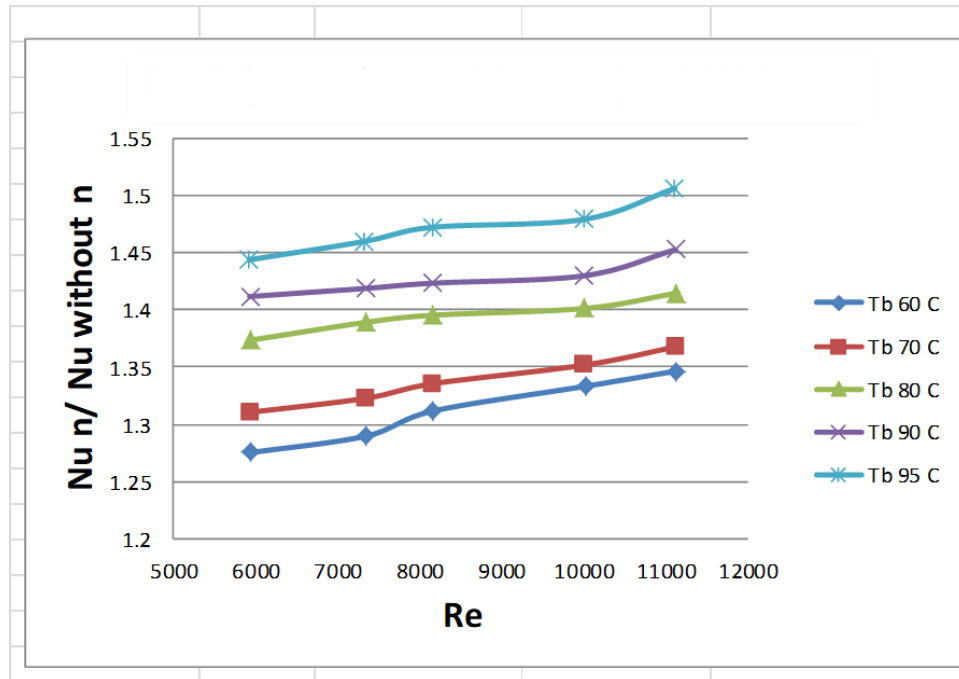


Figure (5 – 21), Variation between Re & (Nu n / Nu without n) with 20% Nano.

5.7.5 The Variation between Re and ($Nu_n / Nu_{Classic}$) :

Also, one of the important things that must be taken into consideration is knowing the effectiveness of the nanomaterial in the manufactured dispersion (Inline) versus the performance of the classic dispersant so that we have a complete idea of the geometric design of the dispersion that we have manufactured (is it effective compared to the dispersants manufactured by large and globally approved companies), and on this basis we must compare the dispersion that contains the nanomaterial with the classic dispersion by obtaining on value Nusselt number with nano dispersion (Inline) divided Nusselt number for the classic heatsink, the result obtained from this equation is to find out which of the two designs is better in the heat dissipation process. If the result is greater than (1), this means that Nusselt number with nano it is bigger than Nusselt number for the classic H.S, but if the result is less than (1), this means that the Nusselt number for the classical H.S is greater than the Nusselt number for the heat sink (Inline) with nano.

Where the result was greater than (1), and this is what is required, and it is clear to us from figure (5 - 22) the change occurring between Reynolds number and between Nusselt for distracted (Inline) divided Nusselt number for the classic H.S.

Figure (5 - 22) represents the relationship between Reynolds and Nusselt when using nanomaterial at a rate of 5% of the number of fins, this means that (6) fins were charged with nanomaterial out of (120) fins, and the curves that we observe in the figure are high because the value Nusselt with nano , it is greater than the value Nusselt for the classic HS.

We find that the first curve, which is at a temperature of 60 °C, ranges between (1.23-1.31), and the last curve, which is at a temperature of 95 °C, ranges between (1.45-1.56), which are good rates fairly.

While we notice that the curves began to rise gradually due to the increase in the nanomaterial used in this experiment to 10%, and this means that (12) fins were charged out of (120) fins, and this is doubled from the previous percentage, which means that the rates of Nusselt and Reynolds number it also increased, as shown in Figure (5 – 23), where we notice that the first curve, which is at 60 °C, is approaching (1.3) and reaching (1.36), which is higher than the first curve for the same degree in the previous figure, and the last curve, which is at The degree of 95 °C ranges between (1.5) and is close to (1.59), which is also higher than the last curve for the same temperature in the previous figure.

As for Figure (5 – 24), which represents the use of nanomaterial at a rate of 15% of the total number of fins, meaning that (18) fins were shipped out of (120) fins. From distraction thermal (Inline), here we notice an increase in Reynolds and Nusselt rates than it was in the previous charts, where the first curve rose from the previous figure, and ranges between (1.38 - 1.42) at a temperature of 60 °C, while the last curve ranges between (1.61 - 1.64), which is at a temperature of 95 °C, which is more than the curve for the same temperature in the previous figure.

While we find that the rates (Reynolds and Nusselt) have increased in figure (5 – 25) with the increase of the nanomaterial, as it was used here by 20% of the number of fins, meaning (24) fins were charged out of (120) of the total fins in the previously mentioned heat sink.

We find that the first curve, which represents the temperature at 60 °C, ranges between (1.49 - 1.54), which is higher than all previous curves in the nanoscale ratios used in this work, while we note that the last curve, which represents the temperature at 95 °C, ranges between (1.63 – 1.68) which is also higher than the other curves in the previous figures to the same degree.

This means that the nanomaterial is effective in the process of heat dissipation, and it is very clear from the diagrams presented in this study, where we notice large changes between the curves at all temperatures to which the heat sink was exposed.

The heat dissipation process differs from one heat sink to another in terms of performance, and this depends on several important things, including (geometric design), where the shape, number, and arrangement of the fins are very important in the process of heat exchange between the surfaces of the fins and the external surroundings, or the overall shape of the heatsink, where it is the dispersion is in some designs (square, rectangular, circular, etc.), and this means that the design affects this process and its the effect is either negative or positive in heat transfer, and the many tests are what show whether this design is good or not.

Here, in this presented study, we have clarified many important matters that show that the heat sink Inline it was good and effective in dispersing heat, even if we did not use nanomaterial in it. The geometric design of the general shape, the shape of the cylindrical fins, and the arrangement of the rows of fins, all of these things combined were of good effectiveness in the performance of this dissipator.

To know the (design effect) of the heat sink, we performed a calculation through division Nusselt number Without the nanomaterial of the dispersion (Inline) on Nusselt number For the classic H.S, make a plot between the result of these values with Reynolds number in this study.

Figure (5 – 26) shows the change between Reynolds number and the result of a division Nusselt number without Nano and Nusselt number For the classic dispersion, the curves are relatively high because at 5% (which is the lowest percentage) the rate is Nusselt a little, as we notice that the first curve, which is at 60 °C, ranges between (1.12 - 1.15) , while the last curve, which is at 95 °C, ranges between (1.33 - 1.37), while that Reynold ranging between (5000 –12000).

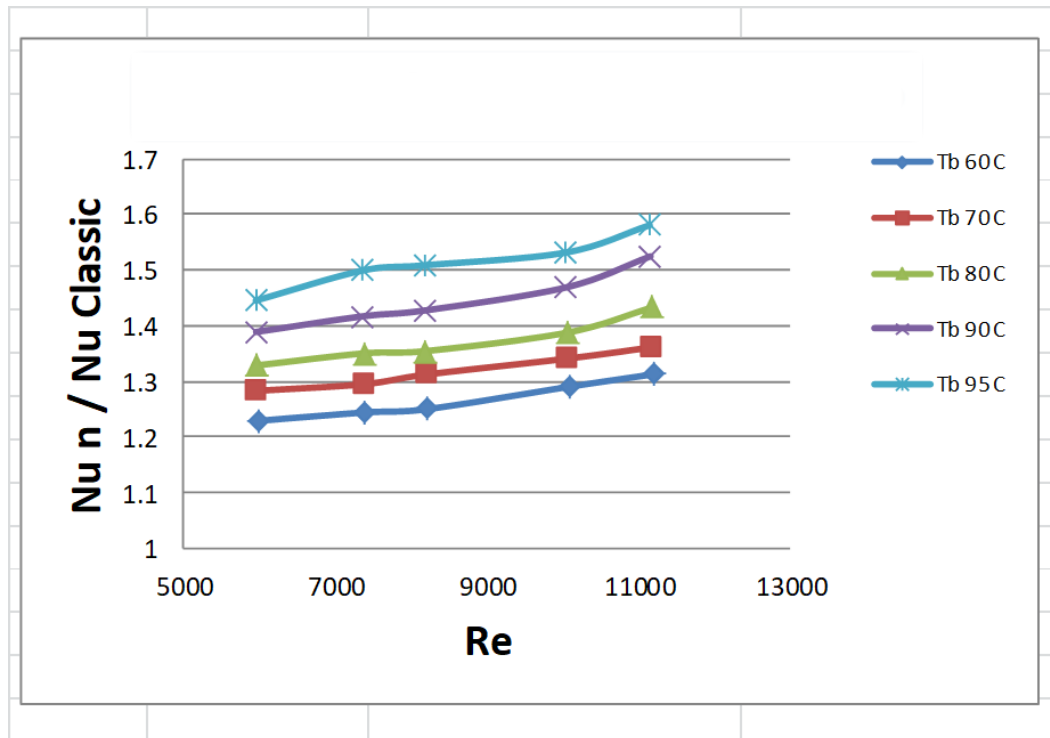


Figure (5 - 22) Variation between Re & ($Nu_n / Nu_{Classic}$) at 5% Nano.

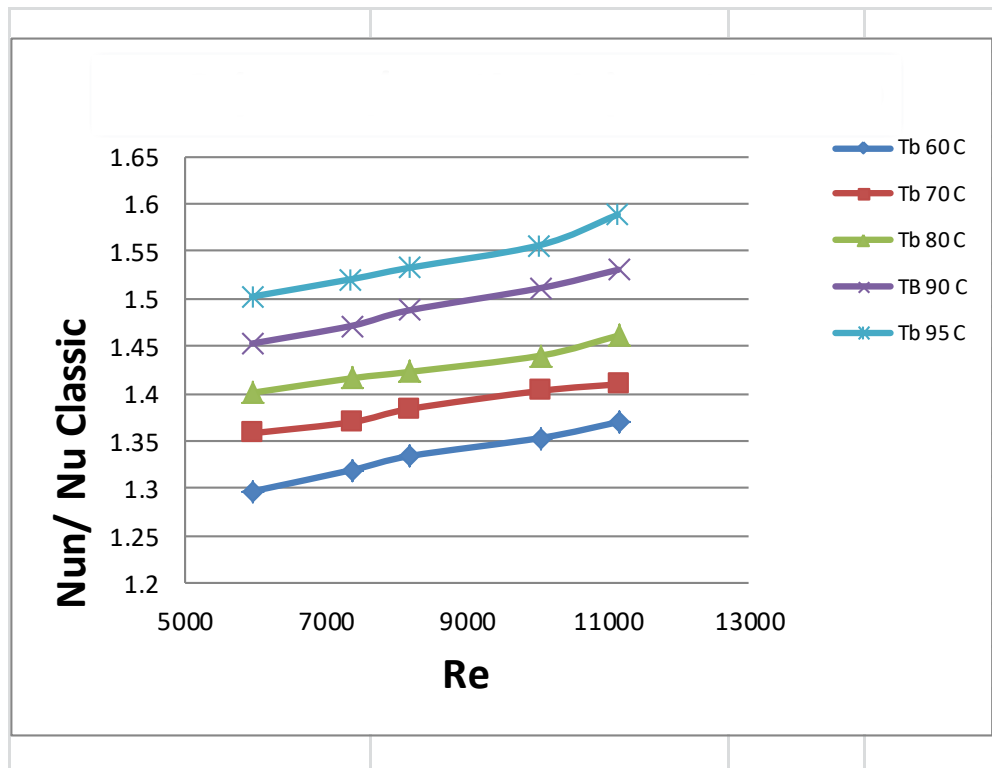


Figure (5 - 23) Variation between Re & ($Nu_n / Nu_{Classic}$) at 10% Nano.

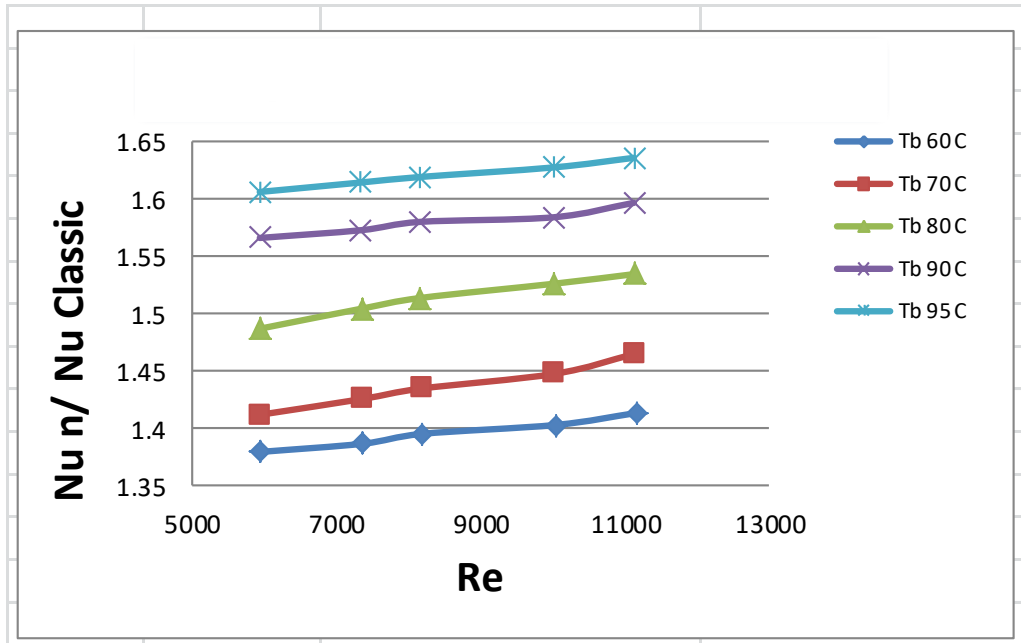


Figure (5 – 24) Variation between Re & ($Nu_n / Nu_{Classic}$) at 15% Nano.

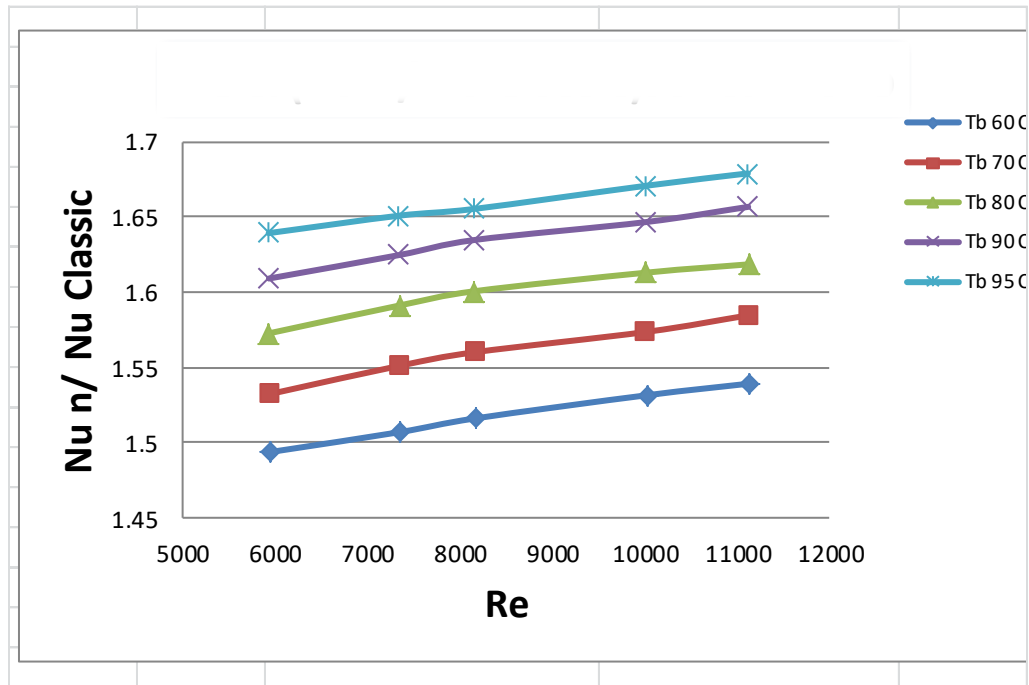


Figure (5 – 25) Variation between Re & ($Nu_n / Nu_{Classic}$) at 20% Nano.

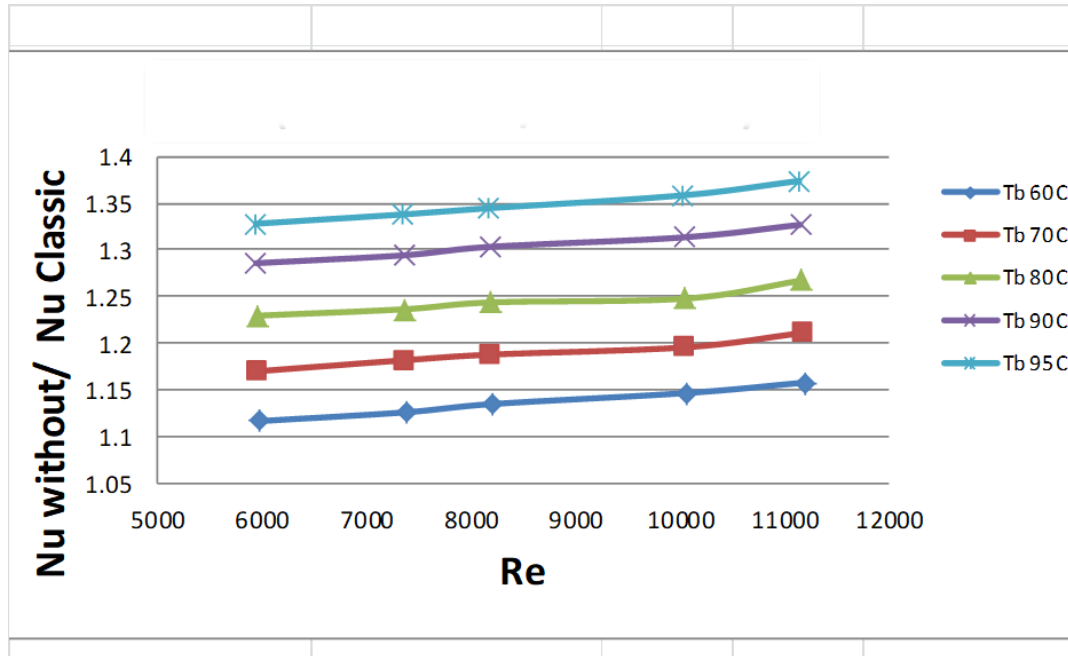


Figure (5 – 26) Variation between Re & (Nu without n / Nu Classic).

5.7.6 The Enhansmenting Ratio of model :

Another important thing is finding the improvement ratio for the dissipator that we designed and manufactured, which is the heat sink (Inline), as it is necessary to know whether this heatsink is as efficient as the classic heatsink or (less or more) efficient, in order to reach a final result to know which is better in terms of thermal dissipation and the ability to transfer heat between the metal and the external environment.

The practical experiments and mathematical equations conducted in this study show that the heat sink (Inline) It is better than the classic dissipator in terms of performance in the thermal dispersion process, by finding the result of the equation that we conducted, which is subtracting the Nusselt coefficient without the nanomaterial from the Nusselt coefficient (with the nanomaterial) divided by the Nusselt coefficient without the nanomaterial, and the result is multiplied (100%) , as define the equation follows:

$$\text{Enhansment Ratio} = \left[\frac{\text{Nu n} - \text{Nu without n}}{\text{Nu without n}} \right] \times 100\% \dots\dots\dots(5.2)$$

Since the result of this equation is what determines who is the best of the dispersers on which this study was conducted, if the result is less than (1), this means that the Inline heat sink is less performance than the original (classic) heat sink. However, if the result is more than (1), this means that the H.S. (Inline) it the best .

The result obtained from this equation is more than (1), and this means that the percentage of improvement that was made on the H.S. (Inline) In terms of dimensions, number of fins, their arrangement, and the general design of the dispersion, it is the best in this study. Figure (5 – 27) shows the change between the improvement percentage that we extracted from the above equation and a Reynold number for each temperature at which the test was performed.

We notice in this figure (when using Nano at a rate of 5%) that the percentage of improvement along the axis (Y) gives a good image through high curves with Reynolds number ,That is, at a temperature of 60 °C, we notice that the first curve ranges between (11 - 15), and the last curve, which is at a temperature of 95 °C, ranges between (30 - 36), and this is a good indicator of the performance of the dispersion in the heat transfer process.

While we notice in Figure (5 – 28) that the value of the curves has increased more than it was, as we used the nanomaterial at a rate of (10%), in the first curve we find that it ranges between (15 - 21), which is at 60 °C, while we notice that the last curve ranges between (33 - 41), which is at 95 °C, which are more than the values in the previous figure, which indicates that by increasing the nanomaterial, the value of Nusselt this leads to an increase in the rate of improvement little by little.

Figure (5 – 29) shows a further increase in the height of the curves by increasing the nanomaterial to (15%). In this figure we notice that the curves increased due to an increase in Nusselt rate on (Y) axis, as the first curve, which is at 60 °C, ranges between (22 - 27), while the last curve, which is at 95 °C, ranges between (45 - 49), and they are more valuable than the curves at the same temperature in the previous figure.

While in figure (5 – 30), we notice that the curves are higher than the previous figures, as the nanomaterial was used at a rate of (20%). This indicates that the Nusselt value has increased significantly from what it was. The first curve ranges between (27 - 33), which is At a temperature of 60 °C, while the last curve ranges between (47 - 51) and is at a temperature of 95 °C, and this indicates that the improvement rate has increased due to the increase in nanomaterial.

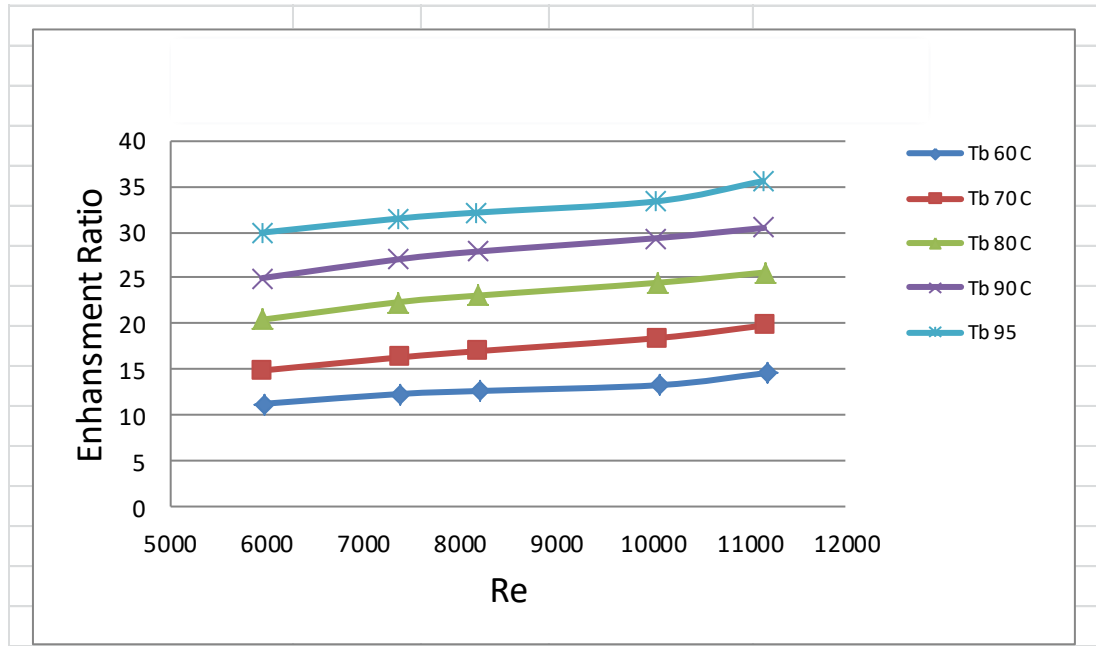


Figure (5 – 27) Variation between Re & Enhancement ratio with 5% Nano.

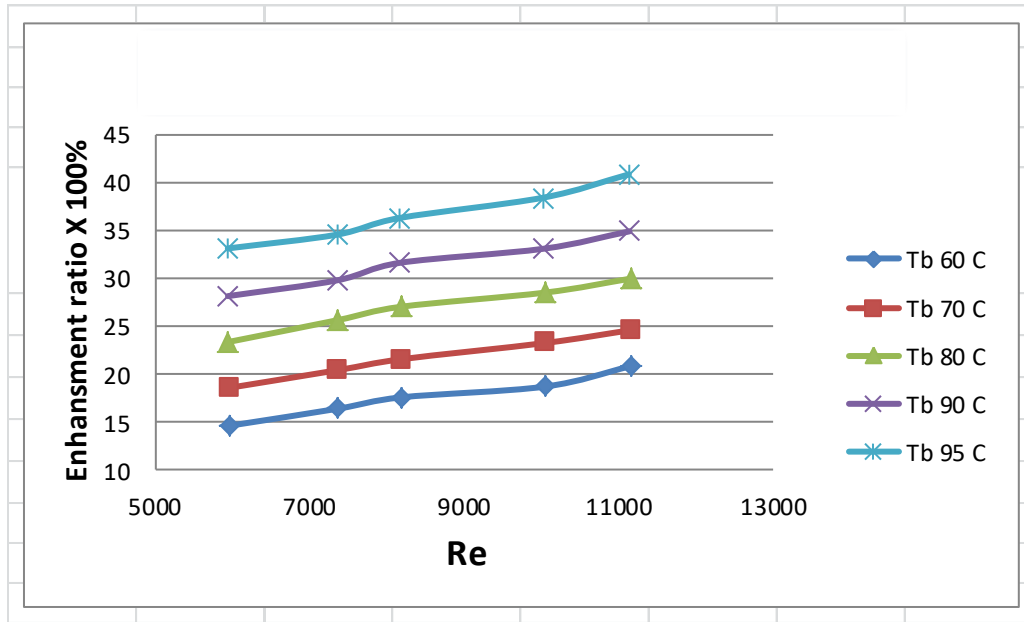


Figure (5 – 28) Variation between Re & Enhancement ratio with 10% Nano.

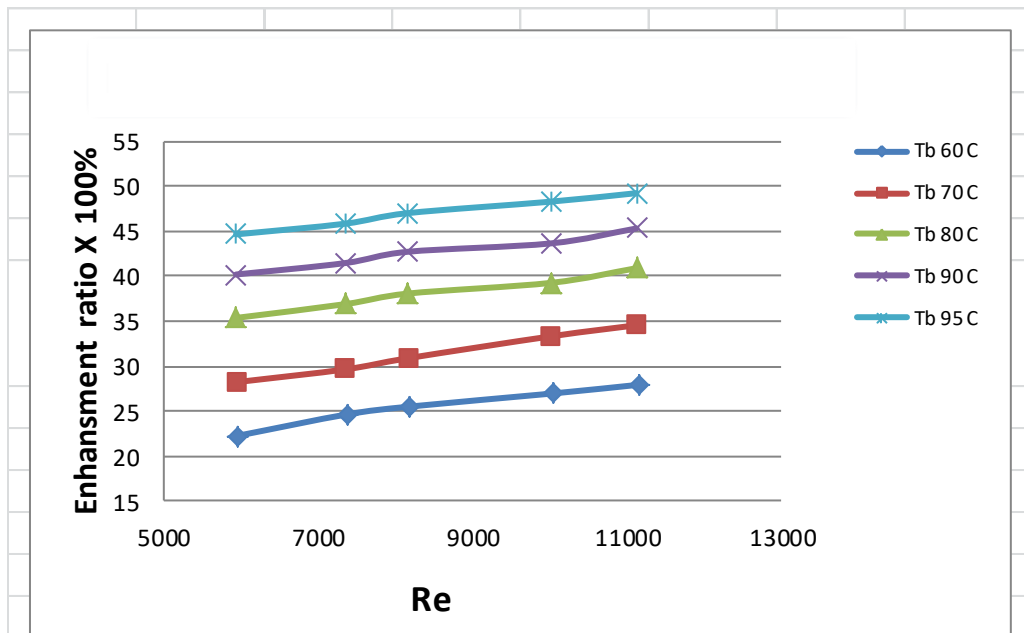


Figure (5 – 29) Variation between Re & Enhancement ratio with 15% Nano.

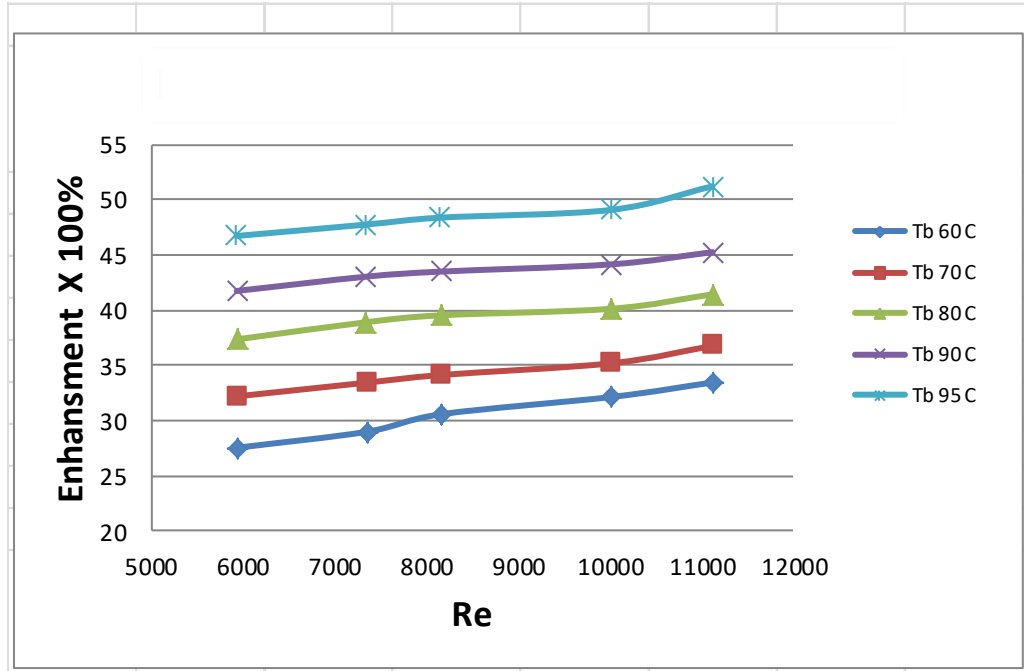


Figure (5 - 30) Variation between Re & Enhancement ratio with 20% Nano.

One of the very important things in this study is (Time).In the process of thermal dispersion, which is an important factor in this process, when practical experiments were conducted on heat sinks, we studied and observed the time it took to reach the maximum temperature to which the heat sink was exposed, which is (95) °C . We performed experiments on the classic and Inline heat sink with all the nanoscale ratios we mentioned previously and exposed to the same mentioned temperature.

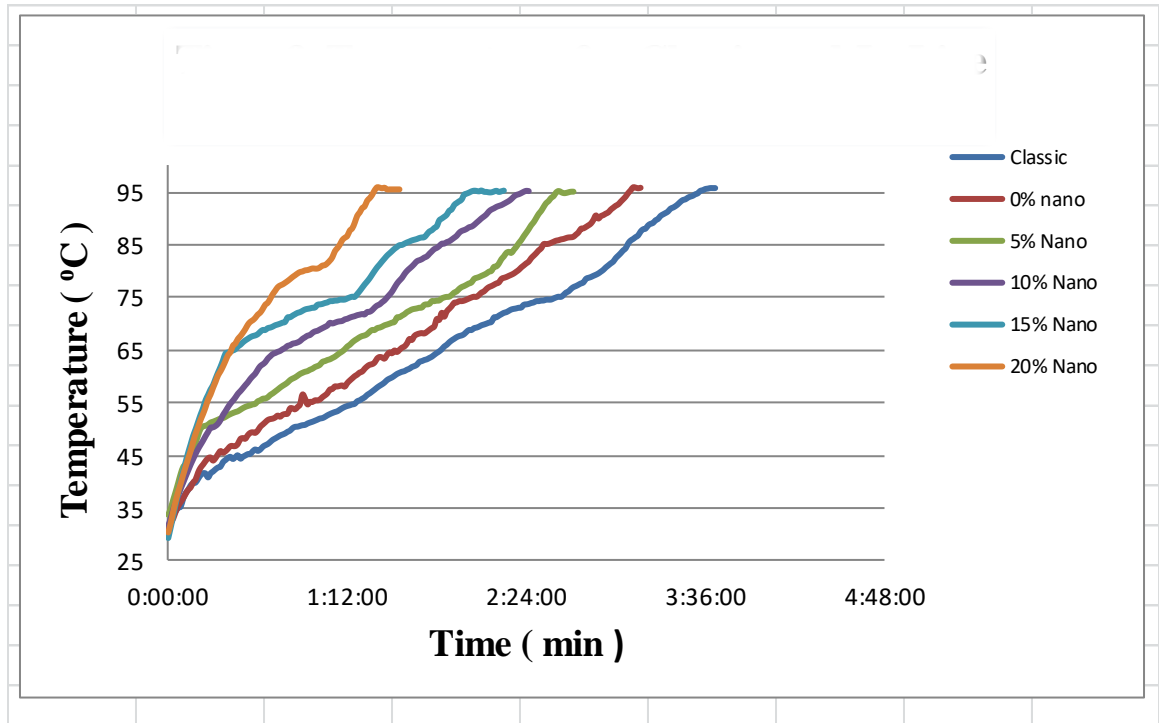


Figure (5 – 31) Variation between the Time and Temperature For Classic and In Line heat sinks.

We noticed through these experiments that the nanomaterial had a significant impact on the process of shortening the time to reach a steady state at the maximum temperature, which is (95) °C.

When we put the classic dispersant in the experiment, it took the longest time to reach this stage (i.e. the required temperature), while the dispersion Inline It is less time than the classic dispersion took, even without the use of nanomaterial, and this indicates that the dispersion Inline It is better than the classic heatsink in terms of dispersion and heat transfer due to the good design of the general shape, arrangement and number of fins, Figure (5 – 31).

We note that the classic heatsink took 3 hours and 38 minutes to reach the required temperature, while the heatsink Inline It took only 3 hours and 8 minutes to reach the same temperature without the nanomaterial, meaning that there was a 30-minute time reduction between them, and this is very important in the thermal management of electrical and electronic devices.

When using the nanomaterial (the nanomaterial is inside the cylindrical fins) in the dispersion, the difference was clear in the process of shortening the time for the same dispersion (without the nano and with the nano), as when using the nanomaterial at a rate of (5%), the dispersion took only 2 hours and 27 minutes to reach. The state of stability is at 95 °C, and this means that the difference between it and the same heat dissipation (in the absence of nano) is (41) minutes, which is approximately a long period of time. That is, the slower the thermal dissipation, the poorer the performance of the dissipator, as it stores The heat in the metal is released slowly to the outside environment. The faster the dispersion, the better the heat transfer process (that is, the heat is not stored inside the metal, but the dispersion carries out the heat exchange process well between it and the external surroundings).

In short, the greater the percentage of nanomaterial, the less time it takes to reach the required temperature.

When this material was used at a rate greater than the previous rate, i.e. it was used at a rate of (10%) in the practical experiment, the time taken to reach the required temperature of 95 degrees Celsius was only 2 hours and 10 minutes, i.e. the difference between it and the previous time (at a rate of 5 %) is 17 minutes, which is a good time in the heat transfer process.

When the nanomaterial was increased to (15%), the time it took for the dispersion to reach a stable state at the required temperature was only 2 hours.

That is, the time period decreases little by little. We notice that there is a difference in time (even if it is small), but it is effective in this process. While if the nanomaterial was increased to (20%), which is the highest percentage of nanomaterials used in this study, this percentage was very effective in the heat exchange process, as the time taken to reach the required temperature was only 1 hour and 33 minutes, which is the shortest period of time. From all previous time periods in the study. That is, the time difference between the classic dispersion and the (inline) dispersion with the nanomaterial at a rate of 20% is 2

hours and 5 minutes, which is a very large period of time in this process, which indicates that this nanomaterial (MWCNT) is effective in the process of conduction and heat transfer because the thermal conductivity coefficient (K) is very high, reaching more than 3500 W/m. C.

5.8 Verification of Model :

A comparison was made with previous work for the purpose of verifying the model that was used to study thermal dispersion by a pin-fin dissipator (inline) without and with the use of nanomaterial (MWCNTs).

Bakhti et al [2021][32], indicated in the study he presented that the average Nusselt number ranged between (3 - 18.5), while the Reynolds number ranged between (50 - 250). In their study, a heat sink with pin fins (Elliptic) was used. Comparing his work with a previous study by the researcher Deshmukh et al [2013][33], who in turn obtained a Nusselt ratio ranging between (2.7 - 19) with same Reynold No. as shown in figure (5– 32), and figure (5 – 33) show the pin-fin of heat sink and designed geometry.

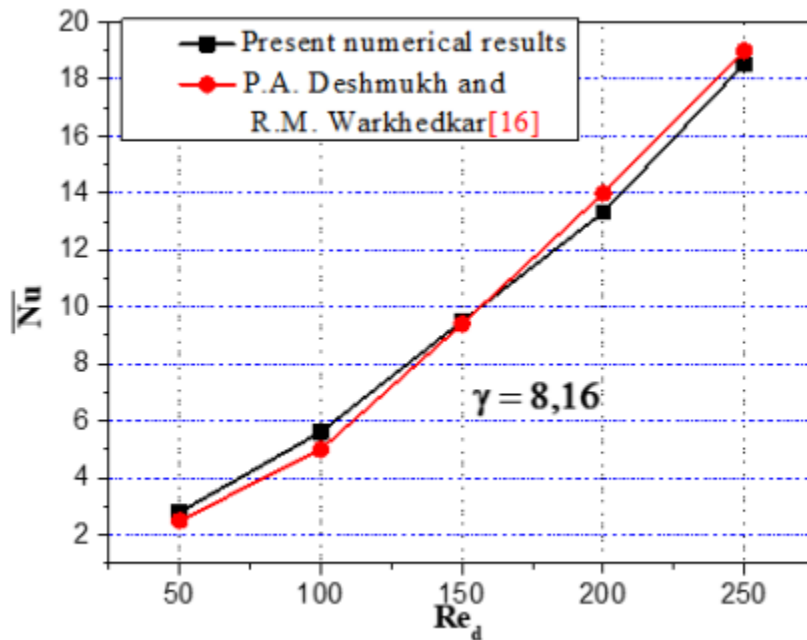


Figure (5 – 32), Average Nusselt number variation versus the Reynolds number.

And this relationship between (Nuslet and Reynolds) was based on a variable measure (γ), which is the ratio of the length of the fin to its elliptical diameter, as shown in the equation (in Appendix).

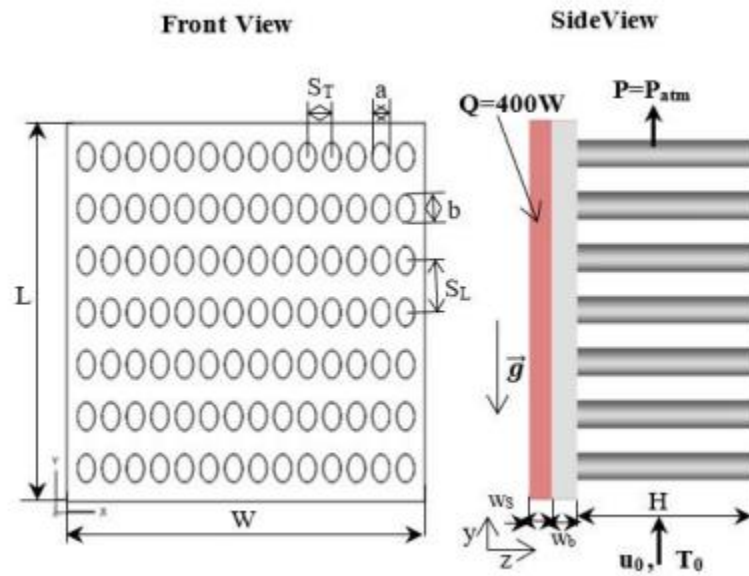


Figure (5 – 33), pin-fin of heat sink and designed geometry.[35]

While in this presented study, better results were obtained by these two researchers by using a heat sink without the nanomaterial, and when placing the nano-filling in the fins, higher results were obtained as shown in the previous diagrams.

Chapter Six
CONCLUSIONS
AND
RECOMMENDATIONS

CHAPTER SIX

CONCLUSIONS AND RECOMMENDATIONS

6.1 CONCLUSIONS

In this study, the total heat transfer, friction factor, thermal efficiency, fin efficiency and thermal resistance were investigated experimentally and numerically in three models of heat sinks (In Line , Staggered , Zigzag) and compare it with the traditional spreader.

- 1- Found the heat transfer coefficient (h) in convection, the value obtained (80 – 90) to the In line H.S when comparing heat sinks.
- 2- calculate the value of the Nusselt number and the Q value of the dispersant.
- 3- Reynolds' value in this study ranged between (5000 – 11800) with nanomaterial.
- 4- Also, it was studied which of the used models of heat sinks had the most effectiveness in dissipation with and without terms of heat the use of nanomaterials.
- 5- It has been shown through experiments that the best of these dispersals in terms of heat dissipation is the type In line, due to the good geometric distribution of the fins, unlike other models.

- 6- The rapid thermal dissipation will help the devices to give a good work in terms of performance and rapid response to the completion of orders related to electronic and electrical devices in general.
- 7 - The use of nanomaterials has a major role in the process of dissipating heat in a short time, which helps keep the devices working within the industrially permissible levels.

6.2 RECOMMENDATIONS

The presented study deals with cooling the central processing unit in electronic and electrical devices in general through the use of several models of heat sinks, including the inline heatsink, which practical experiments have proven to be better than other heatsinks in that study, through the design and arrangement of the pin fins. in it . However, there are several good and effective recommendations that can be taken into account in the future:

1. Choosing a good and pure metal in the manufacture of the heat sink, which has the ability to quickly exchange heat with the external environment.
2. The use of nanomaterials (MWCNTs) as a filler in the fins of the heatsinks, are highly effective in the process of heat exchange between the heatsink and the external environment.
3. Choose a high-speed air fan to help expel heat into the atmosphere through rapid airflow over the surface of the heatsink.
4. The correct and regular arrangement of the fins plays a major role in the process of heat transfer between the heatsink and the external environment, which helps reduce the temperatures of electrical and electronic devices.

REFERENCE:

- [1] Glacial Tech announces Igloo FS125S 30W cold forged pin fin heat sink". Eco-Business.
- [2] https://commons.wikimedia.org/wiki/File:AMD_heatsink_and_fan.jpg
- [3] Overview of Cooling Methods for AC-DC and DC-DC Power Supplies". www.aegispower.com
- [4] Design Considerations for Thermal Management of Power Supplies" (PDF). www.cui.com.
- [5] <https://images.app.goo.gl/Jhfi1YNXsPB6nJuu9>.
- [6] Karthikeyan, R and Rathnasamy, R. Effect of geometric and flow parameters on the performance of pin-fin arrays, Indian Journal of Science and Technology, Vol.4 No. 10 (Oct 2011) 1256 – 1261.
- [7] Nello Sevastopoulos et al., National Semiconductor Voltage Regulator Handbook, National Semiconductor Corp., 1975 chapters 4, 5,6.
- [8] Li, J., & Yang, L. (2023). Recent Development of Heat Sink and Related Design Methods. Energies, 16(20), 7133.

- [9] [https://commons.wikimedia.org/wiki/File:Pinfin, straight fin and flared heat sinks.png](https://commons.wikimedia.org/wiki/File:Pinfin,_straight_fin_and_flared_heat_sinks.png)
- [10] Kily, R.F, and Soul, C.A, Engineering Heat Sink, Power technics Magazine, July, (1990).
- [11] Soul, C.A., Air and Liquid Cooled Techniques for High Power Density Components, Power Conservation and Intelligent Motion, Vol.19, No.11, (1993).
- [12] <https://www.researchgate.net/publication/323826930>.
- [13] <https://www.researchgate.net/publication/323826930>.
- [14] <https://www.researchgate.net/publication/323826930>.
- [15] Baqir, A. S., Qasim, A., & Adnan, A. (2014). Experimental study for staggered perforated array of pins like fins in a rectangular air cross flow. The Iraqi Journal for Mechanical and Material Engineering, 14(2), 261-275.
- [16] Lotfizadeh, H., Mehrizi, A. A., Motlagh, M. S., & Rezazadeh, S. (2015). Thermal performance of an innovative heat sink using metallic foams and aluminum nanoparticles—Experimental study. International Communications in Heat and Mass Transfer, 66, 226-232.
- [17] Patil, A. K., Choudhary, V., Gupta, A., & Kumar, M. (2022). Thermo-hydraulic performance of modified plate fin and pin fin heat sinks. Proceedings of the Institution of Mechanical Engineers, Part A: Journal of Power and Energy, 236(1), 96-108.
- [18] Hung, T. C., Yan, W. M., Wang, X. D., & Chang, C. Y. (2012). Heat transfer enhancement in microchannel heat sinks using nanofluids. International Journal of Heat and Mass Transfer, 55(9-10), 2559-2570.

- [19] Zarma, I., Ahmed, M., & Ookawara, S. (2019). Enhancing the performance of concentrator photovoltaic systems using Nanoparticle-phase change material heat sinks. *Energy Conversion and Management*, 179, 229-242.
- [20] Bondareva, N. S., Gibanov, N. S., & Sheremet, M. A. (2020). Computational study of heat transfer inside different PCMs enhanced by Al₂O₃ nanoparticles in a copper heat sink at high heat loads. *Nanomaterials*, 10(2), 284.
- https://mdpi-res.com/d_attachment/processes/processes-10-01644/article_deploy/processes-10-01644.pdf
- [21] Zhang, B., Zhu, J., & Gao, L. (2020). Topology optimization design of nanofluid-cooled microchannel heat sink with temperature-dependent fluid properties. *Applied thermal engineering*, 176, 115354.
- [22] Awais, A. A., & Kim, M. H. (2020). Experimental and numerical study on the performance of a minichannel heat sink with different header geometries using nanofluids. *Applied Thermal Engineering*, 171, 115125.
- [23] Ma, Y., Shahsavari, A., & Talebizadehsardari, P. (2020). Two-phase mixture simulation of the effect of fin arrangement on first and second law performance of a bifurcation microchannels heatsink operated with biologically prepared water-Ag nanofluid. *International Communications in Heat and Mass Transfer*, 114, 104554.
- [24] Balaji, T., Selvam, C., Lal, D. M., & Harish, S. (2020). Enhanced heat transport behavior of micro channel heat sink with graphene based nanofluids. *International Communications in Heat and Mass Transfer*, 117, 104716.
- [25] Kumar, A., Kothari, R., Sahu, S. K., & Kundalwal, S. I. (2021). Thermal performance of heat sink using nano-enhanced phase change material (NePCM) for cooling of electronic components. *Microelectronics Reliability*, 121, 114144.

- [26] Jung, S. Y., & Park, H. (2021). Experimental investigation of heat transfer of Al_2O_3 nanofluid in a microchannel heat sink. *International Journal of Heat and Mass Transfer*, 179, 121729.
- [27] Kothari, R., Sahu, S. K., & Kundalwal, S. I. (2021). Investigation on thermal characteristics of nano enhanced phase change material based finned and unfinned heat sinks for thermal management system. *Chemical Engineering and Processing-Process Intensification*, 162, 108328.
- [28] Ozbalci, O., Dogan, A., & Asilturk, M. (2022). Heat Transfer Performance of Plate Fin and Pin Fin Heat Sinks Using $\text{Al}_2\text{O}_3/\text{H}_2\text{O}$ Nanofluid in Electronic Cooling. *Processes*, 10(8), 1644.
- [29] Tiwary, B., Kumar, R., & Singh, P. K. (2022). Thermofluidic characteristic of a nanofluid-cooled oblique fin heat sink: An experimental and numerical investigation. *International Journal of Thermal Sciences*, 171, 107214.
- [30] The Global Market for Multi-Walled Carbon Nanotubes 2021–2031, Future Markets. <https://www.researchandmarkets.com/reports/5324906/the-global-market-for-multi-walled-carbon>
- [31] <https://www.scipublications.com/search?q=Junjie%20Chen>
- [32] Bakhti, F.Z., Si-Ameur, M. (2021). Elliptical pin fin heat sink: Passive cooling control. *International Journal of Heat and Technology*, Vol. 39, No. 5, pp. 1417-1429. <https://doi.org/10.18280/ijht.390503>.
- [33] Deshmukh, P.A., Warkhedkar, R.M. (2013). Thermal performance of elliptical pin fin heat sink under combined natural and forced convection. *Experimental Thermal and Fluid Science*, 50: 61-68. <https://doi.org/10.1016/j.expthermflusci.2013.05.005>.

[34] Deshmukh, P.A., Warkhedkar, R.M. (2013). Thermal performance of elliptical pin fin heat sink under combined natural and forced convection. *Experimental Thermal and Fluid Science*, 50: 61-68.

<https://doi.org/10.1016/j.expthermflusci.2013.05.005>.

[35] Bakhti, F.Z., Si-Ameur, M. (2021). Elliptical pin fin heat sink: Passive cooling control. *International Journal of Heat and Technology*, Vol. 39, No. 5, pp. 1417-1429. <https://doi.org/10.18280/ijht.390503>.

[36] M. A. R. Sadiq Al-Baghdadi, Z. M. H. Noor, A. Zeiny, A. Burns, and D. Wen, "CFD analysis of a nanofluid-based microchannel heat sink," *Therm. Sci. Eng. Prog.*, vol. 20, no. August, p. 100685, 2020, doi: 10.1016/j.tsep.2020.100685.

[37] <https://forum.ansys.com/forums/topic/student-ansys-workbench-18-1>.

APPENDIEXES

$$\therefore 1 \text{ m}^3 = 1000 \text{ litter}$$

$$1 \text{ litter} = 1 \text{ Kg}$$

$$1 \text{ Kg} = 1000 \text{ g}$$

Volume of cylindrical

$$V = \frac{\pi}{4} \cdot D^2 \cdot l \quad (D = 1.5 \text{ mm} , l = 14 \text{ mm})$$

$$\begin{aligned} \therefore V &= \left[\frac{\pi}{4} \cdot \left(\frac{1.5}{1000} \right)^2 \cdot \left(\frac{14}{1000} \right) \right] * 1000(\text{Litter}) * 1000(\text{gram}) . \\ &= 0.02474 \text{ m}^3 \end{aligned}$$

$$T_{avg} = \frac{\sum T_{out}}{6} \quad \text{----- 1}$$

(6 No. of the sensors at air outlet)

$$A_{Total} = A_{fin} \times 120 + A_c \times 120 + A_{unfin} \quad \text{----- 2}$$

Where A_{Total} \ Area of all heat sink.

A_{fin} \ Area of fins only.

A_c \ Area of top circle of fins.

A_{unfin} \ Area of heat sink without fins.

120 \ No. of fins in the heat sink.

$$A_{fin} = \pi \cdot D \cdot L \quad \text{----- 3}$$

(D = out diameter of fin , L = Length of fin)

$$A_c = \frac{\pi}{4} \cdot D^2 \quad \text{----- 4}$$

$$A_{unfin} = (81 \times 67) \text{ mm} - A_c \times 120 \quad \text{----- 5}$$

(81 = Length of base the heat sink , 67 = Width of base the heat sink)

$$\Delta T = T_{out} - T_{in} \quad \text{----- 6}$$

(where T_{in} its temp of ambient = 24° C)

$$h = \frac{Q_{convection}}{A_{Total} (T_b - T_{avg})} \quad \text{----- 7}$$

$$Q_{convection} = Q_{Total} - Q_{Loss} \quad \text{----- 8}$$

$$(Q_{Loss} = 0.05 \times Q_{Total}) \quad \text{----- 9}$$

$$\rho_{air} = 0.00001357 \times \left(\frac{T_{in} - T_{avg}}{2}\right)^2 - 0.004668 \times \left(\frac{T_{in} - T_{avg}}{2}\right) + 1.292 \quad \text{-----}$$

$$\text{----- 10}$$

(where ρ_{air} = density of air).

- Thermal Conductivity of air (K_{air}) :

$$K_{air} = 0.00000001905 \times \left(\frac{T_{in} - T_{avg}}{2}\right)^2 + 0.00007533 \times \left(\frac{T_{in} - T_{avg}}{2}\right) + 0.02364$$

$$\text{----- 11}$$

- Reynold No. (Re_{air}) :

$$Re_{air} = \left(\frac{\rho_{air} \cdot V_{air} \cdot D_{duct}}{\mu_{air}}\right)$$

$$= \left(\frac{\rho_{air} \cdot V_{air} \cdot D_{duct}}{0.000019}\right)$$

$$\text{----- 12}$$

(where $\mu_{air} = 0.000019$)

- Nusselt No (Nu_{air}) :

$$Nu_{air} = \left(\frac{h \cdot D_{duct}}{K_{air}} \right) \text{ ----- 13}$$

- *Enhancement ratio* (100%)

$$\text{Enhancement ratio} = \left(\frac{Nu_n - Nu_{without n}}{Nu_{without n}} \right) \times 100 \text{)} \text{ -----14}$$

where $Nu_n = Nu$ with nanomaterial

$Nu_{without n} = Nu$ without nanomaterial .

Where Reynold No.

$$Re = (\rho U_0 d) / \mu$$

$$d = \sqrt{(4ab)}$$

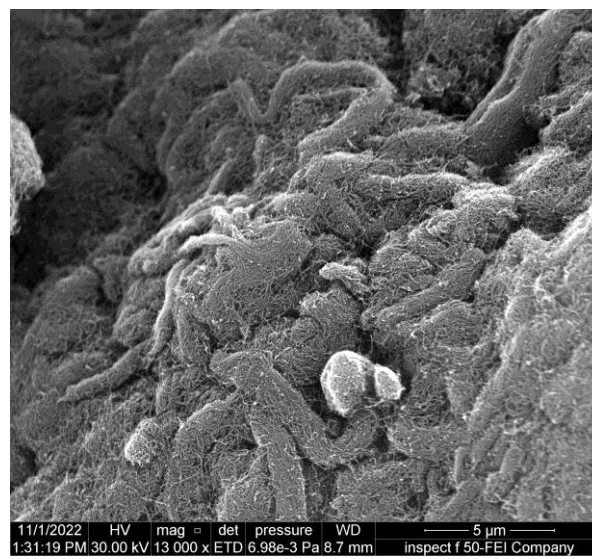
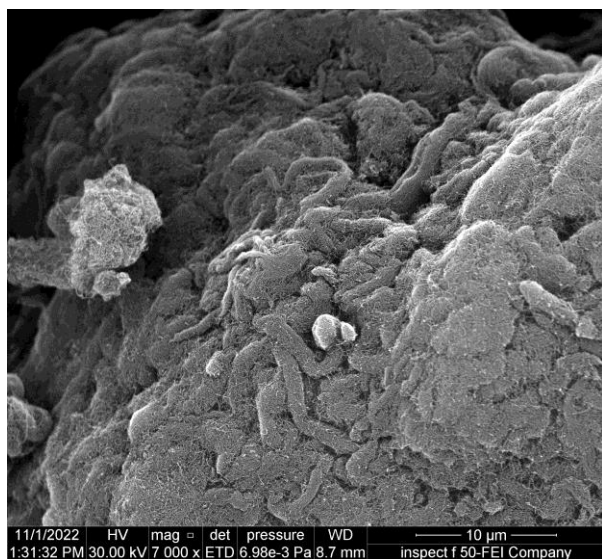
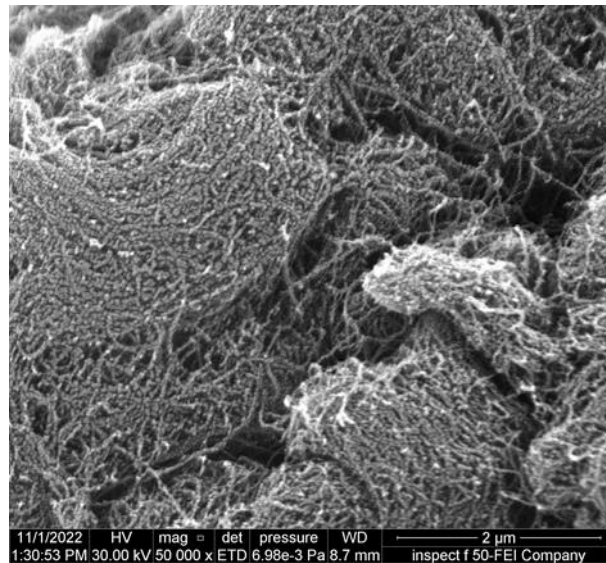
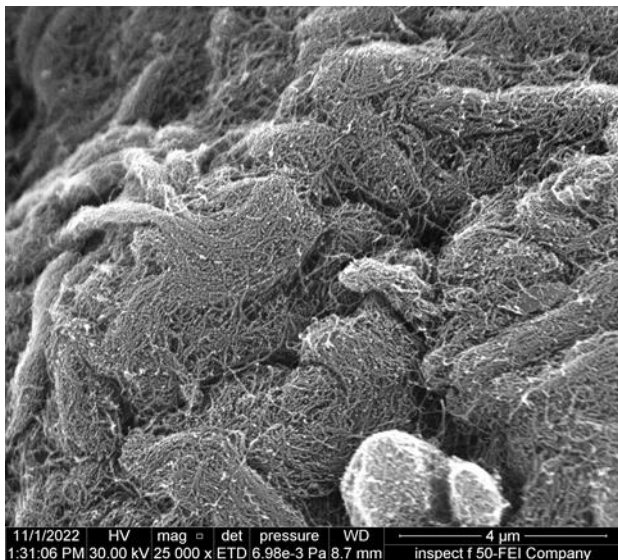
Where d is the mean diameter of elliptical pin fin.

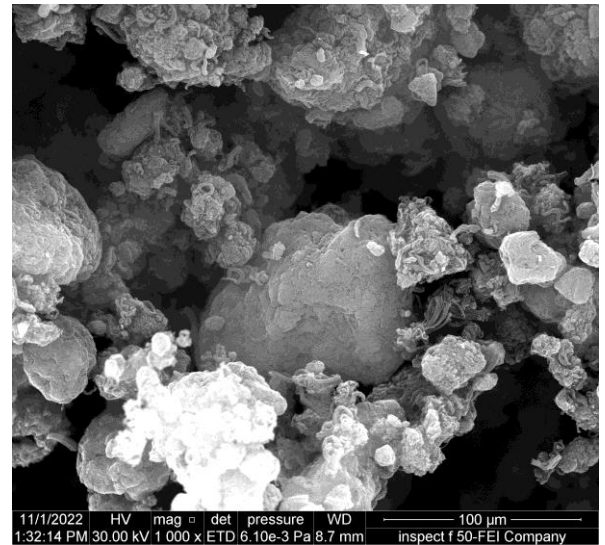
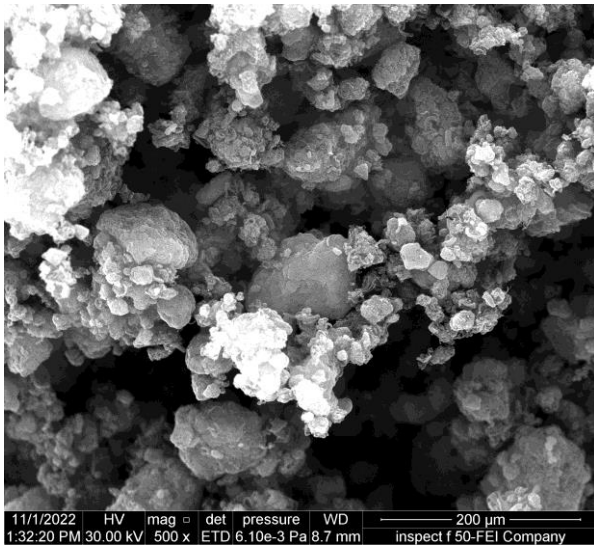
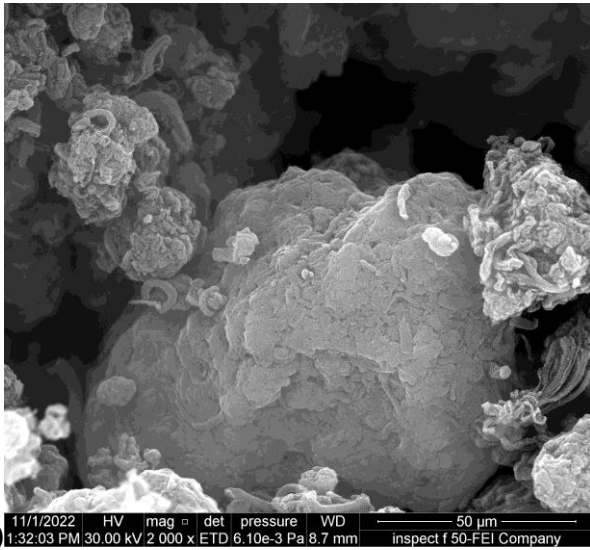
and Nusselt No [$Nu = (h \cdot d) / K$]

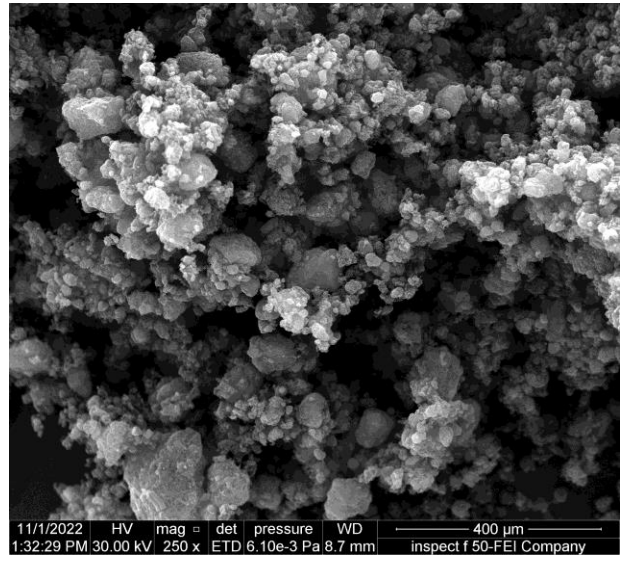
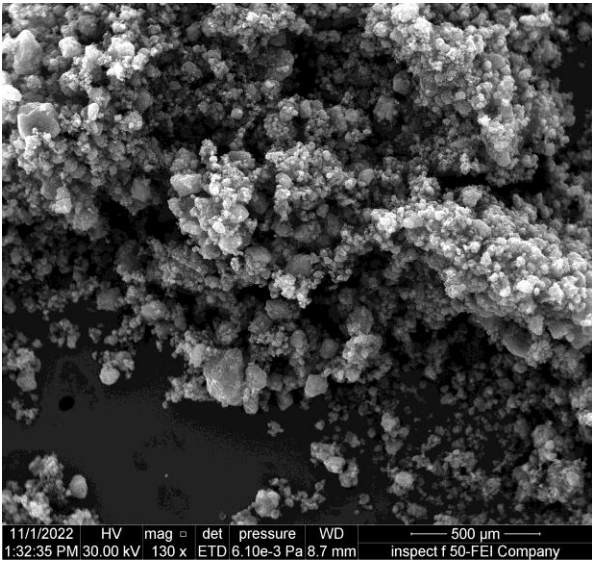
where h is heat transfer coefficient

$$h = q / (A \cdot \Delta T)$$

- The Test Photos of Nano material in (Areej AL- Furat) Lap in Baghdad.







- **List of Publication :**



الخلاصة

اصبحت الادارة الحرارية للأجهزة الكهربائية والالكترونية مشكلة رئيسية في الوقت الحالي . لذلك ومع مرور الوقت ، وبسبب التكنولوجيا المتطورة والحاجة المتزايدة للتبريد في الانظمة الالكترونية المختلفة ، كانت هناك حاجة متزايدة للبحث في العديد من المواد الجديدة والتصميمات المختلفة و المواد النانوية المبتكرة .

حيث تبحث معظم الدراسات المتعلقة بالتحقيقات التجريبية و العديدة في عملية نقل الحرارة من المشتت (في مفاهيم التصميم المثالية التي تزيد من معامل نقل الحرارة و التبريد الحراري (H.S.الحراري

في هذه الدراسة ، تم التحقيق في عملية نقل الحرارة بين مشتت تقليدي ذو زعانف مستطيلة من صنع الشركات المختصة وبين مشتتات ذات زعانف دبوسية قمنا بتصنيعها وهي (إنلاين ، ستاكر ، متعرج) لها (وهي مساوية لمساحة المشتت التقليدي (بعد ازالة جزء 21252.6×10^{-3} نفس المساحة السطحية وهي (منه) . الاختلاف كان في ترتيب صفوف الزعانف ، وكل نموذج من هذه النماذج يحتوي على (120) زعنفة دبوسية ذات قطر خارجي 3 ملم من و قطر داخلي 1.5 ملم ، والزعانف مرة تكون صلدة وغير مجوفة ومرةً (MWCNTs اخرى تحتوي على حشوة من مادة نانوية تسمى أنابيب الكربون النانوية متعددة الجدران) والتي تتميز بخاصية فائقة للتوصيل الحراري ، وبعد اجراء الفحص والاختبارات والاطلاع على النتائج من (مع سرعة الهواء المتدفق h حيث أي من هذه النماذج كان له اعلى قيمة لمعامل انتقال الحرارة بالحمل) على سطح المشتت ، قمنا باختيار المشتت (إنلاين) لأجراء الاختبارات الاخرى وذلك لحصولنا على اعلى (. وعند استخدام مادة النانو ذات الموصلية العالية ، قمنا بتعبئة نسب معينة من زعانف المشتت h قيمة لل (الحراري وليس تعبئة الزعانف بالكامل ، حيث قمنا بتعبئة 5% من عدد الزعانف الكلي أي (6) زعانف ، و 10% أي (12) زعنفة ، و 15% أي (18) زعنفة ، و 20% أي (24) زعنفة من اصل 120 زعنفة .

والاختبارات التي قمنا بها في هذه الدراسة تعتبر من اكثر الاختبارات اهمية من حيث مبدأ انتقال الحرارة بين المشتت والمحيط الخارجي ، والمقارنة بين المشتت وبين المشتت التقليدي ، حيث كانت المقارنات التي اجريت بينهما قد اعتمدت على النتائج الحاصلة من قيمة رقم رينولد ورقم نسلت اللذان كانا اكثر قيمة ، تم الحصول على النتائج من الاختبارات العملية للمشتت (إنلاين) بدون المادة النانوية اولاً ، والحصول على نتائج الاختبارات العملية مع وجود المادة النانوية ثانياً ، حيث هنا اصبحت قيمة رقم رينولد و رقم نسلت اعلى (، مما يعني ان معدل الانتقال h مما كانت عليه وذلك بسبب ارتفاع قيمة معامل انتقال الحرارة بالحمل الحراري بين المشتت والمحيط الخارجي اصبح اكثر مما كان عليه عند الاختبار بدون النانو . وهذا يشير الى ان فعالية المادة النانوية اصبحت مؤثرة الى درجة كبيرة جداً كما تبين هذه الدراسة .



دراسة تجريبية ونظرية للخصائص الحرارية للمشتت الحراري باستخدام تعبئة جزيئات النانو

رسالة مقدمة الى
قسم هندسة تقنيات ميكانيك القوى
كجزء من متطلبات نيل درجة الماجستير في
هندسة تقنيات ميكانيك القوى / الحرارية

تقدم بها
حامد مكي بعيوي
ماجستير في هندسة تقنيات ميكانيك القوى

اشراف

الأستاذ الدكتور
منتظر عبودي الموسوي

الاستاذ الدكتور
علي شاكرا باقر

2023 ميلادي
1445 هجري



جمهورية العراق
وزارة التعليم العالي والبحث العلمي
جامعة الفرات الاوسط التقنية
الكلية التقنية الهندسية/النجف

دراسة تجريبية ونظرية للخصائص الحرارية للمشتت الحراري باستخدام تعبئة
جزيئات النانو

حامد مكي بعيوي

لنيل درجة الماجستير في هندسة تقنيات ميكانيك القوى

2024 ميلادي

1445 هجري